Ionic Liquid Based Polymer Gel Electrolytes

A DISSERTATION
SUBMITTED TO THE FACULTY OF THE GRADUATE SCHOOL
OF THE UNIVERSITY OF MINNESOTA
BY

Keun Hyung Lee

IN PARTIAL FULFILLMENT OF THE REQUIREMENTS
FOR THE DEGREE OF
DOCTOR OF PHILOSOPHY

Advisers: C. Daniel Frisbie and Timothy P. Lodge

November 2012

Acknowledgements

This thesis would not have been completed without the help and support of many people. First and foremost, I would like to thank my advisors, Professors Dan Frisbie and Tim Lodge, for their invaluable assistance and professional guidance during my time in Minnesota. I also thank my current and former lab-mates: Moon Sung Kang, Soo Hyung Choi, Chang-Hyun Kim, Seongho Choi, Sipei Zhang, Yuanyan Gu, Se Hyun Kim, Kihyun Hong, Bong Soo Kim, Wei Xie, Yu Xia, Mingjung Ha, Shun Wang, Soonyong So, Jeong Ho Cho, Jiyoul Lee, Zhifeng Bai, Takeshi Ueki, Yu Lei, Salil Bapat, Can Zhou, Brad Jones, Hau-Nan Lee, Peter Simone, Bryan Paulsen, Chris Smith, David Ellison, Bryan Boudouris, Vivek Kalihari, Yan Liang, and Derek Stevens for their help and valuable discussions in the lab and office.

Thank you to my friends: Jonghyuk Park, Jaewook Nam, Dong-Ha Lim, Won Cheol Yoo, Pyungsoo Lee, Sangwoo Lee, Intaek Lee, Sangwon Kim, Han Seung Lee, Do Young Hong, Jin Oh Song, Hyunwoo Kim, Dong Seong Cho, Seongmin Heo, Mi Young Jeon, Minje Kang, Yong Tae Park, Jong Hee Kim, Sangho Lee, and Sooman Lim for making my life here enjoyable and exciting. I also thank my old friends in Korea: Gwangyoung Lee, Suseong Lee, Bo-Rham Lee, and Jeongwoo Park.

I must thank my entire family: my parents, my brothers, my wife Misun and my daughter Erica. Without their endless love and encouragement throughout my life, I would not have made this achievement.

To my family

Abstract

Ionic liquids have attracted significant interest in a wide variety of applications including electronic, electrochemical, and energy storage devices. This thesis investigates the use of ionic liquid-based polymer electrolytes (ion gels) as a gate insulator material for thin-film transistors. The first objective of thesis is to study the electrical properties of ion gels systematically to understand how the ion gels work as a capacitor to accumulate charge carriers in a semiconductor channel. Accordingly, electrical properties including specific capacitance, resistance and conductivity of ion gels were investigated as a function of film geometry (thickness and area) and temperature.

This research also aims to develop new routes for incorporating an ion gel layer on a device to provide diversity and universality in ion gel processing. The first effort was devoted to prepare a smooth and uniform layer of ion gel by spin casting. Typical thicknesses of spin-coated ion gels were 1~20 μm. Alternatively, transfer printing using an elastomeric stamp was utilized to prepare all-printed (semiconductor, ion gel dielectric, and gate electrode) thin-film transistors. For the last, mechanically free-standing ion gels that can be cut by hand and laminated on a layer of semiconductor using tweezers were developed for thin-film transistors. This ‘cut and stick’ strategy facilitates convenient fabrication of transistors on a variety of semiconductor materials. Overall, these new processes provide reliable routes to employ ion gels on electrical and electrochemical devices.

Table of Content

List of Tables

List of Figures

Chapter 1

Introduction

Ionic liquids consisting of low molar mass cations and anions have attracted great attention as electrolytes for electrical and electrochemical devices, and energy storage applications, due to their negligible vapor pressure, thermal, chemical, and electrochemical stability, high capacitance and ionic conductivity.[1-4] In order to harness these outstanding properties noted above in a solid film, a structuring polymer is blended with ionic liquids to form a network. The polymer network can be designed by using copolymers that are partially soluble in ionic liquids. The resulting solid polymer electrolyte is referred to as an ion gel.[5]

Ion gels have been employed in thin-film transistors as gate insulators (*i.e.* electronic insulators) primarily due to huge specific capacitances (~10 μF/cm^2) coming from nanometer-thick electrical double layers at electrolyte/electrode interfaces.[6] Accordingly, the large capacitance (C) from ion gels allows the same number of charge carriers (Q) in the semiconductor channel with lower applied potential (V): $Q = C \times V$. By using ion gels as gate insulators, transistors operate at low voltages (1−2 V) and have high ON currents (~1 mA).[7-9] For comparison, transistors with traditional insulators (*e.g.* SiO_2) need higher operating voltage (~100 V) and show lower ON current (~10 μA).[10] The operating speeds of ion gel-based transistors are typically ~1−10 kHz.[8] This speed is much slower than SiO_2 gated transistors (>1 MHz), but still highest among transistors using solution-processable gate insulators including poly(ethylene oxide)-based polymer

electrolytes (~1 Hz).[11-13] Therefore ion gel-gated transistors could provide a solution for applications where low voltage operation with moderate working speed is important.

1.1 Thesis overview

The goal of this thesis is to understand electrical and viscoelastic properties of ion gels and thereby develop alternative routes for the gel processing of thin-film transistors. This thesis provides the systematic investigation of geometry (thickness and area) and temperature effects on the electrical properties (resistance, ionic conductivity and capacitance) of ion gels and new deposition methods for ion gels. Reliability of the new processing techniques is verified using thin-film transistors. The remaining chapters are organized as follows. Chapter 2 provides basic concepts of a transistor including geometry and operation mechanisms, and then reviews ionic liquids and their electrical properties. As a way to form solid-like electrolytes, polymer gel electrolytes (ion gels) are also discussed.

Chapter 3 describes experimental techniques used to prepare and characterize ion gels and ion gel-gated transistors. Size exclusion chromatography (SEC), ^{1}H NMR spectroscopy, rheology and impedance spectroscopy are utilized in this thesis. In addition, procedures to prepare a poly(dimethylsiloxane) PDMS stamp and a ZnO film are discussed.

In Chapter 4, electrical properties (resistance, ionic conductivity, and capacitance) of ion gels are investigated as a function of film geometry (thickness and area) and temperature. This work has been published as “Electrical Impedance of Spin-Coatable

Ion Gel Films" by K. H. Lee, S. Zhang, T. P. Lodge, and C. D. Frisbie, *Journal of Physical Chemistry B*, **2011**, *115*, 3315.

In Chapter 5, transfer printing is utilized to employ ion gels on thin-film transistors. Using this method, ion gels with different shapes (hexagon, square, and triangle) are patterned successfully. Contact angle and rheological measurements are carried out to understand the physical origin of the ion gel transfer. Organic thin film transistors are fabricated by transferring all active layers (semiconductor, ion gel, and gate electrode). The results have been prepared for submission as "Thermally Assisted Transfer Printing of Ion Gels for Thin-Film Transistors" by K. H. Lee, S. Zhang, Y. Gu, T. P. Lodge, and C. D. Frisbie.

In Chapter 6, a mechanically free-standing ion gel that can be cut by a razor blade and laminated with tweezers is demonstrated. Using this free-standing ion gel, both p-type (hole transport) and n-type (electron transport) thin-film transistors are fabricated. The ion gel layer is transferred and laminated onto a device using tweezers, which is possible because of the gel's high mechanical strength (~1 MPa). This work has been published as "Cut and Stick Rubbery Ion Gels as High Capacitance Gate Dielectrics" by K. H. Lee, M. S. Kang, S. Zhang, Y, Gu, T. P. Lodge, and C. D. Frisbie, *Advanced Materials*, **2012**, *24*, 4457.

Chapter 7 summarizes this thesis project and describes future research opportunities using ion gels.

1.2 References

1. Armand, M.; Endres, F.; MacFarlane, D. R.; Ohno, H.; Scrosati, B., *Nat. Mater.* **2009**, *8*, 621.
2. Kazarian, S. G.; Briscoe, B. J.; Welton, T., *Chem. Commun.* **2000**, 2047.
3. Huddleston, J. G.; Visser, A. E.; Reichert, W. M.; Willauer, H. D.; Broker, G. A.; Rogers, R. D., *Green Chem.* **2001**, *3*, 156.
4. Galinski, M.; Lewandowski, A.; Stepniak, I., *Electrochim. Acta* **2006**, *51*, 5567.
5. Susan, M. A. B. H.; Kaneko, T.; Noda, A.; Watanabe, M., *J. Am. Chem. Soc.* **2005**, *127*, 4976.
6. Lee, J.; Panzer, M. J.; He, Y.; Lodge, T. P.; Frisbie, C. D., *J. Am. Chem. Soc.* **2007**, *129*, 4532.
7. Cho, J. H.; Lee, J.; Xia, Y.; Kim, B.; He, Y.; Renn, M. J.; Lodge, T. P.; Frisbie, C. D., *Nat. Mater.* **2008**, *7*, 900.
8. Cho, J. H.; Lee, J.; He, Y.; Kim, B. S.; Lodge, T. P.; Frisbie, C. D., *Adv. Mater.* **2008**, *20*, 686.
9. Lee, K. H.; Kang, M. S.; Zhang, S. P.; Gu, Y. Y.; Lodge, T. P.; Frisbie, C. D., *Adv. Mater.* **2012**, *24*, 4457.
10. Kelley, T. W.; Baude, P. F.; Gerlach, C.; Ender, D. E.; Muyres, D.; Haase, M. A.; Vogel, D. E.; Theiss, S. D., *Chemistry of Materials* **2004**, *16*, 4413.
11. Ha, M.; Xia, Y.; Green, A. A.; Zhang, W.; Renn, M. J.; Kim, C. H.; Hersam, M. C.; Frisbie, C. D., *ACS Nano* **2010**, 4388.

12. Gary, F. M., Solid polymer electrolytes: fundamentals and technological applications. Wiley-VCH: New York, 1991.

13. Panzer, M. J.; Frisbie, C. D., *J. Am. Chem. Soc.* **2007**, *129*, 6599.

Chapter 2

Background

2.1 Overview

This chapter discusses basic concepts and material properties that motivate this thesis project. As mentioned in the introduction, this project investigates ionic-liquid based polymer electrolytes (ion gels) as gate insulators in thin-films transistors. The following chapter begins with a brief introduction to a transistor and its operating mechanisms (Section 2.2), and then reviews ionic liquids and their electrical properties (electrochemical stability, ionic conductivity, and capacitance) that are critical for electrochemical applications (Section 2.3). As a way of preventing outflow of ionic liquids, gelled-polymer electrolytes are discussed in Section 2.4.

2.2 Operation mechanisms of a transistor

As shown in Figure 2.1, a field-effect transistor consists of three contact electrodes (the source, drain, and gate), a dielectric, and a semiconductor. A dielectric acts as a capacitor to accumulate charge carriers in a semiconductor by the applied gate bias, V_G. The potential difference between source and drain electrodes, V_D, provides the driving force for carrier conduction through a semiconductor. The resulting drain current I_D in the semiconductor channel is given by the following equation in the linear regime ($V_D << V_G$):

$$I_{\mathrm{D,lin}} = \frac{W}{L}\mu C(V_{\mathrm{G}} - V_{\mathrm{TH}})V_{\mathrm{D}} \qquad (2.1)$$

where μ is the carrier mobility, C is the capacitance of the dielectric layer, W is the width of the channel, L is the length is the channel, and V_{TH} is the threshold voltage at which V_{G} starts to induce mobile carriers in a semiconductor channel. In this regime, $I_{\mathrm{D,\,lin}}$ depends linearly on V_{G} in the I_{D}–V_{G} curve (transfer curve), as expected. I_{D} at the saturation regime ($V_{\mathrm{D}} > V_{\mathrm{G}}$) can be obtained by substituting the onset $V_{\mathrm{D}} = V_{\mathrm{G}}–V_{\mathrm{TH}}$ in Equation 2.1.

$$I_{\mathrm{D,sat}} = \frac{W}{L}\mu C(V_{\mathrm{G}} - V_{\mathrm{TH}})^2 \qquad (2.2)$$

The saturation regime can be recognized by a linear dependence of $I_{\mathrm{D}}^{1/2}$ on V_{G}, as can be seen from Equation 2.2. This regime is more obvious in an I_{D}–V_{D} plot (output curve), as I_{D} remains unchanged above the saturation V_{D}. I_{D} saturation arises because the effective channel length shrinks with V_{D}. The respective current–voltage characteristics (output and transfer curves) of a transistor are displayed in Figure 2.2.[1]

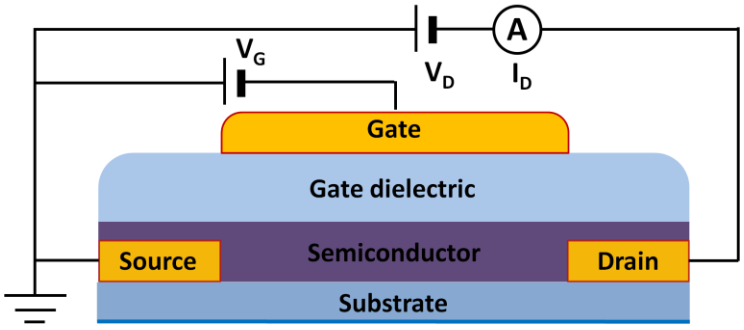

Figure 2.1 Cross-sectional schematic of a top gate, bottom contact transistor.

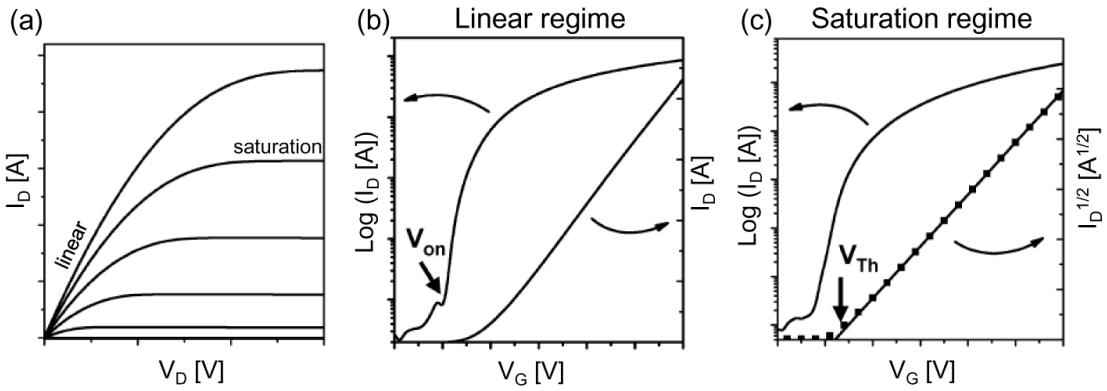

Figure 2.2 Respective current−voltage characteristics of a transistor: a) I_D−V_D curve (output curve) b) I_D−V_G curve (transfer curve) in the linear regime ($V_D << V_G$) and c) I_D−V_G curve in the saturation regime ($V_D > V_G$). Redrawn from ref. 1.

An important factor for transistor operation is the supply voltage of the device. High C is desirable for gate dielectrics because it allows the same number of charge carriers, therefore the same transistor current, with smaller input voltages (V_G and V_D). In other words, low-voltage transistor operation that can be powered by thin-film or conventional AA batteries is possible with high C dielectrics. Several methods for increasing dielectric capacitance have been demonstrated, such as decreasing the dielectric layer thickness using ultrathin films including self-assembled mono- or multilayers, and finding novel organic and inorganic materials with high dielectric constant ($C' = \varepsilon\varepsilon_o/l$, where ε is the dielectric constant, ε_o is the vacuum permittivity and l is the thickness of the dielectric).[2-8]

Recently, it has been shown that traditional dielectrics can be replaced with electrolytes, especially with ionic liquids, because of their capability to form nanometer-thick dielectric layers and their moderately high dielectric constants (ca. ~10), which results in the huge capacitance on the order of 1~10 μF/cm^2.[9] In practical experiments,

solidified electrolytes are often used to prevent the outflow of the liquid electrolytes. For example, to provide mechanical integrity block copolymers are blended with ionic liquids to achieve polymer networks. The resulting soft solid is referred to as an ion gel. More details about the ionic liquids and ion gels will be discussed in the following sections. By using ion gels as gate insulators, thin-film transistors exhibit low operating voltage (< 2 V), large ON current (~1 mA) and high switching speed (~1 kHz).

Note that the idea of using electrolytes in a transistor was first realized in 1947 to amplify a small signal by controlling the electron transport in Si, Ge, and Se semiconductors at Bell Laboratories.[10,11] However, the advantages of electrolytes in electronic devices were somewhat forgotten until Wrighton and others employed liquid electrolytes to modulate the conductivity of polymer semiconductors such as polyaniline, polyacetylene, polythiophene, and polypyrrole in the 1980s.[12-16] Over the past decade, electrolyte-gating has attracted renewed attention in a wide variety of research projects, spanning from fundamental charge transport to practical applications including flexible electronics and biosensors.

Figure 2.3 schematically shows the operation mechanisms of a transistor using an ionically conducting, but electronically insulating, electrolyte as a gate dielectric. Strictly speaking, an electrolyte is not a dielectric because it conducts ionic current.[17] However, electrolyte materials do not conduct holes/electrons and have large capacitances that enable them to work as gate dielectrics in transistor application. In an electrified gate electrode, mobile ions in electrolytes pack to compensate the electric charges on the gate, while accumulating counterions at the semiconductor/electrolyte interface. Through this

polarization process, charge carriers (holes or electrons) are induced in a semiconductor channel from the source contact to neutralize the ionic charges in the electrolyte. The balanced layers of ions and the countercharges are referred to as electrical double layers. The characteristic feature of the double layer depends on the porosity of the materials contacted by the electrolytes.

In case of ion impermeable semiconductors (left, Figure 2.3a) such as organic single crystals and inorganic compounds, the applied gate potential results in the formation of two electrical double layers at the gate/electrolyte and electrolyte/semiconductor interfaces, while leaving a charge neutral regime in between.[18-22] This system can be simply modeled as ultrathin (~1 nm) capacitors connected by a bulk resistor. The specific capacitance of each double layer can be estimated by the Helmholtz equation: $C \sim \varepsilon\varepsilon_o/\lambda$, where ε_o is the vacuum permittivity, and λ is the Debye screening length or the thickness of the double layer. With the λ on the order of 1 nm large C values above 1 $\mu F/cm^2$ are easily attainable in electrolytes, which are orders of magnitude larger than the Cs obtained from conventional dielectrics such as SiO_2.[23,24] If the Cs of two interfaces are equal ($C_1 = C_2 = C$), the total capacitance is one half of the capacitance of each layer: $C_{total} = (C_1^{-1} + C_2^{-1})^{-1} = C/2$. Because the charge carrier density of a semiconductor electrode is much smaller than that of a metallic gate electrode, in most cases C at the semiconductor/electrolyte interface is much smaller than that at the gate electrode/electrolyte interface, thereby dominating C_{total}.[25]

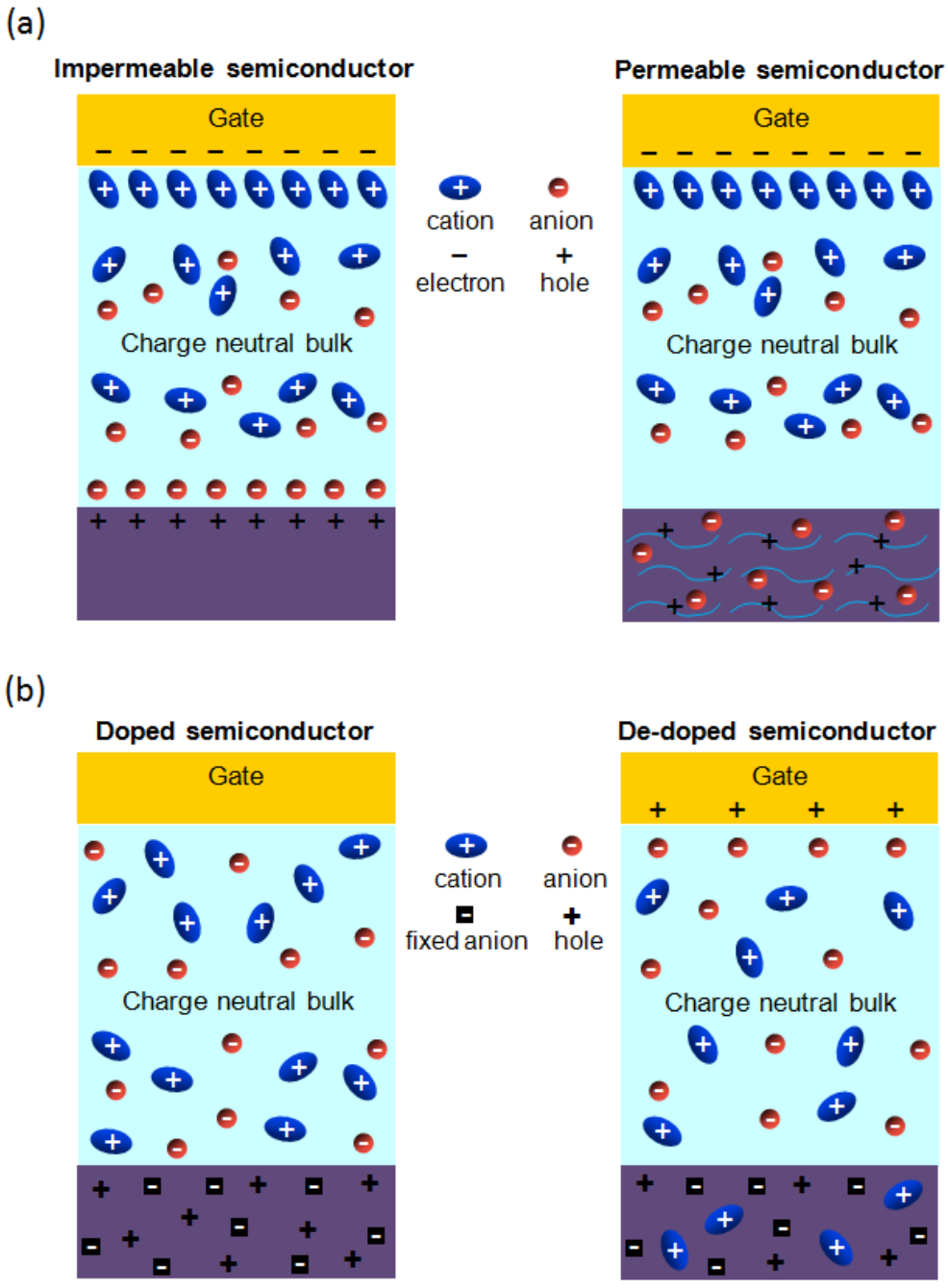

Figure 2.3 a) Carrier accumulation-mode operation of an electrolyte-gated transistor for un-doped ion-impermeable (left) and permeable semiconductors (right) and b) the depletion-mode operation for degenerately doped semiconductors without (left) and with (right) a gate voltage.

The cartoon on the right in Figure 2.3a shows a scheme when a porous semiconductor that is permeable to ions is in contact with the electrolyte. Upon application of a gate voltage an electrical double layer can be formed at the gate/electrolyte interface. However, ions in the semiconductor side can migrate into the film (electrochemical doping) and accumulate countercharges in the semiconductor channel.[26] As a result, a 3D conduction channel is formed in the entire semiconductor film, which leads to a huge transistor current. The transistors operate by the reversible electrochemical doping and de-doping of ions upon application and removal of a gate bias, respectively. Through these processes n-type semiconductors accumulate electrons by electrochemical reduction, whereas p-type semiconductors induce hole carriers by the oxidation.

Figure 2.3a illustrates the transistor operation in accumulation mode because electrons or holes are induced into semiconductors from the source upon application of gate potential. Depletion-mode operation is also possible in electrolyte-gated transistors, as depicted in Figure 2.3b. In the case of using highly doped p-type semiconductors (*e.g.* PEDOT:PSS), application of positive gate bias leads to cation migration into the film and de-dopes hole carriers in the semiconductor, which results in a decrease of channel current. This mode of operation has generated significant interest in the area of chemical- and bio-sensing because a small chemical- or bio-signal at the gate electrode can be amplified in the drain current, thereby lowering the detection limit of the sensors.[27]

In addition to low-voltage operation, another key factor to consider in electrolyte-gated transistors is the device switching time or frequency between ON and OFF states.

Generally, the transistor switching time (τ) is determined by the so-called cut-off time that depends on carrier mobility (μ) and specific operating conditions (channel length (L) and applied source-drain voltage (V_D)); $\tau \approx L^2/\mu V_D$.[28,29] In electrolyte-gated transistors, however, the polarization rate or double layer formation time of the component ions is also important because it can be slow, thereby limiting the working frequency of the devices.

The figure of merit describing the polarization rate of ions is the *RC* time constant, which is the product of the electrolyte resistance (R) and the double layer capacitance (C). A small *RC* time constant is desirable for device operation because it means that component ions in the electrolyte can react rapidly to an input signal. In terms of intrinsic parameters of an electrolyte $RC = C'l/\sigma$, where σ is the ionic conductivity and l is the electrolyte thickness. For common electrolytes σ is $10^{-5} \sim 10^{-2}$ S/cm and C' is ~10 μF/cm^2.[30-34] With a film thickness l of 1 μm the polarization rate can be as small as 0.1 μs. This implies that one can potentially operate an electrochemical device based on electrolytes as rapidly as 10 MHz. However, the operating speed of a transistor gated with an ionic-liquid based gel electrolyte is usually slower, at ~1 kHz. To further increase the operating speed (*i.e.* small *RC* time constant) the electrolyte σ needs to be large. Once the electrolyte material is determined, the *RC* constant can be further engineered by reducing the electrolyte thickness and any parasitic capacitance. Systematic efforts to achieve a small *RC* time constant will be discussed in Chapter 4. Recently, the Frisbie group realized a transistor circuit that operates near 100 kHz by optimizing device configurations.[35]

By using electrolytes as gate insulators low-voltage and moderately high frequency operations are achieved. However, electrolyte-gated transistors generally suffer from relatively larger gate-source/drain leak currents than other oxide and polymer insulators. The large leak current consumes power and ultimately reduces the life time of a power supply. The ratio between electrical energy dissipated to the energy stored in the system can be quantified by the dissipation factor or loss tangent (tan δ)

$$\tan\delta = \frac{Z'}{Z''} \tag{2.3}$$

where Z' and Z'' are the real and imaginary parts of the electrical impedance, respectively, and ($\pi/2 - \delta$) is the phase angle between the input voltage and resulting current.[36] Assuming the gate/electrolyte/semiconductor stack as a resistor and capacitor linked in series, tan δ can be expressed as

$$\tan\delta = \frac{R}{1/(\omega C)} = \omega RC \tag{2.4}$$

Therefore, a smaller RC time constant is not only desirable for fast operating speed of a transistor as discussed previously, but also reduces the energy dissipated by the leak current. At low frequency, tan δ values for electrolytes are typically ~10−15%. At high frequency tan δ becomes huge, indicating a transition to a purely lossy response. Table 1 summarizes the specific capacitances, dissipation factors, and leak currents for oxides, polymers and electrolytes used as dielectrics in transistors. Both values of the dissipation factor and the DC leakage current of electrolytes are larger than those values of polymers and oxides. However, it is also obvious that the specific capacitances of electrolytes are orders of magnitude larger. Thus the decision whether or not to employ an electrolyte as a

gate insulator for a specific application will depend on which figures of merit in Table 1 are most critical to the application.[37]

Table 2.1 Summary of the dielectric properties (C': specific capacitance, l: thickness, ε: dielectric constant, tan δ: dissipation factor, and I_{leak}) for various dielectric materials.

Dielectric		ref	C' ($\mu F/cm^2$)	l (nm)	ε	tan δ	I_{leak} (A/cm^2)
Oxides	HfO_2	38		54	18	0.2 (1 MHz)	2×10^{-9}
		39		190	11.16		7×10^{-9}
		40		20	11		
	TiO_2	41	0.23		40−140	0.02−0.03 (1 kHz)	
		42	0.373	97	41		5×10^{-9}
		43	2.42	7−8	21		1×10^{-10}
	Al_2O_3	41	0.031		8.5	0.005 (1 kHz)	
		44	0.65-0.7	6.5	9-11		
		45		270	7		2×10^{-8} [a]
	SiO_2	41	0.035		3.9	0.001 (1 kHz)	
		46		2	3.9		1×10^{-5}
Polymers	PMMA	47			3.0	0.055 (1 kHz)	
		48	0.0051	560	3.2		3×10^{-8} [a]
	PS	41	0.002		2.6	0.002 (1 kHz)	
		49		500−700	2.5		1×10^{-8} [a]
	PVA	50				0.005 (1 kHz)	
		51	0.0178	500	10		
Electrolytes	PEO/ $LiClO_4$	52	250	5×10^4– 5×10^5		0.16 (10 mHz)	1.5×10^{-6}
	Ionic liquid	19	5	400			1×10^{-6} [a]
		53	100 [c]	3×10^3			2.5×10^{-7} [a]
		54	17 [d]			0.18 [b] (1 Hz)	
		55				0.12 [b] (1 Hz)	
		56	5 [d]	2×10^4			2×10^{-6} [a]
		57	6 [d]	5×10^4			3×10^{-6} [a]
	Ion gel	58	12 [d]	2×10^3		0.09 (1 kHz)	
		59	11 [d]	1×10^4		0.11 (1 kHz)	1×10^{-5} [a]
		60	20 [d]	9×10^3			1×10^{-5} [a]
	P(VPA-AA)	61	10 [e]	54		0.23 (1 kHz)	5×10^{-4} [a]

a: leakage current density from off current and channel dimensions, b: tan ϕ from impedance data, c: capacitance from displacement current measurement, d: capacitance value at 1 Hz, e: capacitance value at 100 Hz. PMMA: poly(methyl methacrylate), PS: polystyrene, PEO: poly(ethylene oxide), PVA: polyvinyl alcohol, P(VPA-AA): poly(vinyl phosphonic acid-*co*-acrylic acid).

2.3 Ionic liquids

Ionic liquids (ILs), also known as room temperature molten salts, consist entirely of ions and have low melting temperatures typically below 100 °C.[62] Ionic liquids generally comprise bulky and asymmetric organic cations and either organic or inorganic anions. The asymmetry and size of component ions reduce the interaction between the cations and anions, which results in low melting temperatures.[63] Ionic liquids are known as 'designer solvents' because of their wide variety of combinations of cation-anion pairs.[64,65] Physicochemical properties such as density, viscosity, self-diffusion coefficient, and ionic conductivity of ionic liquids can be tailored by changing the component ions. There have been systematic studies of IL properties by changing component ions or alkyl chain length in cations.[66-72] Figure 2.4 shows some of common cations (1,3-dialkylimidazolium, *N*-alkylpyridinium, *N*,*N*-dialkylpyrrolidinium, and *N*,*N*,*N*,*N*-tetraalkylammonium) and anions (tetrafluoroborate [BF_4], hexafluorophosphate [PF_6], tris(pentafluoroethyl)trifluorophosphate, [FAP] and bis(trifluoromethylsulfonyl)amide [TFSA]).

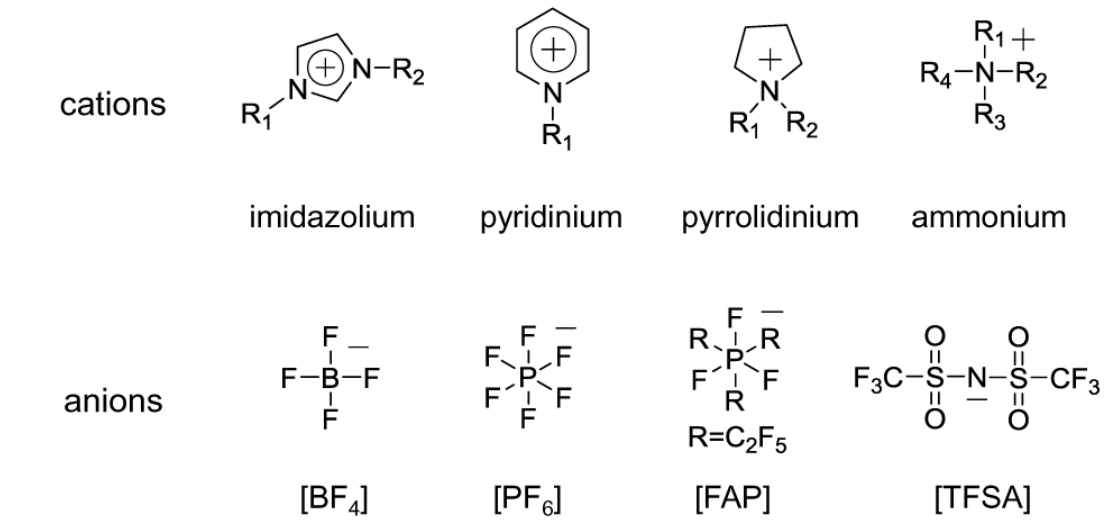

Figure 2.4 Chemical structures of common cations and anions in ionic liquids

Ionic liquids have attracted great interest due to their outstanding properties including high ionic conductivity and specific capacitance, wide electrochemical stability window, negligible vapor pressure, high thermal stability, and good solvation power.[33,34, 65,73-75] Some ionic liquids exhibit high ionic conductivity (~1 mS/cm) and capacitance (10 $\mu F/cm^2$) comparable to those of aqueous electrolytes. They have wide electrochemical stability windows (±3 V) which allow ionic liquids to be used as electrolytes in various applications. Ionic liquids are nonvolatile and nonflammable due to their extremely low vapor pressures (10^{-11}~10^{-10} mbar). They are thermally stable and have wide liquid ranges because of their high decomposition temperatures, typically above 300 °C. They are good solvents for both organic and inorganic molecules.

Such properties of ILs make them suitable candidates for electrochemical and electrical device applications including fuel cells,[76-78] solar cells,[79-82] electrical double

layer capacitors[83-85] and thin-film transistors.[9,57,86-88] Recently, ionic liquids in the form of a solid polymer electrolyte called an ion gel (a polymer network swollen with ionic liquid) have been shown to exhibit outstanding performance as gate insulators in organic thin film transistors.[9,57,87,88] Notably, the high capacitance of ionic liquids boosts the accumulation of charge carriers in the semiconductor channel and results in low transistor operating voltage (< 2 V) and high channel current (> 1 mA). The wide electrochemical windows of ionic liquids facilitate stable operation of the devices.

2.3.1 Physicochemical properties of ionic liquids

Fundamental properties including electrochemical stability, ionic conductivity and capacitance, which are critical to selecting appropriate ionic liquids for electrochemical applications including thin-film transistors, are discussed in this section.

Electrochemical stability window

For practical applications, candidate electrolytes need to be electrochemically stable within an applied potential range. Anodic and cathodic stability limits can be determined from the oxidation and reduction potentials of anions and cations by using cyclic voltammetry.[69,89-91] Therefore, the electrochemical stability of electrolytes can be calculated by subtracting the reduction potential from the oxidation potential. Ionic liquids generally exhibit wide stability windows, comparable to those of conventional organic electrolytes, in the range of 4−7 V.[33,69,89] However, this value far exceeds the electrochemical windows of common aqueous electrolytes.

For a given anion, the electrochemical stability of cations varies depending on the identity of the ions. In general, imidazolium salts are less stable than corresponding

tetraammonium and pyrrolidium salts.[69,89,92] This is because reduction takes place at the C_2−H bond in imidazolium cations due to its relatively high acidity.[93] For a given cation, ionic liquids with heavily fluorinated anions ([BF_4], [PF_6], [FAP], and [TFSA]) show relatively wide stability windows (4−7 V).[33,94-96] ILs with halide anions exhibit narrower windows (~2−4 V) because of their lower oxidation potentials.[33] Koch and colleagues demonstrated that oxidation potentials of anions decrease with increasing highest occupied molecular orbit (HOMO) energies.[97] This is because ions with high HOMO levels can easily donate electrons to other species.

The electrochemical stability of ionic liquids is sensitive to small amounts of impurities. One common impurity in ionic liquids is residual halide from the synthesis. These halide anions shrink the stability windows due to their lower oxidation potentials than those required for commonly used anions listed above.[33] Another prevalent impurity is water. When exposed to air, all ionic liquids can absorb atmospheric moisture to some extent, regardless of their miscibility with water.[95] A few wt% of water in ionic liquids decreases the electrochemical window of ionic liquids by over 2 V by narrowing both reduction and oxidation potentials.[98] This implies that special care is needed to prepare and handle ionic liquids.

Ionic conductivity

The ionic conductivity of ionic liquids is widely studied because it provides insight about ion transport. High ionic conductivity is desirable for fast operation of electrochemical devices, including double layer capacitors and thin-film transistors. High ionic conductivity is a generic property of ionic liquids because they are composed

entirely of ions with low melting temperatures.[62] Reported ionic conductivity values are typically calculated from a plateau resistance at high frequency ($\sigma = l/RA$, where l is the sample thickness and A is the area). Ionic conductivities of common ionic liquids are in the range of 0.1−20 mS/cm at room temperature.[33,99] Imidazolium-based liquids exhibit relatively high conductivities (~10 mS/cm) and are suitable for applications where rapid ion transport is important.[100] Ammonium salts have lower conductivities than the imidazolium family due to their higher melting tempeatures.[99]

The conductivity of ionic liquids is determined by the mobility and the number of free ions. For the same number of free ions, ionic liquids containing ions with high mobility exhibit higher ionic conductivity. The mobility of ions is strongly related to the viscosity of the system. The effect of viscosity is explained by combining the Nernst-Einstein and the Stokes-Einstein equations. The Nernst-Einstein equation correlates a molar conductivity (Λ) of electrolytes and the diffusion coefficient (D) through the following equation (2.5):

$$\Lambda = \frac{z^2 e^2 N_A D}{k_B T} \tag{2.5}$$

where z is the charge of a carrier, e is the elementary charge, N_A is Avogadro's number, and k_B is the Boltzmann constant. Assuming the frictional force follows Stokes' law, the Stokes-Einstein equation explain the relation between the diffusion coefficient and the viscosity (η) of a medium by

$$D = \frac{k_B T}{a\pi r\eta} \tag{2.6}$$

where r is the hydrodynamic radius and a is a constant. In the case of a large solute diffusing in a medium of a small solvent (*i.e.*, the solvent can be considered a continuum), a = 6 as in the normal Stokes-Einstein equation. However, if the size of solutes is comparable to that of solvents, especially for highly viscous solutions, a is reduced to 4, or even to 2.[101] Combining Equations 2.5 and 2.6 and converting the molar conductivity to the ionic conductivity (σ):

$$\sigma = \Lambda c = \Lambda n/V \tag{2.7}$$

where c is the concentration, n is the moles of charge carriers, and V is the volume of the system results in a equation which relates the viscosity and the number of charge carriers (N) to σ.

$$\sigma = \frac{z^2 e^2}{a\pi r V}\frac{N}{\eta} \tag{2.8}$$

Experimentally, the effect of viscosity on ionic conductivity is explained by the Walden product, which is the product of viscosity and molar conductivity.[102] Walden products remain nearly the same for commonly used ionic liquids ($\eta\Lambda = constant$) as shown in Figure 2.5.[103] This result emphasizes that ionic liquids with low viscosity generally exhibit high ionic conductivity.

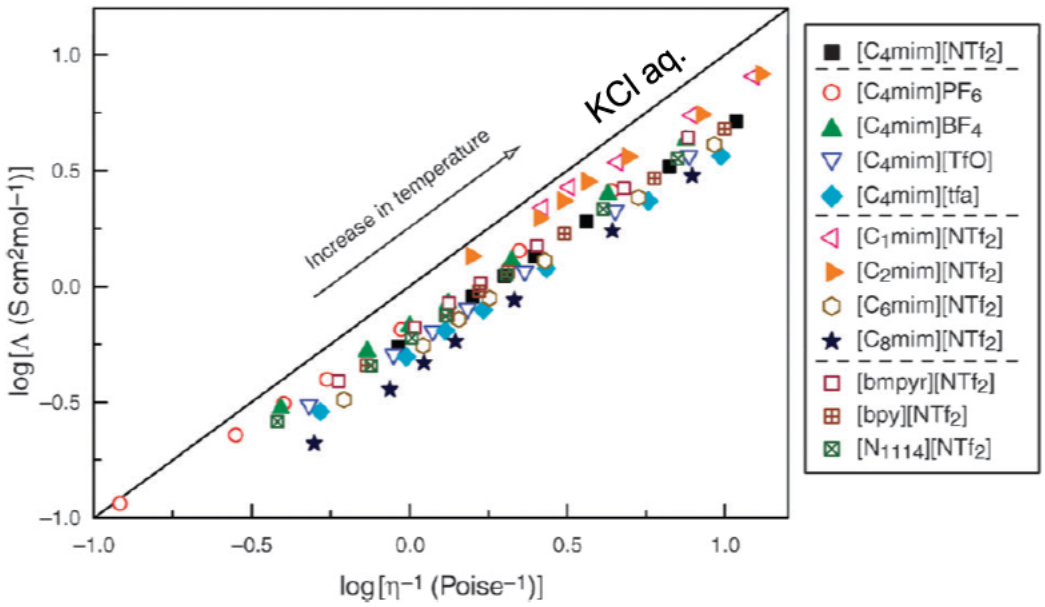

Figure 2.5 Walden plot for typical ionic liquids. The Walden product can be calculated from the slope of the plot. The solid line indicates the ideal Walden line for a fully dissociated KCl aqueous electrolyte. Regenerated from ref. 103

A question that arises at this point is why the Walden rule and Stokes−Einstein relation developed for dilute solutions are applicable to highly concentrated ionic liquids. A model in which ion transport is governed by holes or free volume (notional particle formed by absence of ions) at dilute concentration might provide an explantion.[104,105] Ions in ionic liquids are not closely packed, allowing voids at low concentration. In this case an ion can move only if a hole exists adjacent to the ion and ion motion is depicted as the migration of a hole in the opposite direction. The void volume argument also explains the temperature dependence of ionic-liquid conductivity, which will be discussed shortly. Figure 2.6 shows a schematic of hole transport that explains the ion conduction in ionic liquids.

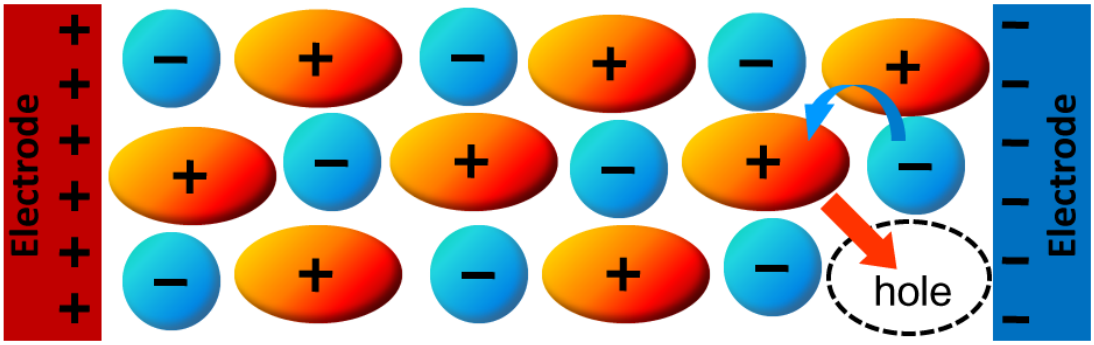

Figure 2.6 Schematic of ion transport in ionic liquids. Ion migration is governed by suitably sized holes in which ions can move.[105]

The ionic conductivity of ionic liquids increases with increasing temperature, following the Vogel-Fulcher-Tamman (VFT) equation:

$$\sigma = \sigma_o exp\left(\frac{-B}{T - T_o}\right) \quad (2.9)$$

where σ_o (S/cm) is the pre-exponential factor, B (K) is the constant related to the entropic barrier to find suitable voids for ion conduction, and T_o(K) is the Vogel temperature. The Vogel temperature is also known as ideal glass transition temperature, which is related to the glass transition temperature and the free volume change upon temperature variation. T_o is usually ~50 °C lower than that of the glass transition temperature (T_g) measured by differential scanning calorimetry (DSC).[106]

For ions with the same mobility, it is clear that ionic liquids with a large number of free ions display high ionic conductivity. The number of free ions in the liquid is determined by interactions between cations and anions, including Coulombic and hydrogen-bonding interactions.[107-110] Once cations and anions form stable aggregates or ion pairs, they can be regarded as neutral species and therefore the number of free ions is decreased, which results in lowering the ionic conductivity. Watanabe and coworkers

suggested a way to calculate the number of free ions in ionic liquids:[66-68,111] the fraction of free ions can be determined by the ratio between conductivity values measured from impedance spectroscopy and those from the Nernst-Einstein equation using ionic self diffusion coefficients measured by pulse-field-gradient spin–echo (PGSE) NMR spectroscopy. While the ionic conductivity from the impedance measurement does not include contribution of neutral ion pairs, the Nernst-Einstein approximation takes into account the contributions from all species in the electrolyte. Through this method, free-ion fractions of ~50−70% were reported for common ionic liquids.[103]

Electrical double layer capacitance

Because we are interested in using ionic liquids as gate insulators in transistor applications, high capacitance of ionic liquids is critical for low voltage operation of the device. In this section, charge storage at an electrode/electrolyte interface will be discussed. When an electrode is immersed in an electrolyte, ions in the electrolyte pack adjacent to the electrode to balance the countercharge on the electrode. This balanced layer of ions and countercharge is called an electrical double layer (EDL). The EDL in ionic liquids is expected to be somewhat different from that of common electrolytes containing non-ionic molecular solvents. This is because ions in ionic liquids directly contact the electrode surface due to their solvent-free nature. In this regard, the properties of the electrode material such as crystallographic orientation and electron density influence the structure of the EDL and the value of the capacitance of ionic liquids.[112]

The Helmholtz relation is the simplest model that can be applied to estimate double layer capacitance (C_{dl}) of an ionic liquid,

$$C_{\mathrm{dl}} = \frac{\varepsilon \varepsilon_{\mathrm{o}}}{\lambda} \tag{2.10}$$

where ε is the relative permittivity, ε_{o} is the permittivity of free space, 8.854×10^{-12} F/m, and λ is the thickness of EDL over which the potential drop occurs. Assuming a value of ε about 10 and λ of 1 nm (typical values for ionic liquids), the Helmholtz model predicts a capacitance ~10 μF/cm^2, a value comparable to reported literature values, in the range of 10~40 μF/cm^2.[9,112-114] Nanjundiah *et al*. measured C_{dl} of 7−15 μF/cm^2 for [EMI] cation with various anions at the potential of zero charge (PZC) using a dropping mercury electrode.[115] The Baldelli group reported C_{dl} values of 10−19 μF/cm^2 for [BMI] cation with four different anions [BF_4], [PF_6], [$N(CN)_2$], and [TFSA] at PZC using a Pt electrode.[116,117]

Reported capacitance values are typically measured at a constant frequency where the capacitive contribution is dominant (typically in a low frequency region).[118-120] In this method, capacitance decreases with increasing frequency, which is known as capacitance dispersion.[121-123] This phenomenon has been attributed to the specific adsorption of ions on the electrodes and the roughness of the electrode surface, and is typical for electrolytes in contact with solid electrodes. It has been suggested that electrode roughness broadens the time distribution of the adsorption process and results in increased capacitance dispersion.[121,124] To address this issue and obtain a frequency independent capacitance, an equivalent circuit using a constant phase element (CPE) can be used to analyze impedance data.[125]

2.4 Ion gels

From an application standpoint, it is desirable to retain the outstanding properties of ionic liquids discussed above in a solid film. This can be achieved by adding a three-dimensional network that percolates ionic liquids, which results in a solid-like electrolyte referred to as an ion gel (or ionogel). Ion gels can be divided into physical and chemical gels, depending on the nature of the network. Physical gels utilize weak interactions including hydrogen bonding, solvent-phobic interactions and crystal junctions to form a network,[126-132] whereas chemical gels are connected by covalent bonding.[133-138] Although inorganic materials such as silica, titania, and carbon nanotubes can form a 3D network with ionic liquids,[139-147] the following section mainly focuses on ion gels containing polymer networks that are directly relevant to the thesis project.

2.4.1 Conventional polymer electrolytes

It is worthwhile to discuss conventional polymer electrolytes that incorporate inorganic salts before moving onto ion gels. They are extensively studied and widely used in electrochemical applications, due to their processability into flexible and thin films over large area.[31] These electrolytes typically exhibit large EDL capacitance (~10 $\mu F/cm^2$) similar to other electrolyte systems. However, conductivity values of the electrolytes are usually lower (in the range of $10^{-6} \sim 10^{-4}$ S/cm at room temperature) than those of other electrolytes, including aqueous electrolytes and ionic liquids.[31]

Conventional polymer electrolytes are also known as salt-in-polymer electrolytes because they are prepared by combining high temperature molten salts and polymers.[148, 149] Most of the work on these electrolytes focus on poly(ethylene oxide) (PEO) and its

derivatives as host polymers, due to their low T_g values (T_g ~ –60 °C) and favorable solubilization. Lithium salts are commonly used in these types of solid electrolytes. The ionic conductivity of these materials displays a maximum with increasing salt concentration because there are two competing processes that occur simultaneously; increasing the salt concentration increases the number of mobile charges but also decreases polymer chain mobility. Polar groups, typically oxygen atoms, in the polymer chain interact with the salts to form cation-polymer complexes, thereby creating mobile free ions that increase conductivity of the system. However, polymer chain mobility decreases (equivalently, the T_g increases) because more than one polymer chain can couple with one cation, effectively creating a transient crosslink. Low ion mobility by elevated T_g offsets the effect by increased free ion density with ion concentration, which explains the maximum conductivity at relatively low salt concentrations. Extensive studies including organic and inorganic additives and host-polymer modification have been conducted for conventional electrolytes to enhance the conductivity.[31,150-155] However, ionic conductivity of these materials still remains at ~10^{-4} S/cm at room temperature, which results in low transistor operating speeds, ~1 Hz.[156]

2.4.2 Polymer electrolytes using ionic liquid (Ion gels)

To overcome the low ionic conductivities associated with inorganic salts and to improve the device speed, ionic liquids have been used. Both chemically and physically crosslinked polymer networks can be utilized to prepare solid electrolytes using ionic liquids. Chemically crosslinked ion gels or chemical gels can be realized by polymerizing vinyl monomers in ionic liquids[133,134] or by crosslinking (macro)monomers with

multifunctional cross-links.[136,137] To make chemical gels, host polymers need to be compatible with the ionic liquid. *In situ* radical polymerization of methyl methacrylate (MMA) or 2-hydroxyethyl methacrylate (HEMA) with a small amount of cross-linker (ethylene glycol dimethacrylate) in imidazolium and pyridinium-based ionic liquids yields transparent chemical gels.[133,134] Other chemical gels were demonstrated by the cross-linking disuccinimidylpropyl poly(ethylene oxide) (SPA-PEG) and tetraamine PEG,[136] or by curing a mixture of bisphenol A diglycidyl ether and tetrafuntional epoxy resin with tetraethylenepentamine in ionic liquids.[137] Polyurethane resins can be used to prepare chemical gels with ionic liquids.[157] These chemical gels show higher ionic conductivity, on the order of 10^{-3} S/cm, than that of conventional polymer electrolytes. However, once the chemical gels are formed, their structures are irreversible due to the nature of covalent bonds.

Physical crosslinking provides an alternative way to prepare ion gels that can reversibly change their states with external stimulus such as pH or temperature. Among various kinds of physical gels, a block copolymer ion gel is a versatile candidate because the gel structures and properties can be tailored by varying the block length, identity and sequence. For example, an ABA triblock copolymer with ionic-liquid insoluble A end blocks and a soluble B middle block can form a soft gel in ionic liquids. Here, the microphase-separated A blocks act as cross-linkers bridged by soluble B blocks, as shown in Figure 2.7.[131] Lodge and others reported the first ion gel utilizing a triblock copolymer, poly(styrene-*b*-ethylene oxide-*b*-styrene) (SOS) in [BMI][PF_6].[158] In this ion gel, physical gelation can be achieved by adding SOS at concentrations as low as 4 wt%

in [BMI][PF_6]. This low polymer weight fraction leads to a high ionic conductivity, comparable to that of a pure ionic liquid (~10 mS/cm). Using these highly conductive ion gels, the Frisbie group demonstrated a transistor circuit with a ~10 μs response time.

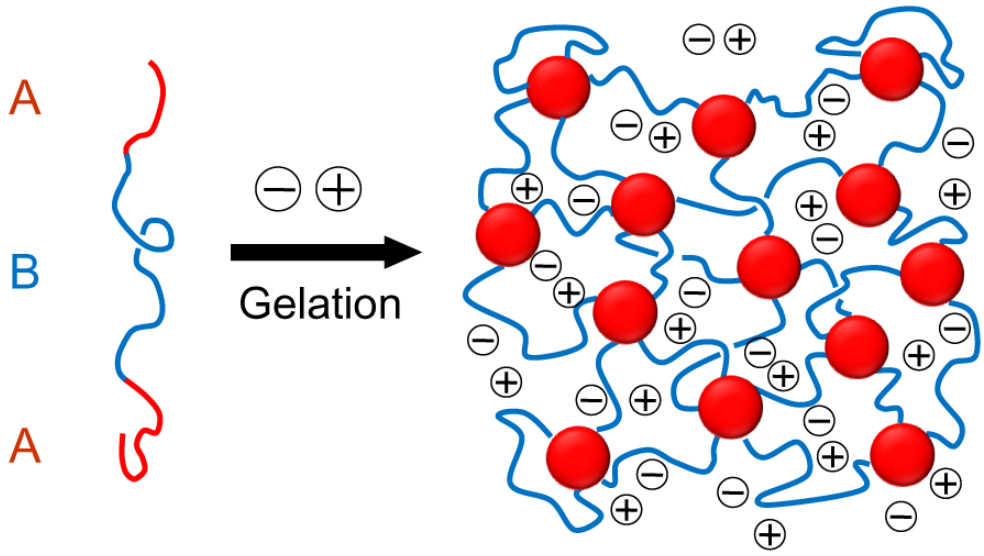

Figure 2.7 Ion gel formed by self assembly of an ABA tribolck copolymer with insoluble A blocks and soluble B block in an ionic liquid. + and – symbols correspond to cation and anion, respectively.

By modifying the A blocks in triblock polymers, thermoreversible ion gels that respond to temperature variation can be achieved. A thermoresponsive gel is particularly advantageous in material processing because the material can be deposited in the liquid state and used in the solid state. SOS gels with short PS end blocks (M_{PS}<4000) can melt at high temperatures due to low enthalpic barriers for pulling PS chains out from the network cores, forming a congested micelle solution with PS cores and PEO coronas.[159, 160] In the case of combining SOS with M_{PS} = 3000 and M_{PEO} = 35000 in [EMI][TFSA], a

gelation temperature (T_{gel}) at ~60 °C was measured.[159] For this ion gel, the measured T_{gel} or longest relaxation time ($\tau_{1,\,gel}$) was independent of polymer concentration.

Another thermoreversible ion gel can be prepared through upper critical solution temperature (UCST) or lower critical solution temperature (UCST) type phase separation of block polymers. An ion gel with UCST type gelation exhibits solid-like characteristics at low temperatures and becomes a liquid at temperature higher than T_{gel}. He *et al*. reported a thermoreversible ion gel with poly(N-isopropyl acrylamide-*b*-ethylene oxide-*b*-N-isopropyl acrylamide) (NON) triblock copolymer in [EMI][TFSA], using the UCST behavior of a poly(N-isopropyl acrylamide) block.[160,161] However, NON gel is a liquid at room temperature because of its low T_{gel} of ~17 °C. In order to increase T_{gel} above room temperature for practical applications, insoluble PS blocks are incorporated to obtain NSOSN pentablock polymers. The resulting T_{gel} of the NSOSN gel was increased from 17 °C to ~50 °C by using PS blocks with M_{PS} = 3800. The thermoresponsive SOS and NSOSN gels were applied to transfer print the gel layers on thin-film transistors, and the results will be discussed in Chapter 5.

In case of LCST type gelation, ion gels show liquid like properties at temperature lower than T_{gel} and become solid at high temperatures. Watanabe and others reported a thermoreversible ion gel with poly(benzyl methacrylate-*b*-methyl methacrylate-*b*-benzyl methacrylate) (BMB) triblock copolymer in [EMI][TFSA], using the LCST behavior of a poly(benzyl methacrylate) block.[130] The ion gel with 20 wt% BMB in [EMI][TFSA] shows T_{gel} of 100 °C. Another thermoreversible ion gel using ABA triblock copolymers that are fully soluble in ionic liquid with C homopolymers, where A and C form strong

hydrogen bonds has also been reported.[127-129] Ion gels with poly(2-vinyl pyridine) as hydrogen bonding accepting A blocks, poly(vinyl phenol) as hydrogen bond donating C and PEO middle block show tunable melting temperatures in the range of 110 ~ 160 °C depending on the number of hydrogen bonds.[129]

2.5 References

1. Zaumseil, J.; Sirringhaus, H., *Chem. Rev.* **2007**, *107*, 1296.
2. Halik, M.; Klauk, H.; Zschieschang, U.; Schmid, G.; Dehm, C.; Schutz, M.; Maisch, S.; Effenberger, F.; Brunnbauer, M.; Stellacci, F., *Nature* **2004**, *431*, 963.
3. DiBenedetto, S. A.; Frattarelli, D.; Ratner, M. A.; Facchetti, A.; Marks, T. J., *J. Am. Chem. Soc.* **2008**, *130*, 7528.
4. DiBenedetto, S. A.; Frattarelli, D. L.; Facchetti, A.; Ratner, M. A.; Marks, T. J., *J. Am. Chem. Soc.* **2009**, *131*, 11080.
5. Yoon, M.-H.; Yan, H.; Facchetti, A.; Marks, T. J., *J. Am. Chem. Soc.* **2005**, *127*, 10388.
6. Tate, J.; Rogers, J. A.; Jones, C. D. W.; Vyas, B.; Murphy, D. W.; Li, W.; Bao, Z.; Slusher, R. E.; Dodabalapur, A.; Katz, H. E., *Langmuir* **2000**, *16*, 6054.
7. Yu, X. J.; Xu, J. B.; Cheung, W. Y.; Ke, N., *J. Appl. Phys.* **2007**, *102*, 103711.
8. Naber, R. C. G.; Tanase, C.; Blom, P. W. M.; Gelinck, G. H.; Marsman, A. W.; Touwslager, F. J.; Setayesh, S.; de Leeuw, D. M., *Nat. Mater.* **2005**, *4*, 243.
9. Lee, J.; Panzer, M. J.; He, Y.; Lodge, T. P.; Frisbie, C. D., *J. Am. Chem. Soc.* **2007**, *129*, 4532.
10. Brattain, W. H.; Gibney, R. B. *US patent 2,524,034*, **1948**.

11. Brattain, W. H.; Garrett, C. G. B., *Bell. Telephone Syst. Tech. Publ. Monogr.* **1955**, *2372*, 1.

12. White, H. S.; Kittlesen, G. P.; Wrighton, M. S., *J. Am. Chem. Soc.* **1984**, *106*, 5375.

13. Chao, S.; Wrighton, M. S., *J. Am. Chem. Soc.* **1987**, *109*, 2197.

14. Chao, S.; Wrighton, M. S., *J. Am. Chem. Soc.* **1987**, *109*, 6627.

15. Ofer, D.; Crooks, R. M.; Wrighton, M. S., *J. Am. Chem. Soc.* **1990**, *112*, 7869.

16. Ofer, D.; Park, L. Y.; Schrock, R. R.; Wrighton, M. S., *Chem. Mater.* **1991**, *3*, 573.

17. Wilk, G. D.; Wallace, R. M.; Anthony, J. M., *J. Appl. Phys.* **2001**, *89*, 5243.

18. Panzer, M. J.; Frisbie, C. D., *Adv. Mater.* **2008**, *20*, 3177.

19. Panzer, M. J.; Newman, C. R.; Frisbie, C. D., *Appl. Phys. Lett.* **2005**, *86*, 103503.

20. Takeya, J.; Yamada, K.; Hara, K.; Shigeto, K.; Tsukagoshi, K.; Ikehata, S.; Aoyagi, Y., *Appl. Phys. Lett.* **2006**, *88*, 112102.

21. Dhoot, A. S.; Israel, C.; Moya, X.; Mathur, N. D.; Friend, R. H., *Phys. Rev. Lett.* **2009**, *102*, 136402.

22. Ye, J. T.; Inoue, S.; Kobayashi, K.; Kasahara, Y.; Yuan, H. T.; Shimotani, H.; Iwasa, Y., *Nat. Mater.* **2009**, *9*, 125.

23. Min, Y.; Akbulut, M.; Sangoro, J. R.; Kremer, F.; Prud'homme, R. K.; Israelachvili, J., *J. Phys. Chem. C* **2009**, *113*, 16445.

24. Fedorov, M. V.; Kornyshev, A. A., *Electrochim. Acta* **2008**, *53*, 6835.

25. Memming, R., *Semiconductor electrochemistry*. Wiley-VCH: Weinheim ; New York, 2001.

26. Lee, J.; Kaake, L. G.; Cho, J. H.; Zhu, X. Y.; Lodge, T. P.; Frisbie, C. D., *J. Phys. Chem. C* **2009**, *113*, 8972.

27. Owens, R. M.; Malliaras, G. G., *MRS Bull.* **2010**, *35*, 449.

28. Herlogsson, L.; Noh, Y.-Y.; Zhao, N.; Crispin, X.; Sirringhaus, H.; Berggren, M., *Adv. Mater.* **2008**, *20*, 4708.

29. Klauk, H., *Chem. Soc. Rev.* **2010**, *39*, 2643.

30. MacCallum, J. R.; VIncent, C. A., *Polymer electrolyte Review 1 and 2*. Elsevier: New York, 1987, 1989.

31. Gary, F. M., *Solid polymer electrolytes: fundamentals and technological applications*. Wiley-VCH: New York, 1991.

32. Bard, A. J.; Faulkner, L. R., *Electrochemical Methods: Fundamentals and Applications*. Wiley: New York, 2001.

33. Galinski, M.; Lewandowski, A.; Stepniak, I., *Electrochim. Acta* **2006**, *51*, 5567.

34. Hapiot, P.; Lagrost, C., *Chem. Rev.* **2008**, *108*, 2238.

35. Ha, M.; Frisbie, C. D., *Manuscript in preparation*.

36. Daniel, V. V., *Dielectric Relaxation* Academic Press: London and New York 1965.

37. Sarjeant, W. J.; Zirnheld, J.; MacDougall, F. W., *IEEE Trans. Plasma Sci.* **1998**, *26*, 1368.

38. Hu, H.; Zhu, C.; Lu, Y. F.; Wu, Y. H.; Liew, T.; Li, M. F.; Cho, B. J.; Choi, W. K.; Yakovlev, N., *J. Appl. Phys.* **2003**, *94*, 551.

39. Wei, C.-Y.; F., A.; Lin, Y.-J.; Li, Y.-C.; Huang, T.-J.; Chou, D.-W.; Wang, Y.-H., *IEEE Electron Device Lett.* **2009**, *30*, 1039.

40. Tardy, J. E., M.; Deman, A. L.; Gagnaire, A.; Teodorescu, V.; Blanchin, M. G.; Canut, B.; Barau, A.; Zaharescu, M. , *Microelectron. Reliab.* **2007**, *47*, 372.

41. Jackson, N. F., *Phys. Educ.* **1968**, *3*, 253.

42. Wang, G.; Moses, D.; Heeger, A. J.; Zhang, H.-M.; Narasimhan, M.; Demaray, R. E., *J. Appl. Phys.* **2004**, *95*, 316.

43. Majewski, L. A.; Schroeder, R.; Grell, M., *Adv. Mater.* **2005**, *17*, 192.

44. Majewski, L. A.; Schroeder, R.; Grell, M., *J. Phys. D: Appl. Phys.* **2004**, *37*, 21.

45. Lee, J.; Kim, J. H.; Im, S., *Appl. Phys. Lett.* **2003**, *83*, 2689.

46. Muller, D. A.; Sorsch, T.; Moccio, S.; Baumann, F. H.; Evans-Lutterodt, K.; Timp, G., *Nature* **1999**, *399*, 758.

47. Brandrup, J.; Immergut, E. H.; Grulke, E. A., *Polymer Handbook* Wiley-Interscience: New York, 1999; Vol. 4th ed.

48. Cheng, J.-A.; Chuang, C.-S.; Chang, M.-N.; Tsai, Y.-C.; Shieh, H.-P. D., *Org. Electron.* **2008**, *9*, 1069.

49. Yan, H.; Chen, Z.; Zheng, Y.; Newman, C.; Quinn, J. R.; Dotz, F.; Kastler, M.; Facchetti, A., *Nature* **2009**, *457*, 679.

50. Singh, K. P.; Gupta, P. N., *Eur. Polym. J.* **1998**, *34*, 1023.

51. Parashkov, R.; Becker, E.; Ginev, G.; Riedl, T.; Johannes, H.-H.; Kowalsky, W., *J. Appl. Phys.* **2004**, *95*, 1594.

52. Liu, X.; Osaka, T., *J. Electrochem. Soc.* **1996**, *143*, 3982.

53. Panzer, M. J.; Frisbie, C. D., *Adv. Funct. Mater.* **2006**, *16*, 1051.

54. Lockett, V.; Sedev, R.; Ralston, J.; Horne, M.; Rodopoulos, T., *J. Phys. Chem. C* **2008**, *112*, 7486.

55. Zhao, F.; Wu, X.; Wang, M.; Liu, Y.; Gao, L.; Dong, S., *Anal. Chem.* **2004**, *76*, 4960.

56. Uemura, T.; Yamagishi, M.; Ono, S.; Takeya, J., *Appl. Phys. Lett.* **2009**, *95*, 103301.

57. Ono, S.; Seki, S.; Hirahara, R.; Tominari, Y.; Takeya, J., *Appl. Phys. Lett.* **2008**, *92*, 103313.

58. Lee, K. H.; Zhang, S. P.; Lodge, T. P.; Frisbie, C. D., *J. Phys. Chem. B* **2011**, *115*, 3315.

59. Lee, K. H.; Kang, M. S.; Zhang, S.; Gu, Y.; Lodge, T. P.; Frisbie, C. D., *Adv. Mater.* **2012**, *24*, 4457.

60. Cho, J. H.; Lee, J.; Xia, Y.; Kim, B.; He, Y.; Renn, M. J.; Lodge, T. P.; Frisbie, C. D., *Nat. Mater.* **2008**, *7*, 900.

61. Herlogsson, L.; Crispin, X.; Robinson, N. D.; Sandberg, M.; Hagel, O. J.; Gustafsson, G.; Berggren, M., *Adv. Mater.* **2007**, *19*, 97.

62. MacFarlane, D. R.; Seddon, K. R., *Aust. J. Chem.* **2007**, *60*, 3.

63. Welton, T., *Chem. Rev.* **1999**, *99*, 2071.

64. Freemantle, M., *Chem. Eng. News* **1998**, *76*, 32.

65. Abedin, S. Z. E.; Endres, F., *Acc. Chem. Res.* **2007**, *40*, 1106.

66. Tokuda, H.; Ishii, K.; Susan, M. A. B. H.; Tsuzuki, S.; Hayamizu, K.; Watanabe, M., *J. Phys. Chem. B* **2006**, *110*, 2833.

67. Tokuda, H.; Hayamizu, K.; Ishii, K.; Susan, M. A. B. H.; Watanabe, M., *J. Phys. Chem. B* **2005**, *109*, 6103.

68. Tokuda, H.; Hayamizu, K.; Ishii, K.; Susan, M. A. B. H.; Watanabe, M., *J. Phys. Chem. B* **2004**, *108*, 16593.

69. Sun, J.; Forsyth, M.; MacFarlane, D. R., *J. Phys. Chem. B* **1998**, *102*, 8858.

70. Every, H. A.; Bishop, A. G.; MacFarlane, D. R.; Oradd, G.; Forsyth, M., *Phys. Chem. Chem. Phys.* **2004**, *6*, 1758.

71. Zech, O.; Stoppa, A.; Buchner, R.; Kunz, W., *J. Chem. Eng. Data* **2010**, *55*, 1774.

72. Stoppa, A.; Zech, O.; Kunz, W.; Buchner, R., *J. Chem. Eng. Data* **2009**, *55*, 1768.

73. Kazarian, S. G.; Briscoe, B. J.; Welton, T., *Chem. Commun.* **2000**, 2047.

74. Huddleston, J. G.; Visser, A. E.; Reichert, W. M.; Willauer, H. D.; Broker, G. A.; Rogers, R. D., *Green Chem.* **2001**, *3*, 156.

75. Reichardt, C., *Org. Process Res. Dev.* **2007**, *11*, 105.

76. de Souza, R. F.; Padilha, J. C.; Gonçalves, R. S.; Dupont, J., *Electrochem. Commun.* **2003**, *5*, 728.

77. Nakamoto, H.; Noda, A.; Hayamizu, K.; Hayashi, S.; Hamaguchi, H.; Watanabe, M., *J. Phys. Chem. C* **2007**, *111*, 1541.

78. Noda, A.; Susan, M. A. B. H.; Kudo, K.; Mitsushima, S.; Hayamizu, K.; Watanabe, M., *J. Phys. Chem. B* **2003**, *107*, 4024.

79. Papageorgiou, N.; Athanassov, Y.; Armand, M.; Bonhote, P.; Pettersson, H.; Azam, A.; Grätzel, M., *J. Electrochem. Soc.* **1996**, *143*, 3099.

80. Kawano, R.; Watanabe, M., *Chem. Commun.* **2003**, 330.

81. Wang, P.; Zakeeruddin, S. M.; Moser, J.; Grätzel, M., *J. Phys. Chem. B* **2003**, *107*, 13280.

82. Kawano, R.; Kubo, W.; Masaki, N.; Kitamura, T.; Wada, Y.; Watanabe, M.; Yanagida, S., *J. Phys. Chem. B* **2007**, *111*, 4763.

83. Balducci, A.; Bardi, U.; Caporali, S.; Mastragostino, M.; Soavi, F., *Electrochem. Commun.* **2004**, *6*, 566.

84. Ue, M.; Takeda, M.; Takahashi, T.; Takehara, M., *Electrochem. Solid-State Lett.* **2002**, *5*, A119.

85. McEwen, A. B.; Ngo, H. L.; LeCompte, K.; Goldman, J. L., *J. Electrochem. Soc.* **1999**, *146*, 1687.

86. Thiemann, S.; Sachnov, S.; Porscha, S.; Wasserscheid, P.; Zaumseil, J., *J. Phys. Chem. C* **2012**, *116*, 13536.

87. Yuan, H.; Shimotani, H.; Tsukazaki, A.; Ohtomo, A.; Kawasaki, M.; Iwasa, Y., *Adv. Funct. Mater.* **2009**, *19*, 1046.

88. Cho, J. H.; Lee, J.; He, Y.; Kim, B. S.; Lodge, T. P.; Frisbie, C. D., *Adv. Mater.* **2008**, *20*, 686.

89. Bonhote, P.; Dias, A.-P.; Papageorgiou, N.; Kalyanasundaram, K.; Gratzel, M., *Inorg. Chem.* **1996**, *35*, 1168.

90. Suarez, P. A. Z.; Selbach, V. i. M.; Dullius, J. E. L.; Einloft, S.; Piatnicki, C. M. S.; Azambuja, D. S.; de Souza, R. F.; Dupont, J., *Electrochim. Acta* **1997**, *42*, 2533.

91. Dzyuba, S. V.; Bartsch, R. A., *ChemPhysChem.* **2002**, *3*, 161.

92. MacFarlane, D. R.; Meakin, P.; Sun, J.; Amini, N.; Forsyth, M., *J. Phys. Chem. B* **1999**, *103*, 4164.

93. Suarez, P. A. Z.; Consorti, C. S.; Souza, R. F. d.; Dupont, J.; Gonçalves, R. S., *J. Braz. Chem. Soc.* **2002**, *13*, 106.

94. Howlett, P. C.; Izgorodina, E. I.; Forsyth, M.; MacFarlane, D. R., *Z. Phys. Chem.* **2006**, *220*, 1483.

95. Buzzeo, M. C.; Hardacre, C.; Compton, R. G., *ChemPhysChem.* **2006**, *7*, 176.

96. Ignat'ev, N. V.; Welz-Biermann, U.; Kucheryna, A.; Bissky, G.; Willner, H., *J. Fluorine Chem.* **2005**, *126*, 1150.

97. Koch, V. R.; Dominey, L. A.; Nanjundiah, C.; Ondrechen, M. J., *J. Electrochem. Soc.* **1996**, *143*, 798.

98. Schroder, U.; Wadhawan, J. D.; Compton, R. G.; Marken, F.; Suarez, P. A. Z.; Consorti, C. S.; Souza, R. F. d.; Dupont, J., *New J. Chem.* **2000**, *24*, 1009.

99. McFarlane, D. R.; Sun, J.; Golding, J.; Meakin, P.; Forsyth, M., *Electrochim. Acta* **2000**, *45*, 1271.

100. Every, H.; Bishop, A. G.; Forsyth, M.; MacFarlane, D. R., *Electrochim. Acta* **2000**, *45*, 1279.

101. Cussler, E. L., *Diffusion: Mass Transfer in Fluid Systems*. Cambridge University Press: New York, 1997.

102. Walden, P., *Bull. Acad. Imp. Sci. St Petersbourg* **1914**, *8*, 405.

103. Ueno, K.; Tokuda, H.; Watanabe, M., *Phys. Chem. Chem. Phys.* **2010**, *12*, 1649.

104. Abbott, A. P., *ChemPhysChem* **2004**, *5*, 1242.

105. Abbott, A. P., *ChemPhysChem.* **2005**, *6*, 2502.

106. Hiemenz, P. C.; Lodge, T. P., *Polymer Chemistry*. CRC Press: New York, 2007.

107. Turner, E. A.; Pye, C. C.; Singer, R. D., *J. Phys. Chem. A* **2003**, *107*, 2277.

108. Tsuzuki, S.; Tokuda, H.; Hayamizu, K.; Watanabe, M., *J. Phys. Chem. B* **2005**, *109*, 16474.

109. Hyk, W.; Caban, K.; Donten, M.; Stojek, Z., *J. Phys. Chem. B* **2001**, *105*, 6943.

110. Katoh, R.; Hara, M.; Tsuzuki, S., *J. Phys. Chem. B* **2008**, *112*, 15426.

111. Noda, A.; Hayamizu, K.; Watanabe, M., *J. Phys. Chem. B* **2001**, *105*, 4603.

112. Islam, M. M.; Alam, M. T.; Ohsaka, T., *J. Phys. Chem. C* **2008**, *112*, 16568.

113. Ohno, H., *Electrochemical aspects of ionic liquids*. Wiley: Hoboken, New Jersey, 2005.

114. Islam, M. M.; Alam, M. T.; Okajima, T.; Ohsaka, T., *J. Phys. Chem. C* **2009**, *113*, 3386.

115. Nanjundiah, C.; McDevitt, S. F.; Koch, V. R., *J. Electrochem. Soc.* **1997**, *144*, 3392.

116. Baldelli, S., *J. Phys. Chem. B* **2005**, *109*, 13049.

117. Baldelli, S., *Acc. Chem. Res.* **2008**, *41*, 421.

118. Alam, M. T.; Islam, M. M.; Okajima, T.; Ohsaka, T., *J. Phys. Chem. C* **2007**, *111*, 18326.

119. Lockett, V.; Sedev, R.; Ralston, J.; Horne, M.; Rodopoulos, T., *J. Phys. Chem. C* **2008**, *112*, 7486.

120. Alam, M. T.; Islam, M. M.; Okajima, T.; Ohsaka, T., *J. Phys. Chem. C* **2008**, *112*, 16600.

121. Pajkossy, T., *J. Electroanal. Chem.* **1994**, *364*, 111.

122. Kerner, Z.; Pajkossy, T., *Electrochim. Acta* **2000**, *46*, 207.

123. Pajkossy, T., *Solid State Ionics* **2005**, *176*, 1997.

124. Pajkossy, T., *Solid State Ionics* **2005**, *176*, 1997.

125. Brug, G. J.; van den Eeden, A. L. G.; Sluyters-Rehbach, M.; Sluyters, J. H., *J. Electroanal. Chem.* **1984**, *176*, 275.

126. Noro, A.; Hayashi, M.; Matsushita, Y., *Soft Matter* **2012**, *8*, 6416.

127. Noro, A.; Matsushita, Y.; Lodge, T. P., *Macromolecules* **2008**, *41*, 5839.

128. Noro, A.; Matsushita, Y.; Lodge, T. P., *Macromolecules* **2009**, *42*, 5802.

129. Lei, Y.; Lodge, T. P., *Soft Matter* **2012**, *8*, 2110.

130. Kitazawa, Y.; Ueki, T.; Niitsuma, K.; Imaizumi, S.; Lodge, T. P.; Watanabe, M., *Soft Matter* **2012**, *8*, 8067.

131. Lodge, T. P., *Science* **2008**, *321*, 50.

132. Jansen, J. C.; Friess, K.; Clarizia, G.; Schauer, J.; Izak, P., *Macromolecules* **2011**, *44*, 39.

133. Noda, A.; Watanabe, M., *Electrochim. Acta* **2000**, *45*, 1265.

134. Susan, M. A. B. H.; Kaneko, T.; Noda, A.; Watanabe, M., *J. Am. Chem. Soc.* **2005**, *127*, 4976.

135. Lee, S. W.; Lee, H. J.; Choi, J. H.; Koh, W. G.; Myoung, J. M.; Hur, J. H.; Park, J. J.; Cho, J. H.; Jeong, U., *Nano Lett.* **2009**, *10*, 347.

136. Klingshirn, M. A.; Spear, S. K.; Subramanian, R.; Holbrey, J. D.; Huddleston, J. G.; Rogers, R. D., *Chem. Mater.* **2004**, *16*, 3091.

137. Matsumoto, K.; Endo, T., *Macromolecules* **2008**, *41*, 6981.

138. Jana, S.; Parthiban, A.; Chai, C. L. L., *Chem. Commun.* **2010**, *46*, 1488.

139. Shi, F.; Zhang, Q.; Li, D.; Deng, Y., *Chem. Eur. J.* **2005**, *11*, 5279.

140. Neouze, M.-A.; Bideau, J. L.; Leroux, F.; Vioux, A., *Chem. Commun.* **2005**, 1082.

141. Shi, F.; Deng, Y., *Spectrochim. Acta A* **2005**, *62*, 239.

142. Ueno, K.; Hata, K.; Katakabe, T.; Kondoh, M.; Watanabe, M., *J. Phys. Chem. B* **2008**, *112*, 9013.

143. Wang, P.; Zakeeruddin, S. M.; Exnar, I.; Gratzel, M., *Chem. Commun.* **2002**, 2972.

144. Wang, P.; Zakeeruddin, S. M.; Comte, P.; Exnar, I.; Gratzel, M., *J. Am. Chem. Soc.* **2003**, *125*, 1166.

145. Stathatos, E.; Lianos, P.; Zakeeruddin, S. M.; Liska, P.; Gratzel, M., *Chem. Mater.* **2003**, *15*, 1825.

146. Usui, H.; Matsui, H.; Tanabe, N.; Yanagida, S., *J.Photoch. Photobio. A* **2004**, *164*, 97.

147. Fukushima, T.; Kosaka, A.; Ishimura, Y.; Yamamoto, T.; Takigawa, T.; Ishii, N.; Aida, T., *Science* **2003**, *300*, 2072.

148. Vincent, C. A., *Prog. Solid State Chem.* **1987**, *17*, 145.

149. Ratner, M. A.; Shriver, D. F., *Chem. Rev.* **1988**, *88*, 109.

150. Kaskhedikar, N.; Burjanadze, M.; Karatas, Y.; Wiemhofer, H. D., *Solid State Ionics* **2006**, *177*, 3129.

151. Guilherme, L. A.; Borges, R. S.; Moraes, E. M. S.; Silva, G. G.; Pimenta, M. A.; Marletta, A.; Silva, R. A., *Electrochim. Acta* **2007**, *53*, 1503.

152. Uno, T.; Kawaguchi, S.; Kubo, M.; Itoh, T., *J. Power Sources* **2008**, *178*, 716.

153. Weston, J. E.; Steele, B. C. H., *Solid State Ionics* **1982**, *7*, 75.

154. Adebahr, J.; Best, A. S.; Byrne, N.; Jacobsson, P.; MacFarlane, D. R.; Forsyth, M., *Phys. Chem. Chem. Phys.* **2003**, *5*, 720.

155. Cheung, I. W.; Chin, K. B.; Greene, E. R.; Smart, M. C.; Abbrent, S.; Greenbaum, S. G.; Prakash, G. K. S.; Surampudi, S., *Electrochim. Acta* **2003**, *48*, 2149.

156. Panzer, M. J.; Frisbie, C. D., *J. Am. Chem. Soc.* **2007**, *129*, 6599.

157. Berns, B.; Deligöz, H.; Tieke, B.; Kremer, F., *Macromol. Mater. Eng.* **2008**, *293*, 409.

158. He, Y.; Boswell, P. G.; Buhlmann, P.; Lodge, T. P., *J. Phys. Chem. B* **2007**, *111*, 4645.

159. Zhang, S.; Lee, K. H.; Sun, J.; Frisbie, C. D.; Lodge, T. P., *Macromolecules* **2011**, *44*, 8981.

160. He, Y.; Lodge, T. P., *Macromolecules* **2008**, *41*, 167.

161. Ueki, T.; Watanabe, M., *Chem. Lett.* **2006**, *35*, 964.

Chapter 3

Experimental Section

3.1 Overview

This chapter outlines the materials and experimental techniques used in this thesis. The following sections describe general procedures for block copolymer synthesis and characterization, and experimental techniques to prepare and characterize polymer/ionic liquid composites (ion gels) and thin-film transistors. Specific experimental details, such as sample preparation and device fabrication, will also be described in the following chapters, where the experimental data using the techniques are presented.

3.2 Block polymer synthesis

This section describes the method used to synthesize the triblock copolymer poly(styrene-*b*-methyl methacrylate-*b*-styrene) (SMS), which imparts mechanical strength to an ion gel. In order to prepare polymers with narrow molecular weight distribution, atom transfer radical polymerization (ATRP), a type of controlled/living radical polymerization, was used.

The synthesis of SMS copolymer consists of two steps. First, a PMMA middle block that acts as a macroinitiator for the second step is created from a bifunctional initiator. By growing polystyrene at both ends of PMMA macroinitiators, SMS triblock copolymers are obtained. For the SMS synthesis, a difunctional initiator (diethyl meso-2-5-dibromoadipate), a ligand for methyl methacrylate (*N*,*N*,*N*´,*N*´,*N*´´-pentamethyldiethylenetriamine (PMDETA)), a ligand for styrene (4,4´-dinonyl-2-2´-

bipyridine (dNbpy)), a solvent (anisole), copper catalysts (CuBr and $CuBr_2$), methyl methacrylate (MMA), and styrene monomers were used.[1-3] Copper catalyst was stored in a nitrogen-filled glovebox to prevent water absorption. MMA and styrene monomers were passed through active alumina columns prior to use.

The following procedure was used to obtain ~30 g of SMS (13-65-13). Numbers in parenthesis represent the molecular weights of each polymer block (M_{PS} and M_{PMMA}) in kg/mol. To begin, copper catalysts, CuBr (56.57 mg) and $CuBr_2$ (8.83 mg), and the initiator (0.285 g) were dissolved in anisole (100 mL). Upon formation of a homogeneous solution, MMA monomer (100 mL) and PMDETA (105 μL) were added to a high-pressure glass reactor. In order to remove the oxygen from the reactants, a freeze-pump-thaw-degassing process was carried out at least four cycles. The solution was then heated to 60 °C under argon atmosphere for 6 hours to obtain PMMA. The polymerization was terminated by cooling the reactor in an ice bath. After termination, the solution was poured into methanol (3 L) to remove the copper catalyst. The product PMMA was precipitated in methanol. The PMMA precipitate was dissolved in ethyl acetate and then passed through a neutral alumina column. The solution was then precipitated in hexane. The resulting white polymer was filtered and dried under vacuum.

To synthesize styrene blocks, copper catalysts (CuBr (97 mol%) and $CuBr_2$ (3 mol%) mixture, 0.163 g), PMMA (25 g) obtained from the previous step, dNbpy (0.953 g), and styrene monomer (100 mL) were placed in a high-pressure glass reactor. At least four freeze-pump-thaw-degassing cycles were carried out to remove oxygen from the solution. The reactor was then immersed in an oil bath at 100 °C for 60 hours. The

reaction was stopped by cooling the reactor in an ice bath. The following purification steps were the same as in the PMMA synthesis, with an additional precipitation in cyclohexane to remove PS homopolymers. The product SMS polymer was then filtered and dried under vacuum. The synthetic procedures for SMS are outlined in Figure 3.1.

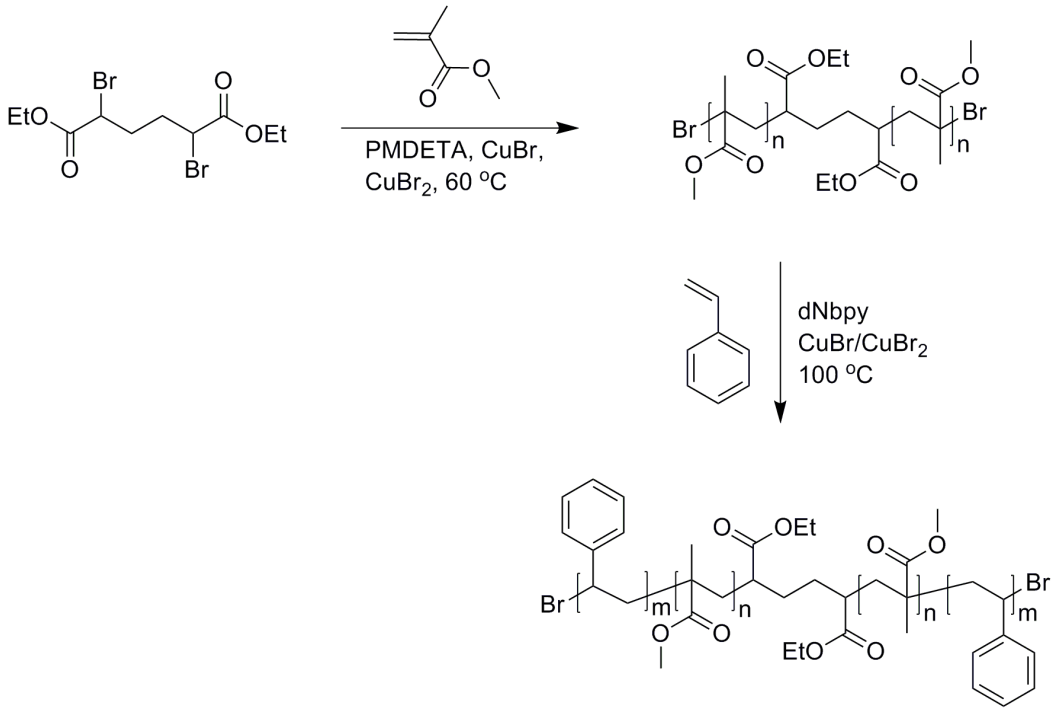

Figure 3.1 Synthetic procedures for SMS triblock copolymer.

The PMMA and SMS polymers were confirmed by ^{1}H NMR spectroscopy and size exclusion chromatography (SEC). Representative ^{1}H NMR and SEC results for PMMA(65) and SMS(13-65-13) are displayed in Figures 3.2 and 3.3, respectively. M_{PMMA} was determined by SEC, a Alltech 426 HPLC pump with refractive index (RI) and light scattering (LS) detectors. M_{PS}s in SMS were calculated from M_{PMMA}, the mole ratio between MMA and styrene, and molecular weights of monomers ($M_{styrene}$ and M_{MMA} are 104.15 and 100.12 g/mol, respectively). Both PS end blocks were assumed to be

symmetric in the estimation of M_{PS}s. The mole ratio between MMA and styrene in SMS was calculated from ^{1}H NMR by comparing the peak areas of the three methoxy protons (3.6 ppm) on the PMMA block to the five benzyl protons (6.5 and 7.1 ppm) on the PS blocks using the following equation.

$$\text{Mole ratio of styrene} = \frac{\frac{[\text{Area}(6.5) + \text{Area}(7.1)]}{5}}{\frac{[\text{Area}(6.5) + \text{Area}(7.1)]}{5} + \frac{\text{Area}(3.6)}{3}} \quad (3.1)$$

Polydispersity indices for PMMA(65) and SMS(13-65-13) were 1.3. This SMS polymer was used to study the electrical properties of ion gels, and the results will be discussed in Chapter 4.

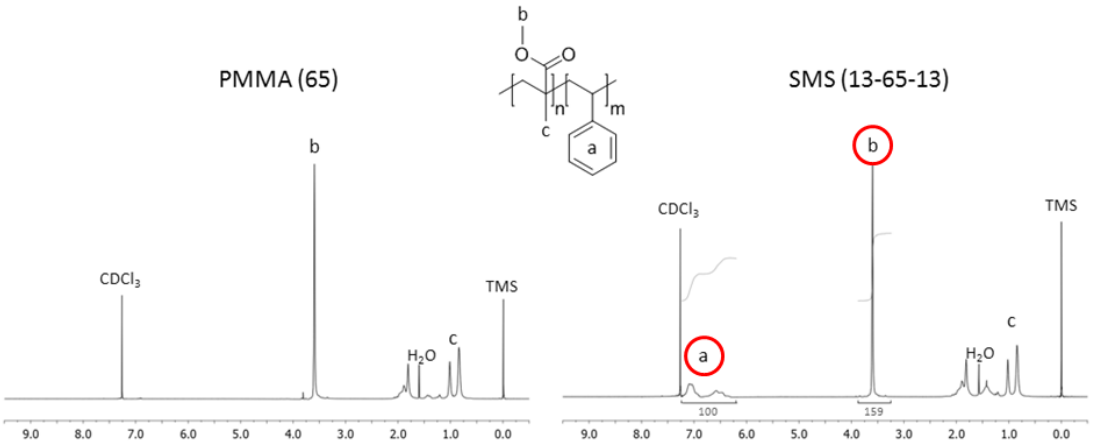

Figure 3.2 ^{1}H NMR spectra for PMMA(65) homopolymer and SMS(13-65-13) triblock copolymer.

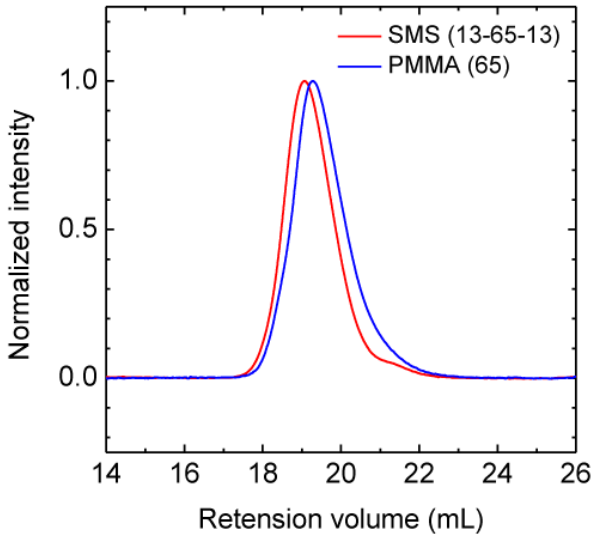

Figure 3.3 SEC traces for PMMA(65) homopolymer and SMS(13-65-13) triblock copolymer.

3.3 Rheology

Rheology was used to study the mechanical properties of polymer electrolytes. In rheological experiments, a sinusoidal strain (or stress) was applied and the resulting sinusoidal stress (or strain) was measured. The resulting behavior of a polymer sample was described by a complex dynamic modulus (G^*). This modulus consists of the storage modulus (G') and the loss modulus (G''), which corresponds to real and imaginary parts of G^*, respectively:

$$G^* = G' + iG'' \tag{3.2}$$

where i is the imaginary unit.

More specifically, rheological measurements can be applied to investigate the properties of ion gels such as the critical gelation concentration (C_{gel}) and temperature

(T_{gel}), network modulus, and terminal relaxation time ($\tau_{1,gel}$). The measurements were conducted on an ARES rheometer (Rheometric Scientific) using a parallel plate geometry. Depending on the gel modulus, 25 and 50 mm diameter plates were used. For frequency sweep tests, samples were thermally equilibrated for 20 min at each temperature and the gap between two plates was adjusted to compensate for the thermal expansion of the equipment. From the experiments, frequency-dependent dynamic moduli *G*' and *G*" were obtained at a given frequency range. To study the gelation of ion gels, low frequency response of *G*' and *G*" can be utilized. Below C_{gel}, the homogeneous polymer/ionic liquid solution can flow and show characteristics of a liquid: $G' \sim \omega$, $G'' \sim \omega^2$ and $G'' > G'$, as evidenced by the 1 wt% results in Figure 3.4.[4] When the solution is chemically or physically crosslinked to form a network, $G' > G''$ and *G*' becomes frequency independent, as shown by 10 wt% data.[4] When the transition from a viscous liquid to a network solid (*i.e.*, gelation) occurs, both *G*' and *G*" values become similar and show the same power law dependence, $G' \approx G'' \sim \omega^n$.[4]

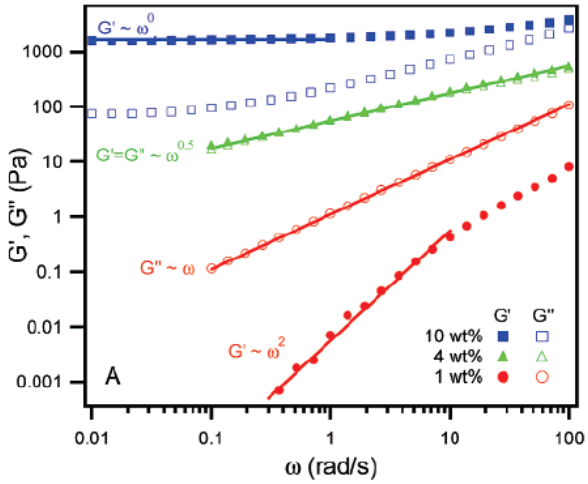

Figure 3.4 The storage (*G*') and loss (*G*'') moduli for a polymer solution consisting of poly(styrene-*b*-ethylene oxide-*b*-styrene) SOS and 1-butyl-3-methylimidazolium hexafluorophosphate [BMI][PF_6] with different concentrations. Redrawn from ref. 4.

The *G*' and *G*" measured from dynamic frequency sweep tests at different temperatures can be used to obtain a terminal relaxation time, $\tau_{1,gel}$, of thermoreversible ion gels. The loss tangents (tan δ) were horizontally shifted by time-temperature superposition (tTS) (Figure 3.5a) and the same shift factors were employed to *G*' and *G*'' to generate tTS master curves in Figure 3.6. At high frequency, both *G*' and *G*'' values are large, and *G*' > *G*'', indicating solid-like behavior. With decreasing frequency *G*' and *G*'' decrease, and *G*'' > *G*', indicating a liquid-like flow response. At the reference temperature of 120 °C, $\tau_{1,gel}$ of 0.4 s is determined from the crossover of *G*' and *G*''. The $\tau_{1,gel}$ values for different temperatures can be calculated by using the same shift factors shown in Figure 3.5b.

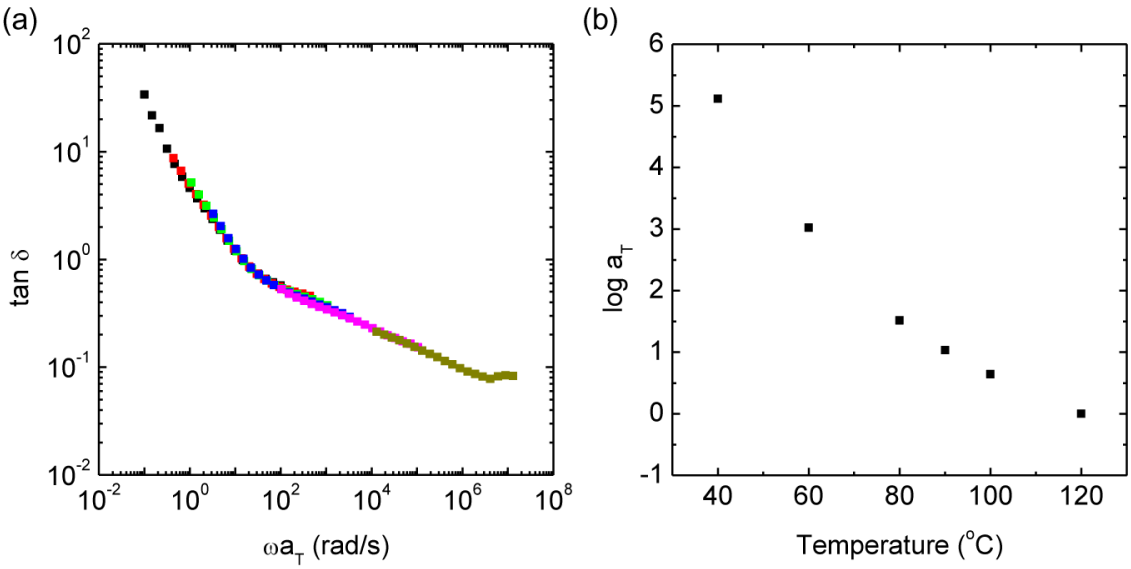

Figure 3.5 a) Horizontally shifted tan δ to obtain a master curve and b) temperature dependence of the shift factors used to superpose tan δ for an ion gel with 10 wt% SOS in 1-ethyl-3-methylimidazolium bis(trifluoromethylsulfonyl)amide [EMI][TFSA].

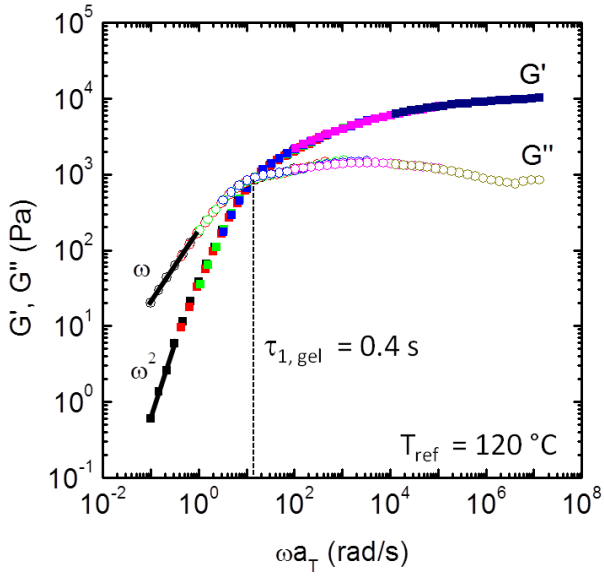

Figure 3.6 tTS master curves of *G*' and *G*" referenced to 120 °C for an ion gel with 10 wt% SOS in [EMI][TFSA].

The gelation temperature (T_{gel}) of ion gels can be measured by the crossover of *G*' and *G*" from the dynamic temperature ramp result as shown in Figure 3.7. At low temperatures the values of *G*' and *G*'' are high, and *G*' > *G*'', indicating solid-like behavior. With increasing temperature both *G*' and *G*'' decrease, and *G*'' > *G*', indicating a liquid-like response. The particular ion gel shown below has T_{gel} at ~17 °C.[5]

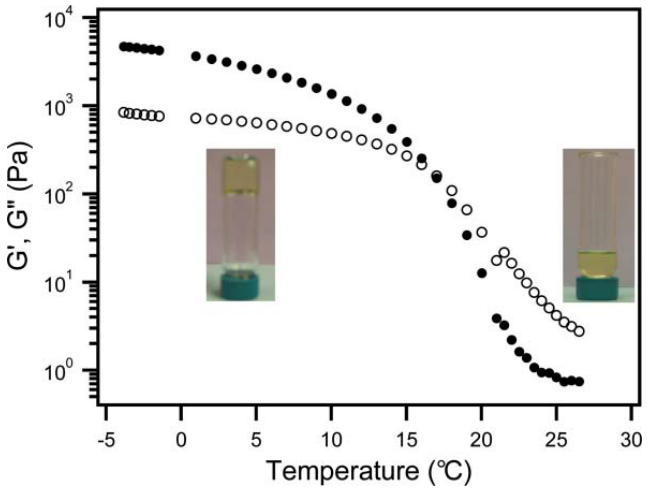

Figure 3.7 Temperature dependent dynamic shear moduli (*G*' and *G*'') for 10 wt% poly(N-isopropyl acrylamide-*b*-ethylene oxide-*b*-N-isopropyl acrylamide) (NON) in [EMI][TFSA]. Redrawn from ref. 5.

3.4 Impedance spectroscopy

Impedance spectroscopy was employed to characterize the electrical properties such as ionic conductivity and specific capacitance of ion gel films. In the measurements, a sinusoidal voltage was applied and the resulting sinusoidal current was measured. Impedance is the measure of the opposition of a sample to the current passage under the applied voltage. In this regard, impedance is a more general concept than resistance in the DC condition because it takes into account not only the magnitude but also the phase

difference. In order to express the magnitude and the phase difference together, impedance is represented as a complex quantity (Z^*)

$$Z^* = Z' + iZ'' \tag{3.3}$$

where i is the imaginary unit, and Z' and Z'' are the real and imaginary parts of the impedance, respectively. The impedance can be plotted in the complex plane with either rectangular or polar coordinates as shown in Figure 3.8.

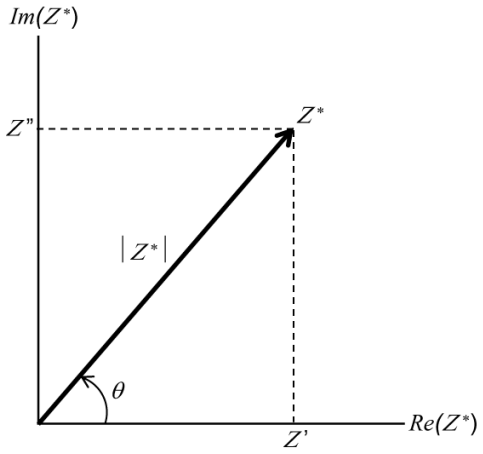

Figure 3.8 Complex impedance (Z) plane.

In the rectangular coordinates, impedance can be expressed as

$$Z' = |Z^*|\cos(\theta),\ Z'' = |Z^*|\sin(\theta) \tag{3.4}$$

with the magnitude

$$|Z^*| = [(Z')^2 + (Z'')^2]^{1/2} \tag{3.5}$$

and phase angle (θ).

$$\theta = \tan^{-1}(Z''/Z') \tag{3.6}$$

In this thesis project, all room temperature impedance experiments for ion gels were conducted on a Solartron 1255B frequency response analyzer with a SI 1287

electrochemical interface controlled by ZPlot and ZView software. Measurements were performed over the frequency range of 1 ~ 10^6 Hz with an AC amplitude of 10 mV; no DC voltage was applied. The variable temperature measurements were conducted under vacuum (~10^{-6} torr) in a Desert Cryogenics probe station (Lakeshore) with a HP-4192A LF impedance analyzer. Resistance and conductivity values were extracted from the plateau *Z*' results at high frequency, and the capacitance was calculated from *Z*" data using the following equations:

$$R = \frac{l}{\sigma A} + R_{lead} \tag{3.7}$$

$$C' = \frac{-1}{2\pi f \, Z'' A} \tag{3.8}$$

where l is the thickness of an ion gel, A is the area of the top contact, R_{lead} is the lead resistance, and f represents the frequency.

3.5 PDMS stamp fabrication

A poly(dimethylsiloxane) PDMS stamp was used to transfer-print ion gels and other polymer layers to fabricate thin-film transistors. A PDMS stamp was prepared by curing a mixture of PDMS precursor and curing agent (Sylgard 184, Dow Corning) in a ratio of 10:1 by weight on a pre-patterned master. The pre-patterned master was created by standard photolithography using SU-8 photoresist (MicroChem Corp.) in the Nanofabrication Center (NFC). A standard procedure used to prepare a 20 μm-thick PDMS stamp is listed below:

PDMS stamp fabrication (20 μm thick)

1. Prebake a 3'' or 4'' wafer 115 °C for 1 min.
2. Spin coat MicroChem SU8−2010 photoresist on a wafer at 1000 rpm for 30 s with acceleration of 100 rpm/s
3. Soft bake the spin-coated wafer at 65 °C for 1 min and 95 °C for 3 min.
4. Exposure the wafer for 12 s (140 mJ/cm^2, soft contact, gap 20 μm)
5. Post-exposure bake the wafer at 65 °C for 1 min and 95 °C for 5 min.
6. Develop the wafer using SU8 developer for 3 min 20 s.
7. Rinse the wafer with isopropyl alcohol (IPA) and dry it with house nitrogen.
8. Hard bake the wafer at 150 °C for more than 5 min.
9. Check the thickness of recessed regions using a P-16 surface profiler.
10. Mix PDMS prepolymer (Sylgard 184, Dow corning) and curing agent (10:1 wt %) more than 10 min.
11. Degas the mixture in a vacuum chamber more than 1 hr until there is no bubble.
12. Put the patterned face of the wafer up in a petri-dish and pour the PDMS mixture into the petri-dish.
13. Cure the PDMS at 60 °C for more than 6 hr.
14. Peel off PDMS from the wafer.

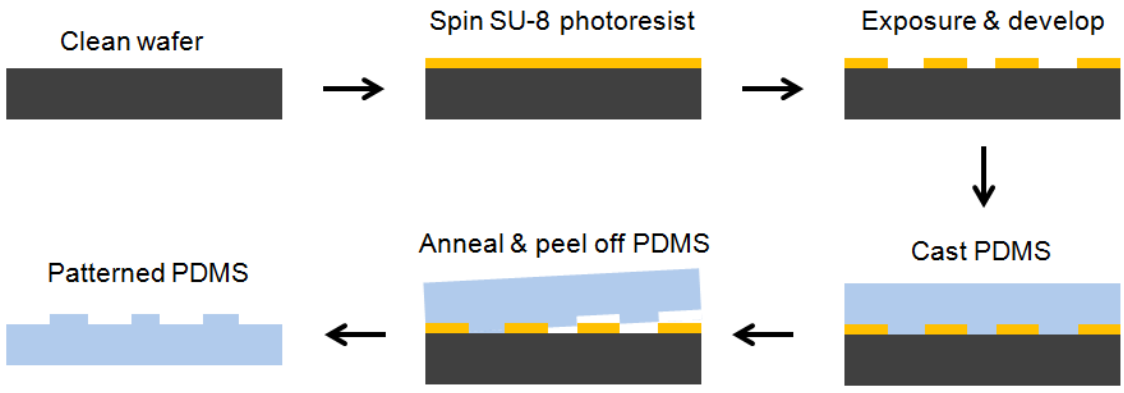

Figure 3.9 Schematic procedures to fabricate a patterned PDMS stamp.

3.6 P3HT transistor fabrication and characterization

Thin-film transistors were fabricated on a 300 nm thick SiO_2 or polyimide substrate in a bottom contact configuration. Metal source and drain electrodes were patterned on these substrates by thermal evaporation using a stainless stencil mask or by e-beam evaporation on lift-off channels created by photolithography. A lift-off process was applied for a batch production of source/drain electrodes on wafers and the process was conducted in NFC. A standard lift-off procedure is outlined below:

Source/drain electrode fabrication through a lift-off technique

1. Prebake a 4" wafer at 115 °C for 1 min.
2. Spin coat hexamethyldisilazane (HMDS) on a wafer at 3000 rpm for 30 s.
3. Spin coat Shipley S-1818 photoresist on the wafer at 3000 rpm for 30 s.
4. Soft bake the spin-coated wafer at 105 °C for 1 min.
5. Exposure the wafer for 10 s (120 mJ/cm^2, soft contact, gap 35 μm)
6. Develop the wafer using a water:351 developer = 5:1 mixture for 30 s.
7. Rinse the wafer with DI water and dry it with house nitrogen.
8. Evaporate 25 Å Cr/375 Å Au on the wafer using a CHA e-beam evaporator.
9. Soak the whole wafer in acetone overnight
10. Sonicate the wafer in acetone for 5 min and dry with nitrogen blowing

To fabricate a transistor, patterned substrates were sequentially sonicated in acetone, isopropyl alcohol, and methyl alcohol for 10 min, rinsed with methyl alcohol, and then dried with nitrogen gas prior to use. The semiconductor regioregular poly(3-hexylthiophene) (P3HT) was deposited by spin coating or by transfer printing from a PDMS stamp. An ion-gel layer was then prepared by simple lamination of a free-standing ion gel or by transfer printing. A gate PEDOT:PSS electrode was deposited by aerosol jet printing or by transfer printing on ion gels for top-gated organic thin-film transistors. All

electrical characterization of thin-film transistors was conducted in a Desert Cryogenic vacuum probe station (Lakeshore) at ~10^{-6} torr using Keithley 236, 237, and 6517a electrometers. Dynamic gate-displacement current measurements were performed with a Keithley 2612 electrometer. In the measurements, the source and drain electrodes were connected to ground and the gate potential was swept at different rates.

3.7 ZnO transistor fabrication

In addition to p-type (hole transport) transistors, an important objective in this thesis was to gate n-type (electron transport) semiconductors using ion gels. In this regard, an inorganic n-type ZnO was studied. Semiconductor ZnO thin films were created by spin coating a zinc hydroxide precursor followed by sintering at 300 °C for 10 min.[6] A standard procedure to create the precursor solution and ZnO film is listed below:

ZnO film preparation

1. Dissolve $Zn(NO_3)_2$▪6 H_2O (0.9807 g) in DI water (15 mL) to prepare 0.5 M Zn solution.
2. Add 10 mL of 2.5M NaOH (1 g of NaOH in 10 mL of DI water) in drop-wise for ~5 min while vigorously stirring the solution.
3. Centrifuge the mixture and remove supernatant liquid (upper part).
4. Suspend the precipitate in 20 mL of water and agitate for 2 min.
5. Repeat steps 3 and 4 more than 4 times. This step is to remove Na^+ and $NO3^-$.
6. After the final centrifugation, decant the supernatant liquid and then dissolve hydrated precipitate in 50 mL of 7.5 M NH_3 (aq) (BDH ARISTAR®) to make a precursor solution. Final Zn concentration is ~0.14 M.
7. Filter the precursor solution with 0.45 μm PTFE filter.
8. Spin coat the precursor on a substrate at 3000 rpm for 30 sec.
9. Cure the film on a preheated hot plate at 300 °C for 10 min.

A smooth ZnO film with surface roughness of 0.3 nm was obtained as shown by the atomic force microscopy (AFM) image in Figure 3.10.

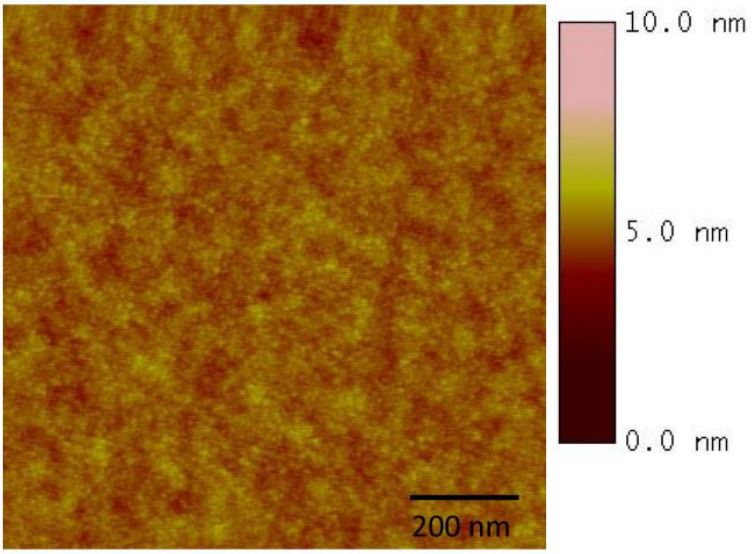

Figure 3.10 AFM height image of a ZnO film. Surface roughness of the film is 0.3 nm. Taken by Yanfei Wu.

Electron transport in the ZnO film (thickness ~10 nm) was tested by creating transistors using a 300 nm thick SiO_2 as a gate dielectric. The devices have a channel length of 100 μm and width of 2 mm. Al contacts were used to facilitate electron injection to the ZnO channel. Transfer (I_D–V_G) and output (I_D–V_D) characteristics for a ZnO transistor in Figure 3.11 demonstrate reliable electron transport through the ZnO film. A maximum drain current above 100 μA, ON/OFF current ratio of ~10^4, and electron mobility of 1 cm^2/Vs were obtained, comparable values to those of SiO_2 gated ZnO transistors reported previously.[6-8] A SiO_2 capacitance value of 11.5 nF/cm^2 was used for the mobility calculation. The spin-coated ZnO films were used to demonstrate ion gel gated n-type transistors and the results will be presented in Chapter 6.

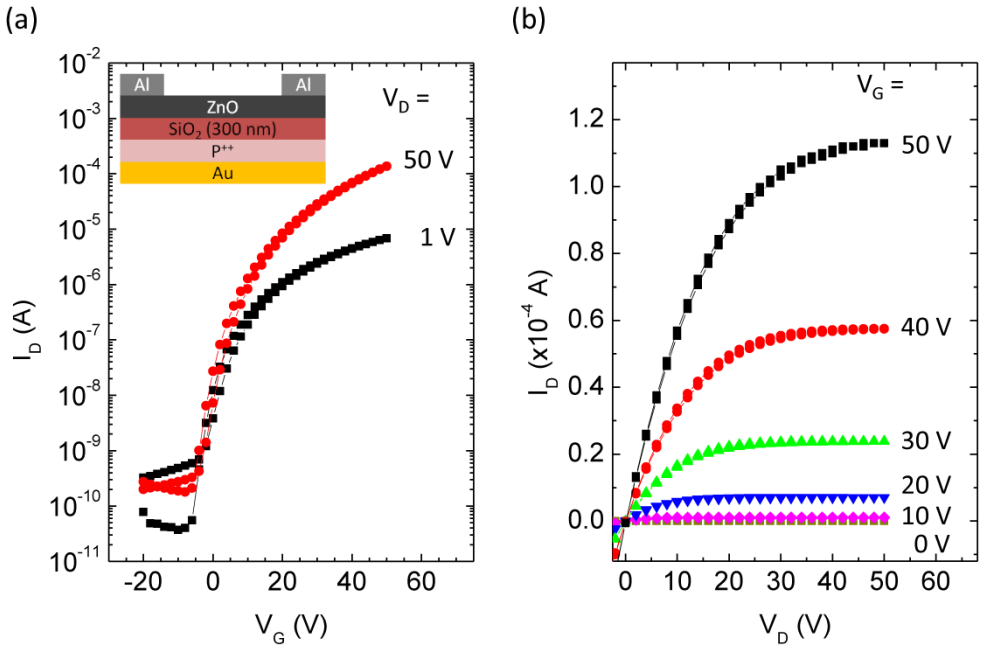

Figure 3.11 a) Transfer I_D-V_G and b) output I_D-V_D characteristics of a ZnO transistor using a 300 nm thick SiO_2 as a gate dielectric. Al source and drain electrodes were thermally deposited after a ZnO layer was created. Inset shows a schematic of a bottom-gated ZnO transistor. The devices have channel lengths of 100 μm and channel widths of 2 mm. The gate voltage was swept at a rate of 50 mV/s. Thickness of a ZnO layer was 10 nm.

3.8 References

1. Matyjaszewski, K.; Xia, J., *Chem. Rev.* **2001**, *101*, 2921.
2. Xia, J.; Matyjaszewski, K., *Macromolecules* **1997**, *30*, 7697.
3. Shipp, D. A.; Wang, J.; Matyjaszewski, K., *Macromolecules* **1998**, *31*, 8005.
4. He, Y.; Boswell, P. G.; Buhlmann, P.; Lodge, T. P., *J. Phys. Chem. B* **2007**, *111*, 4645.
5. He, Y.; Lodge, T. P., *Chem. Commun.* **2007**, 2732.

6. Meyers, S. T.; Anderson, J. T.; Hung, C. M.; Thompson, J.; Wager, J. F.; Keszler, D. A., *J. Am. Chem. Soc.* **2008**, *130*, 17603.

7. Redinger, D.; Subramanian, V., *IEEE Trans. Electron Devices* **2007**, *54*, 1301.

8. Cheng, H.-C.; Chen, C.-F.; Lee, C.-C., *Thin Solid Films* **2006**, *498*, 142.

Chapter 4

Electrical Properties of Ion Gels with SMS Triblock Copolymers[1]

4.1 Overview

In this chapter, we study electrical properties (capacitance, resistance and conductivity) of ion gel films as a function of film geometry and temperature by using electrical impedance spectroscopy. Ion gel films consisting of poly (styrene-*b*-methyl methacrylate-*b*-styrene) (SMS) and 1-ethyl-3-methylimidazolium bis(trifluoromethylsulfonyl)amide, [EMI][TFSA], are prepared by spin coating from ethyl acetate solution. The thickness (2.2 ~ 13.4 μm) and the area (0.01 ~ 0.06 cm^2) of the gel film sandwiched between two gold electrodes are varied systematically to investigate the relation between the electrical properties and the geometry of the film. The resistance (R) is directly proportional to the thickness and the reciprocal area, as expected, whereas the specific capacitance (C') is insensitive to the film geometry. Importantly, the gel polarization time constants (RC, where $C = C' \times$ Area) are as small as 2.8 μs for 2.2 μm thick ion gel films. Conductivity and capacitance of the film both increase with increasing temperature, with conductivity following the Vogel-Fulcher-Tamman equation, indicating entropically activated behavior, and capacitance at 10 Hz showing Arrhenius-type activation.

---

[*] Reproduced in part with permission from Lee, K.H.; Zhang, S.; Lodge, T. P.; and Frisbie, C. D. *Journal of Physical Chemistry B* **2011**, *115*, 3315-3321. Copyright 2011 American Chemical Society.

4.2 Introduction

Ionic liquids, or room temperature molten organic salts, have attracted great interest due to their unique properties including high thermal stability, wide electrochemical window, negligible vapor pressure, and large ionic conductivity and specific capacitance.[1-3] Such properties of ionic liquids make them suitable electrolytes for electrochemical and electrical device applications such as fuel cells,[4-6] solar cells,[7-10] electrical double layer capacitors[11-13] and thin film electrochemical transistors.[14-17] In these applications, the motion of ions in the liquids is central to device operation. At an electrified interface, ions in the electrolyte pack to compensate the countercharge on the electrode; the interfacial structure is referred to as an electrical double layer. In the functioning of capacitors and thin film transistors, the dynamic response or the electrical double layer formation time is important, because it ultimately limits the switching frequency of these devices.[18-20]

The figure of merit describing the polarization rate or double layer formation time is the *RC* time constant, which is the product of the electrolyte resistance (R) and the interfacial capacitance (C). A small *RC* time constant is desirable in device operation because it implies that ions in the electrolyte can respond quickly to an input signal. In terms of intrinsic parameters of an electrolyte $RC = C'l/\sigma$, where σ is the conductivity, C' is the specific capacitance ($C' \approx \varepsilon\varepsilon_o/\lambda$ where ε is the relative permittivity, ε_o is the permittivity of free space, and λ is the double layer thickness (~1 nm)), and l is the thickness of a film. For typical ionic liquids σ is $10^{-4} \sim 10^{-2}$ S/cm and C' is ~10 μF/cm^2.[3, 21-23] With a film thickness l of 1 μm the polarization response time can be as small as 0.1

μs. This means that potentially one can switch an electrochemical device based on ionic liquids as fast as 10 MHz.

However, from an applications perspective it is desirable to harness the excellent characteristics of ionic liquids noted above in a solid film. This can be fulfilled by adding a structuring polymer network to ionic liquids. Both chemical and physical polymer networks have been utilized in preparing solid-state electrolytes based on ionic liquids. For example, to produce a solid electrolyte containing a chemical network, *in situ* radical polymerization of vinyl monomers[24,25] or crosslinking of telechelic polymers by molecular gelators[26-28] have been reported. A physical polymer network can be designed using ABA type block copolymers consisting of an ionic liquid soluble B midblock and insoluble A endblocks.[29-31] These triblock copolymers dissolved in ionic liquids form a solid polymer electrolyte, termed a physical ion gel or simply an ion gel,[25] through non-covalent association of the A blocks. In this chapter, we show for the first time that ion gel films based on ionic liquids and triblock polymers can be reproducibly spin-coated from ethyl acetate solution. In this way the thickness of the ion gel film can be well-controlled. We used an ion gel consisting of poly(styrene-*b*-methyl methacrylate-*b*-styrene), (SMS) and 1-ethyl-3-methylimidazolium bis(trifluoromethylsulfonyl)amide, [EMI][TFSA]; the structures of these materials are shown in Figure 4.1a.

This chapter demonstrates systematic characterization of the film specific capacitance, resistance and conductivity by impedance spectroscopy. The main findings are that: (1) the resistance depends linearly on the thickness of the film and is inversely proportional to the area of the film; (2) the specific capacitance and the conductivity are

independent of the film geometry, as expected; (3) the *RC* time constant decreases with decreasing thickness of the ion gel, and is as low as 2.8 μsec for a 2.2 μm thick ion gel film; (4) conductivity values of ~1 mS/cm are achieved, which are ~10 times higher than that of traditional polymer electrolytes based on poly(ethylene oxide) and lithium salts[32]; (5) the conductivity obeys the Vogel-Fulcher-Tamman equation; and (6) the capacitance at 10 Hz displays Arrhenius behavior with temperature.

4.3 Experimental Section

4.3.1 Materials

A poly(styrene-*b*-methyl methacrylate-*b*-styrene) triblock copolymer SMS(13-65-13) was synthesized using two-step atom transfer radical polymerization (ATRP) from a difunctional initiator, following procedures described in Chapter 3.[33-36] The molecular weights (MWs) of each block, M_{PS} = 13000 and M_{PMMA} = 65000, were determined by a combination of size exclusion chromatograph (SEC) and ^{1}H NMR spectroscopy. Both PS end blocks were assumed to be the same in the MW calculation. The polydispersity index by SEC is 1.3 for the polymer used in the present study. [EMI][TFSA] (high purity) was purchased from EMD Chemicals Inc. The ionic liquid was dried in a vacuum oven for 24 h at a temperature of 70 °C. The dried ionic liquid was stored in a nitrogen filled glovebox.

4.3.2 Spin coating ion gel films

The spin coating solution was prepared by co-dissolving SMS(13-65-13) and [EMI][TFSA] in ethyl acetate. The weight ratio between the polymer and the ionic liquid

was kept to 1:4 in the experiments, and the amount of solvent was varied. The ethyl acetate solution was filtered with 0.45 μm poly(tetrafluoroethylene) filters and then spin coated onto a bottom electrode. The bottom electrode was fabricated by sequentially depositing Cr (2.5 nm) and Au (37.5 nm) on SiO_2 substrates. Spin coating conditions were changed systematically (polymer to solvent ratio from 9 to 12 wt %, spin speed between 1500 and 5000 rpm, and spin time of 30 and 60 s) to change the thickness of the ion gel films. Spin coated ion gels were placed in a vacuum oven for 24 h to remove the residual solvent. Thicknesses of spin coated ion gel films were measured by an HS200A optical profiler (Hyphenated-Systems, LLC).

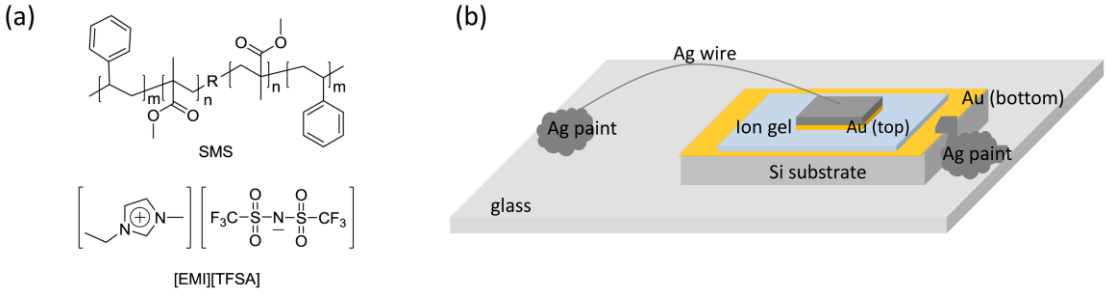

Figure 4.1 a) Chemical structures of the triblock copolymer and ionic liquid: poly(styrene-*b*-methyl methacrylate-*b*-styrene) (top) and 1-ethyl-3-methylimidazolium bis(trifluoromethylsulfonyl)amide (bottom). b) Schematic of an Au/spin-coated ion gel/Au capacitor (not to scale).

4.3.3 Capacitor fabrication

Metal-ion gel-metal (MIM) capacitors were created by placing a top electrode on the spin coated ion gel film. A schematic diagram of the MIM capacitor is shown in Figure 4.1b. The fabrication of the top electrode was started by depositing Cr (2.5 nm)/Au (37.5 nm) on SiO_2 substrates. Silver paint was carefully applied on the side and

back of the substrates and silver wire (diameter of 0.05 mm) was then connected to the top electrode using silver paint. The MIM capacitor was placed on a glass slide with double-sided tape and then silver paint was used to make two electrical contacts (one at the bottom electrode and the other at the end of the silver wire) for impedance analysis.

4.3.4 Impedance measurement

All room temperature impedance measurements were performed on a Solartron 1255B frequency response analyzer with a SI 1287 electrochemical interface controlled by ZPlot and ZView software. Experiments were conducted over the frequency range of $1 \sim 10^6$ Hz with an AC amplitude of 10 mV; no DC voltage was applied. Measurements were performed on three to five capacitors for each thickness or area. The variable temperature experiments for ion gel capacitors were performed in vacuum ($\sim 10^{-6}$ torr) with a Desert Cryogenics probe station and a Hewlett-Packard 4192A LF impedance analyzer. Liquid nitrogen was introduced into the probe station to control the temperature. The impedance (Z^*) was obtained in the form of $Z^* = Z' + i\,Z''$ where i is the imaginary unit, and Z' and Z'' are the real and imaginary parts of the impedance, respectively. Resistance and conductivity values were extracted from the plateau Z' results at high frequency, and the capacitance was calculated from Z'' data.

4.4 Results and Discussion

4.4.1 Spin coating and impedance spectroscopy

Uniform and smooth ion gel films were obtained on a flat substrate using spin coating. Deposited films were transparent, soft solids (elastic modulus ~10 kPa[30,37]) at

room temperature. The thickness of the film was controlled by changing the concentration of the spin solution and the spin speed and time, as shown in Figure 4.2.

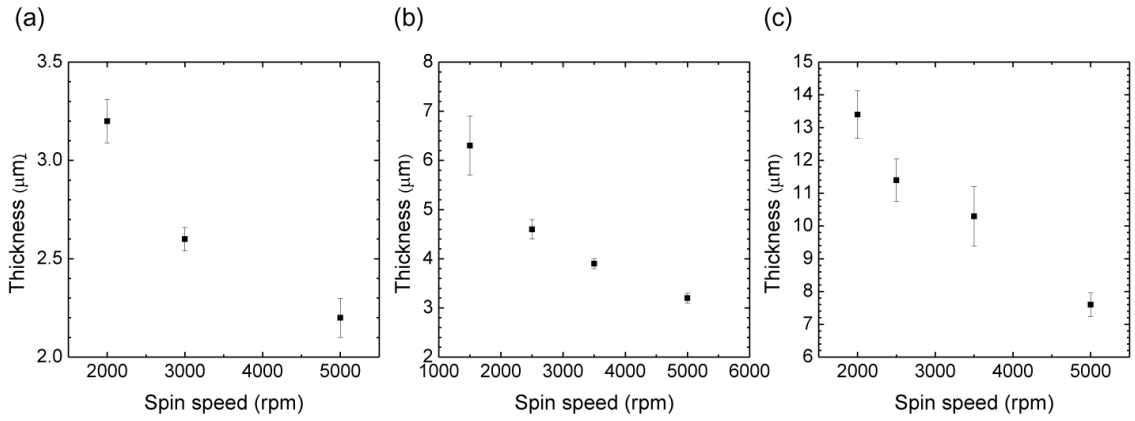

Figure 4.2 Thickness of the ion gels with different spin conditions. The polymer concentrations in ethyl acetate were a) 9 wt%, b) 10 wt%, and c) 12 wt%. Spin times were 60 s for a, and 30 s for b and c. The weight ratio between the polymer and [EMI][TFSA] was 1:4 for all cases.

Figure 4.3a displays a Nyquist plot, *Z*' vs. *Z*", for films ranging in thickness from 2.2 to 13.4 μm. For an ideal resistor and capacitor linked in series, the Nyquist plot would show a straight vertical line. The data in Figure 4.3a are clearly not simply explained by an ideal *RC* equivalent circuit, as *Z*' vs. *Z*" consistently has a positive slope. However, such behavior is typical of electrolytes contacted by solid electrodes.[38-40] The slope is due to "capacitance dispersion", which has been attributed to the adsorption of ions on the electrodes and the roughness of the electrode surface.[39-41] It has been demonstrated that increased electrode roughness broadens the time constant distribution of the adsorption process and results in increased capacitance dispersion.[40,41] The main conclusion from Figure 4.3a is that the ion gel appears to behave as a typical electrolyte.

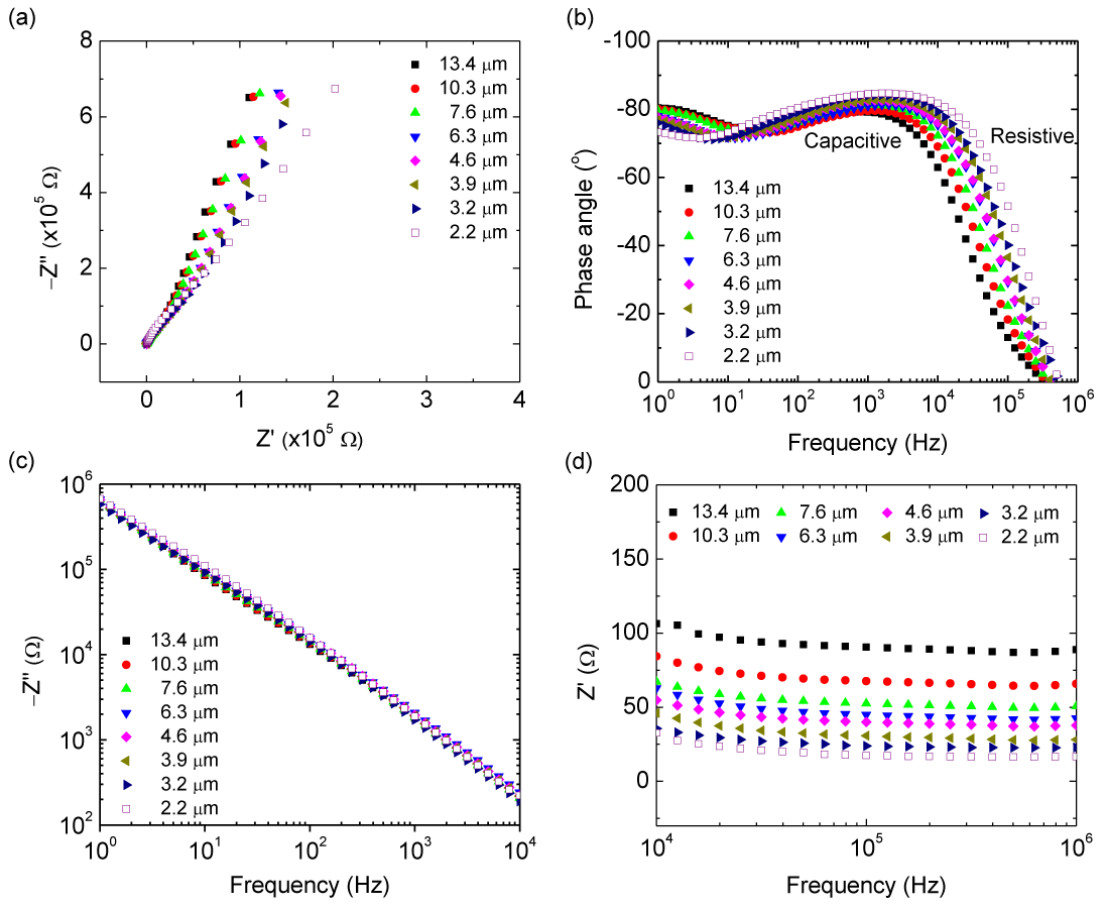

Figure 4.3 a) Nyquist plot, b) phase angle vs. frequency plot, c) *Z*'' vs. frequency plot below 10 kHz (where the capacitive contribution is dominant), and d) *Z*' vs. frequency plot above 10 kHz (where the resistive contribution is prominent) for ion gel-based capacitors with different gel thicknesses. The weight ratio between SMS polymer and [EMI][TFSA] was 1:4. The frequency range covered was 1–10^6 Hz.

Further insight is gained from the phase angle ($\theta = \tan^{-1}$ (*Z*''/ *Z*')), *Z*'', and *Z*' versus frequency plots in Figures 4.3b, c and d. The phase angle in the low frequency region is close to –80°. A phase angle of –90° is indicative of a purely capacitive response. Thus, inspection of Figure 4.3b suggests that the ion gel behaves largely as a capacitor for frequencies below 10 kHz. Above this frequency the phase angle collapses,

indicating a transition to a more resistive response. Figures 4.3c and 4.3d emphasize these two distinctive regions separately. Figure 4.3c displays Z' vs. frequency at frequencies below 10 kHz where the capacitive contribution is dominant. All eight lines corresponding to different gel thicknesses overlap each other and have an average slope of –0.86. This result implies that the capacitance obtained from Z' is independent of the thickness of the film. For an ideal RC series circuit the slope would be –1. The deviation in slope is again attributed to the capacitance dispersion and corroborates the capacitance results in the following sections. At frequencies >10 kHz the nearly frequency independent Z' values in Figure 4.3d indicate the total impedance is largely due to resistance. These observations support the calculation of the ion gel capacitance from the low frequency impedance data and the gel resistance from the high frequency results, similar to procedures used for standard electrolytes.[42]

An important point to note in Figure 4.3b is that the phase angle roll-off frequency shifts to higher values as the thicknesses of the ion gel films decrease. If the transition between capacitive and resistive character is taken to occur at a phase angle of –45°, the thinnest film shows a transition at ~125 kHz whereas the thickest changes at ~20 kHz.[43] This six-fold difference in the roll-off frequency is comparable to the thickness ratio of the films.

4.4.2 Thickness dependence

The film thickness dependences of the specific capacitance, resistance and conductivity are displayed in Figure 4.4. Three to five capacitors were examined at each thickness and eight different thicknesses (2.2 ~ 13.4 μm) were achieved by changing the

solution concentration (9 ~ 12 wt % of polymer to ethyl acetate), the spin speed (1500 ~ 5000 rpm) and spin time (30 and 60 s). The area of the top gold contact was kept constant at 0.02 cm^2.

The specific capacitance (*C*') in Figure 4.4a was calculated according to

$$C' = \frac{-1}{2\pi f \, Z'' A} \tag{4.1}$$

where f represents the frequency and A is the area of the top contact. Calculated capacitances are independent of the thickness of the ion gel film at a given frequency in the investigated thickness range. The average capacitances are 12.2 ± 0.9 μF/cm^2 at 1 Hz and 8.4 ± 0.4 μF/cm^2 at 10 Hz, where the errors are the standard deviation of capacitances at each thickness. The thickness insensitivity of the ion gel capacitance is different from conventional dielectric materials, which follow equation 4.2:

$$C' = \frac{\varepsilon\varepsilon_0}{l} \tag{4.2}$$

where l is the thickness of the dielectric layer. With a thickness on the order of 1 μm (this is the experimental thickness range), a capacitance value above 1 μF/cm^2 is not attainable with traditional dielectrics. The large capacitance value of ~10 μF/cm^2 and the thickness independent character of spin-coated ion gel films indicate that the films form ultrathin electrical double layers at the electrode interfaces. The capacitance of the electrical double layer can be estimated by the Gouy-Chapman model. At very low bias, this model has the same formula as equation 4.2, where dielectric layer thickness is replaced with the Debye screening length (λ). Measured λ values for ionic liquids are on the order of 1-4

nm,[44] which is comparable to other reported double layer thickness values around 1 nm.[45] Assuming a value of ε about 12,[46-48] the Gouy-Chapman model predicts a capacitance of 3 – 11 μF/cm^2. The measured capacitances at the low frequency region are comparable to the prediction and are also similar to literature values.[21-23]

The resistance (R) of an ion gel, on the other hand, increases linearly with increasing film thickness according to the following equation:

$$R = \frac{l}{\sigma A} + R_{lead} \tag{4.3}$$

where in our case the lead resistance is ~8 Ω. The conductivity of ion gels could in principle change with film thickness, because it is possible for the films to have different compositional ratios due to altered spin coating conditions. Composition changes or gradients will influence the conductivity of ion gels.[37] However, the nearly constant conductivity values in Figure 4.4b mean $\sigma \neq$ f(l). Therefore, with the same area and conductivity, resistances of these ion gels are directly proportional to the thickness of the films.

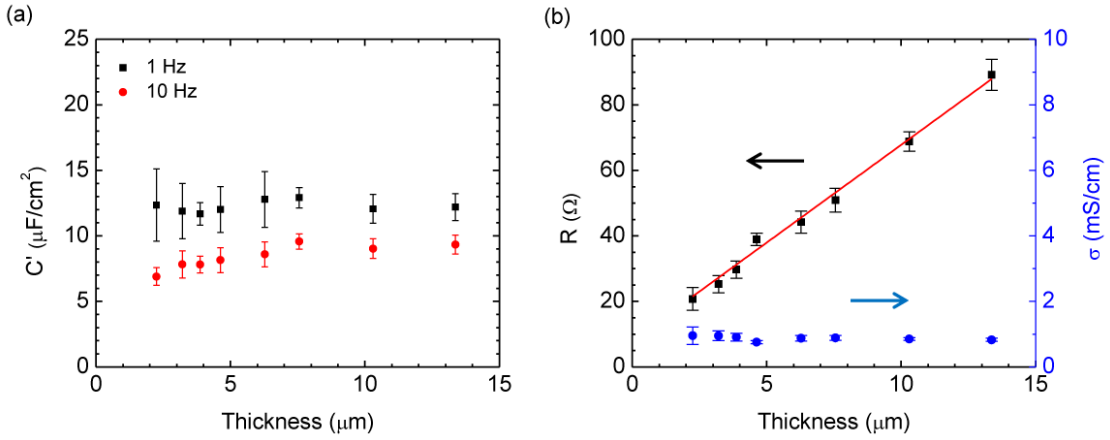

Figure 4.4 Thickness dependence of (a) capacitance at 1 and 10 Hz and (b) resistance at frequency >100 kHz (black squares: experimental data and red line: linear fit) and conductivity (blue circles) of ion gels. Area of top gold contact was 0.02 cm^2. The zero thickness intercept gives the lead and contact resistance.

The measured *R* and *C* values were employed to compute the *RC* polarization response times, Figure 4.5, as a function of gel film thickness. It is clear that the *RC* time constants increase linearly with thickness. However, the *RC* values depend on the test frequency because of capacitance dispersion. Importantly, for the thinnest 2.2 μm film a very fast response, *RC* ~ 3 μs, is achieved. This means that the polarization of an ion gel based capacitor can be switched at frequencies >100 kHz. Potentially, even shorter response times could be obtained for even thinner films. Recently, researchers in the Frisbie group realize a transistor circuit which works at ~10 μs using ion gel as a gate dielectric and carbon nanotube as a semiconductor.[49]

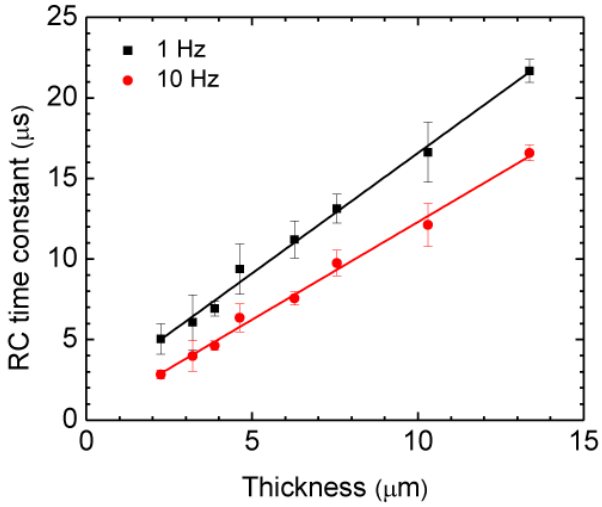

Figure 4.5 Gel thickness dependence of the *RC* time constant of capacitors at 1 and 10 Hz.

4.4.3 Area dependence

Electrical properties of the ion gel films were further investigated by changing the area of the top gold contact, as shown in Figure 4.6. Three to five capacitors with different contact areas (0.01, 0.02, 0.04 and 0.06 cm^2) were examined. The thickness of the films was kept constant at 13.4 μm. Capacitance values in Figure 4.6a increase linearly with increasing contact area, as expected. Straight lines fit the experimental data very well, indicating that the specific capacitances remain nearly the same within the investigated area range. The specific capacitances from the slopes were 9.9 ± 0.3 $\mu F/cm^2$ at 1 Hz and 7.1 ± 0.2 $\mu F/cm^2$ at 10 Hz. The difference in capacitance at different test frequencies is due to capacitance dispersion. On the other hand, resistances of the gels are inversely proportional to the area of the top contact (Figure 4.6b), as expected from equation 4.3. The results in Figures 4.4 and 4.6 confirm that the gel films can be formed

reproducibly with similar properties and that the geometric scaling of both capacitance and resistance is consistent with expectation for a high conductivity solid electrolyte.

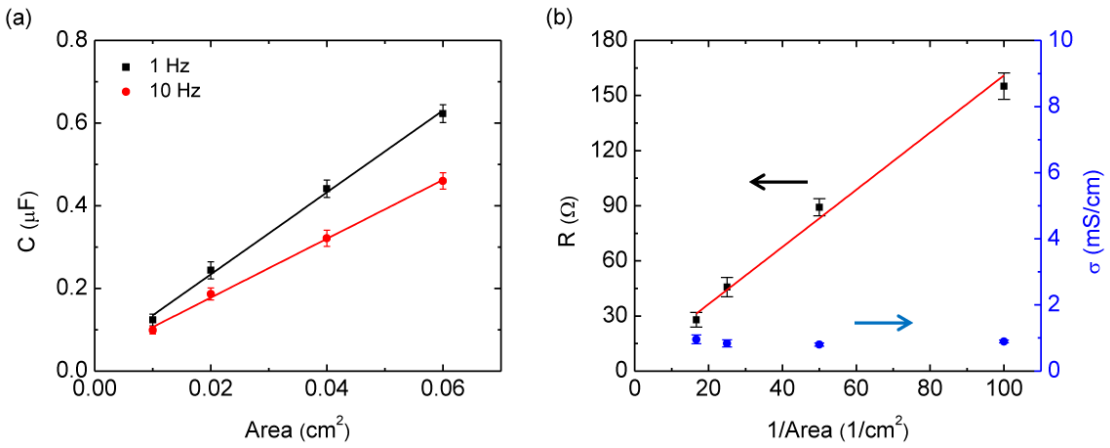

Figure 4.6 Area dependence of (a) capacitance at 1 and 10 Hz and (b) resistance at frequency >100 kHz (black squares: experimental data and red line: linear fit) and conductivity (blue circles) of ion gels. Thickness of ion gel layer was 13.4 μm. The zero reciprocal area intercept gives the lead and contact resistance.

4.4.4 Temperature dependence

Figure 4.7 displays the temperature dependence of the ion gel capacitance at different frequencies. For a traditional electrolyte that obeys the Gouy-Chapman model, the capacitance decreases with increasing temperature.[50] This trend in normal electrolytes is explained by the expanded electrical double layer due to the accelerated thermal motion of ions at high temperature. However, the capacitance of the ion gel increases with increasing temperature. This trend has been reported for both room temperature ionic liquids and high temperature molten inorganic salts.[51-57] The physical origin(s) of this behavior are still under discussion. One interpretation correlates the capacitance increase with increasing temperature to an increased concentration of free cations and

anions.[57,58] In ionic liquids there are a number of inter-ionic interactions, including electrostatic, van der Waals, and hydrogen bonding. The strength of these interactions directly influences the number of free ions. Once cations and anions form stable aggregates (ion pairs) they can be regarded as neutral species and the number of free ions decreases. With higher temperature the free ion concentration increases following an Arrhenius behavior[59], which facilitates the formation of thinner electrical double layers and efficient screening of the electrode potential. Thus, this model proposes that dissociation of ion-pairs can result in the opposite temperature dependence of capacitance for ionic liquids (and ion gels) as compared to conventional electrolytes.[56-58]

The Arrhenius-type temperature dependence of the capacitance at 10 Hz gives a pre-exponential factor of 599 $\mu F/cm^2$ and activation energy of 10.0 kJ/mol for a 13.4 μm thick ion gel. The extracted activation energy is comparable to that of a weak hydrogen bond. Formation of hydrogen bonds with three acidic carbon atoms on the imidazolium cation as hydrogen donors and nitrogen or oxygen atoms in the amide anion as hydrogen acceptors has been reported.[60-63] In addition, the lifetime of hydrogen bonds decreases with increasing temperature in 1-n-butyl-3-methylimidazolium hexafluorophosphate ([BMI][PF_6]).[64] This trend describes the weakened interaction between cations and anions, which accelerates the dissociation of ion pairs present in the double layer at elevated temperature. Therefore, more free ions are available at high temperature[59], which is consistent with the model for capacitance increase described above. However, this picture may not be consistent with the temperature dependence of free ion concentration reported by Watanabe and co-workers.[65-67] They report that the number

density of free ions in ionic liquids is insensitive to temperature based on nearly the same ratio between conductivity values measured from impedance and those from the Nernst-Einstein approximation. Although our result is qualitatively well explained by an increased free ion concentration with increasing temperature, the origin of the temperature dependence of ion gel capacitance is not yet clear at this point.

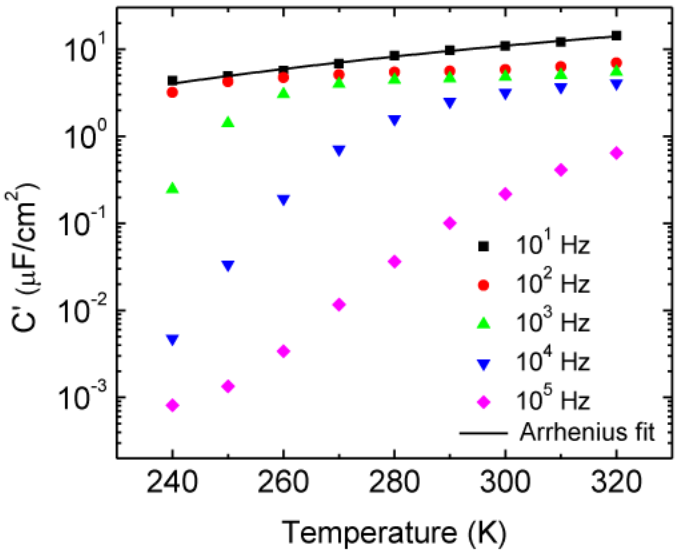

Figure 4.7 Temperature dependence of capacitance at different frequencies (filled symbols: experimental data and line: Arrhenius fit)

In Figure 4.7, a sharp decrease in capacitance is observed with increasing frequency at low temperatures and the capacitance roll-off temperature shifts to higher values. These observations indicate that double layer formation becomes less effective at high frequencies and low temperatures because ion motion becomes sluggish. When temperature is too low or the excitation frequency is too high, such that ions cannot respond to external potentials, electrical double layer formation will be impeded. In this case, the capacitance of the ion gel will be that of a conventional dielectric material in

which dipolar relaxation is dominant. For example, with a dielectric constant of 12[46-48] and ion gel thickness of 13.4 μm the dielectric capacitance of the ion gel is only 8×10^{-4} μF/cm^2. High frequency capacitance data approach this value at low temperature. In this regime, capacitance is essentially temperature independent if the dielectric constant and volume changes with temperature are negligible.

Figure 4.8a displays the temperature dependence of ion gel capacitance at 10 Hz, which recaps the argument discussed above. At high temperatures capacitance values are greater than 1 μF/cm^2, indicating the ions in the gel can move to the electrode interface to compensate the countercharges. With decreasing temperature, a sharp drop in capacitance is observed at ~ −40 °C, suggesting impeded ion motion at the gel/electrode interfaces. The capacitance roll-off temperature corresponds to the crystallization temperature of [EMI][TFSA] measured by differential scanning calorimetry (DSC).

A DSC thermogram in Figure 4.8b shows that [EMI][TFSA] crystallizes at ~ −40 °C (exothermic peak observed in the cooling scan) and melts at ~ −10 °C (endothermic peak shown in the heating scan). The small exothermic peak in the heating curve indicates that some of the [EMI][TFSA] crystallizes on heating through the crystallization temperature. This phenomenon occurs because sufficient time wasn't allowed on cooling for extensive crystallization of [EMI][TFSA]. Therefore, capacitance roll-off at low temperature is due to the crystallization of component ions in the ion gel.

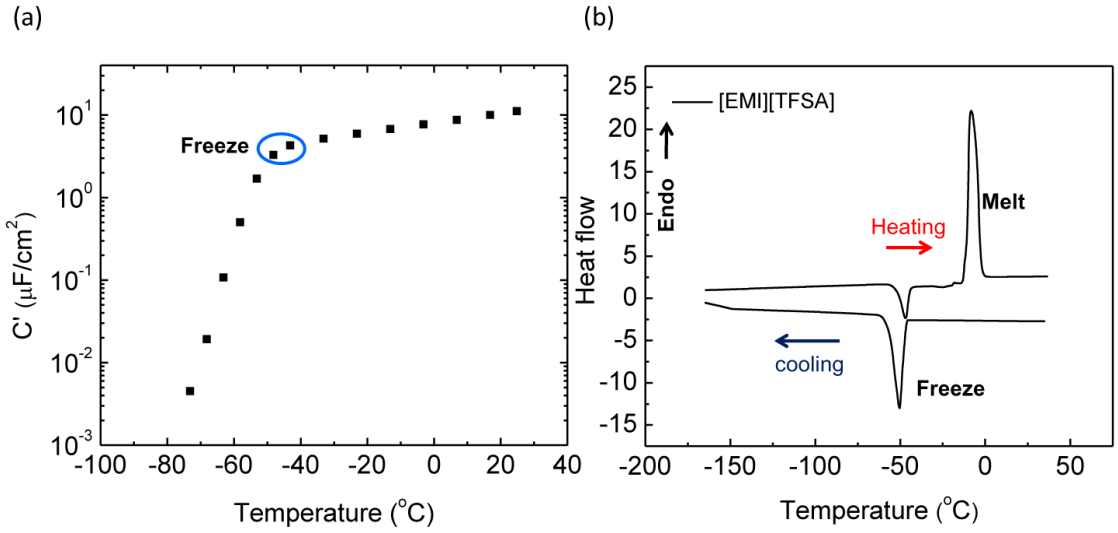

Figure 4.8 Temperature dependence of (a) capacitance at 10 Hz for a 4.6 μm thick ion gel film. (b) DSC thermogram of pure [EMI][TFSA]. The samples were tightly sealed in Al pans, and the measurements were carried out while heating up the sample to 40 °C, followed by cooling down to –170 °C, and reheating up to 40 °C, at a heating and cooling rate of ±10 °C/min.

Temperature measurements of the bulk conductivity (σ) of an ion gel were also performed, and the results were fit with the VFT equation (Figure 4.9):

$$\sigma = \sigma_0 \exp\left(\frac{-B}{T - T_0}\right) \tag{4.4}$$

where σ_o (S/cm) is the pre-exponential factor, B (K) is the constant related to the entropic barrier for conduction, and T_o (K) is the Vogel temperature. The VFT equation fits the experimental data very well with fit parameters of σ_o = 264 mS/cm, B = 825 K, and T_o = 161 K, which implies that free volume is the limiting factor for ion transport in the gel. This conduction mechanism is exactly the same as that of pure ionic liquids.[3] However, conductivity values are ~10 % of those of neat ionic liquids at a given temperature.[66] The

[EMI][TFSA] conductivity in Figure 4.9 was regenerated for comparison using VFT parameters listed in ref. 66. The reduction in conductivity for the gels compared to neat ionic liquids can be understood by impeded ion motion due to the surrounding polymer network.[30]

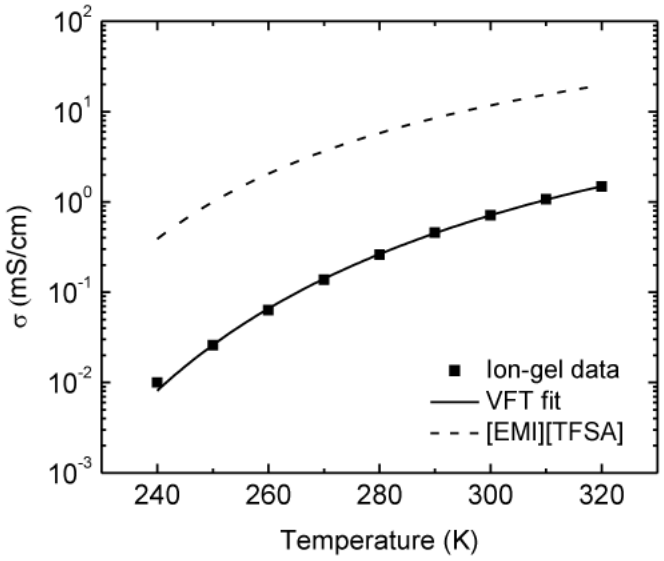

Figure 4.9 Temperature dependence of conductivity, ■: experimental data for a spin-coated ion gel film, solid line: Vogel-Fulcher-Tamman (VFT) fit, and dotted line: [EMI][TFSA] conductivity regenerated using VFT parameters listed in ref. 66.

Note that the conductivity increase with temperature is much stronger than the double layer capacitance increase with temperature. As noted, we propose that an increase in free ion concentration with increasing temperature is responsible for the double layer capacitance vs. temperature trend. Increases in free ions will also enhance the conductivity. However, it appears that the free volume increase with increasing temperature dominates the conductivity behavior and leads to a much stronger increase in conductivity with temperature. This result also indicates that the *RC* time constant will

decrease, and the maximum device operating frequency will increase, with increasing temperature.

4.5 Summary

In this chapter, we investigated the electrical properties of spin coated ion gel films based on SMS(13-65-13) triblock copolymer (20 wt%) and [EMI][TFSA] (80 wt%) by impedance measurements. The resistances of the ion gel films show a linear dependence on the thickness of the film, while the specific capacitance remains constant, over the investigated thickness range. As a result, the *RC* time constant depends linearly on the thickness of the film. An *RC* time constant of a few μs is achieved by simply reducing the film thickness. As expected, the resistance is also inversely proportional to the area of the top contact, whereas capacitance is directly proportional to the contact area. The capacitance of the ion gel at 10 Hz increases with temperature, probably due to dissociation of ion-pairs. The conductivity shows entropically activated behavior, which is also typical of pure ionic liquids. In summary, our results demonstrate that spin coatable ion gel films composed of ionic liquids and network forming block polymers can serve as high capacitance, high conductivity, solution processable solid electrolytes with short polarization response times.

4.6 References

1. Kazarian, S. G.; Briscoe, B. J.; Welton, T., *Chem. Commun.* **2000**, 2047.
2. Huddleston, J. G.; Visser, A. E.; Reichert, W. M.; Willauer, H. D.; Broker, G. A.; Rogers, R. D., *Green Chem.* **2001**, *3*, 156.

3. Galinski, M.; Lewandowski, A.; Stepniak, I., *Electrochim. Acta* **2006**, *51*, 5567.

4. de Souza, R. F.; Padilha, J. C.; Gonçalves, R. S.; Dupont, J., *Electrochem. Commun.* **2003**, *5*, 728.

5. Nakamoto, H.; Noda, A.; Hayamizu, K.; Hayashi, S.; Hamaguchi, H.; Watanabe, M., *J. Phys. Chem. C* **2007**, *111*, 1541.

6. Noda, A.; Susan, M. A. B. H.; Kudo, K.; Mitsushima, S.; Hayamizu, K.; Watanabe, M., *J. Phys. Chem. B* **2003**, *107*, 4024.

7. Papageorgiou, N.; Athanassov, Y.; Armand, M.; Bonhote, P.; Pettersson, H.; Azam, A.; Grätzel, M., *J. Electrochem. Soc.* **1996**, *143*, 3099.

8. Kawano, R.; Watanabe, M., *Chem. Commun.* **2003**, 330.

9. Wang, P.; Zakeeruddin, S. M.; Moser, J.; Grätzel, M., *J. Phys. Chem. B* **2003**, *107*, 13280.

10. Kawano, R.; Kubo, W.; Masaki, N.; Kitamura, T.; Wada, Y.; Watanabe, M.; Yanagida, S., *J. Phys. Chem. B* **2007**, *111*, 4763.

11. Balducci, A.; Bardi, U.; Caporali, S.; Mastragostino, M.; Soavi, F., *Electrochem. Commun.* **2004**, *6*, 566.

12. Ue, M.; Takeda, M.; Takahashi, T.; Takehara, M., *Electrochem. Solid-State Lett.* **2002**, *5*, A119.

13. McEwen, A. B.; Ngo, H. L.; LeCompte, K.; Goldman, J. L., *J. Electrochem. Soc.* **1999**, *146*, 1687.

14. Ono, S.; Seki, S.; Hirahara, R.; Tominari, Y.; Takeya, J., *Appl. Phys. Lett.* **2008**, *92*, 103313.

15. Yuan, H.; Shimotani, H.; Tsukazaki, A.; Ohtomo, A.; Kawasaki, M.; Iwasa, Y., *Adv. Funct. Mater.* **2009**, *19*, 1046.

16. Lee, J.; Panzer, M. J.; He, Y.; Lodge, T. P.; Frisbie, C. D., *J. Am. Chem. Soc.* **2007**, *129*, 4532.

17. Cho, J. H.; Lee, J.; He, Y.; Kim, B. S.; Lodge, T. P.; Frisbie, C. D., *Adv. Mater.* **2008**, *20*, 686.

18. Cho, J. H.; Lee, J.; Xia, Y.; Kim, B.; He, Y.; Renn, M. J.; Lodge, T. P.; Frisbie, C. D., *Nat. Mater.* **2008**, *7*, 900.

19. Xia, Y.; Zhang, W.; Ha, M.; Cho, J. H.; Renn, M. J.; Kim, C. H.; Frisbie, C. D., *Adv. Funct. Mater.* **2010**, *20*, 587.

20. Lee, J.; Kaake, L. G.; Cho, J. H.; Zhu, X. Y.; Lodge, T. P.; Frisbie, C. D., *J. Phys. Chem. C* **2009**, *113*, 8972.

21. Nanjundiah, C.; McDevitt, S. F.; Koch, V. R., *J. Electrochem. Soc.* **1997**, *144*, 3392.

22. Alam, M. T.; Islam, M. M.; Okajima, T.; Ohsaka, T., *J. Phys. Chem. C* **2008**, *112*, 16600.

23. Drüschler, M.; Huber, B.; Passerini, S.; Roling, B., *J. Phys. Chem. C* **2010**, *114*, 3614.

24. Noda, A.; Watanabe, M., *Electrochim. Acta* **2000**, *45*, 1265.

25. Susan, M. A. B. H.; Kaneko, T.; Noda, A.; Watanabe, M., *J. Am. Chem. Soc.* **2005**, *127*, 4976.

26. Klingshirn, M. A.; Spear, S. K.; Subramanian, R.; Holbrey, J. D.; Huddleston, J. G.; Rogers, R. D., *Chem. Mater.* **2004**, *16*, 3091.

27. Matsumoto, K.; Endo, T., *Macromolecules* **2008**, *41*, 6981.

28. Berns, B.; Deligöz, H.; Tieke, B.; Kremer, F., *Macromol. Mater. Eng.* **2008**, *293*, 409.

29. Lodge, T. P., *Science* **2008**, *321*, 50.

30. He, Y.; Boswell, P. G.; Buhlmann, P.; Lodge, T. P., *J. Phys. Chem. B* **2007**, *111*, 4645.

31. He, Y.; Lodge, T. P., *Chem. Commun.* **2007**, 2732.

32. Gary, F. M., *Solid polymer electrolytes: fundamentals and technological applications*. Wiley-VCH: New York, 1991.

33. Patten, T. E.; Xia, J.; Abernathy, T.; Matyjaszewski, K., *Science* **1996**, *272*, 866.

34. Xia, J.; Matyjaszewski, K., *Macromolecules* **1997**, *30*, 7697.

35. Shipp, D. A.; Wang, J.; Matyjaszewski, K., *Macromolecules* **1998**, *31*, 8005.

36. Matyjaszewski, K.; Xia, J., *Chem. Rev.* **2001**, *101*, 2921.

37. Zhang, S.; Lee, K. H.; Frisbie, C. D.; Lodge, T. P., *Macromolecules* **2011**, *ASAP*.

38. Motheo, A. J.; Sadkowski, A.; Neves, R. S., *J. Electroanal. Chem.* **1997**, *430*, 253.

39. Kerner, Z.; Pajkossy, T., *Electrochim. Acta* **2000**, *46*, 207.

40. Pajkossy, T., *J. Electroanal. Chem.* **1994**, *364*, 111.

41. Pajkossy, T., *Solid State Ionics* **2005**, *176*, 1997.

42. Brug, G. J.; van den Eeden, A. L. G.; Sluyters-Rehbach, M.; Sluyters, J. H., *J. Electroanal. Chem.* **1984**, *176*, 275.

43. Larsson, O.; Said, E.; Berggren, M.; Crispin, X., *Adv. Funct. Mater.* **2009**, *19*, 3334.

44. Min, Y.; Akbulut, M.; Sangoro, J. R.; Kremer, F.; Prud'homme, R. K.; Israelachvili, J., *J. Phys. Chem. C* **2009**, *113*, 16445.

45. Fedorov, M. V.; Kornyshev, A. A., *Electrochim. Acta* **2008**, *53*, 6835.

46. Krossing, I.; Slattery, J. M.; Daguenet, C.; Dyson, P. J.; Oleinikova, A.; Weingärtner, H., *J. Am. Chem. Soc.* **2006**, *128*, 13427.

47. Izgorodina, E. I.; Forsyth, M.; MacFarlane, D. R., *Phys. Chem. Chem. Phys.* **2009**, *11*, 2452.

48. Wakai, C.; Oleinikova, A.; Ott, M.; Weingärtner, H., *J. Phys. Chem. B* **2005**, *109*, 17028.

49. Ha, M.; Frisbie, C. D., *Manuscript in preparation*.

50. Bard, A. J.; Faulkner, L. R., *Electrochemical Methods: Fundamentals and Applications*. Wiley: New York, 2001.

51. Boda, D.; Henderson, D.; Chan , K.-Y., *J. Chem. Phys.* **1999**, *110*, 5346.

52. Ukshe, E. A.; Bukun, N. G.; Leikis, D. I.; Frumkin, A. N., *Electrochim. Acta* **1964**, *9*, 431.

53. Zistler, M.; Wachter, P.; Schreiner, C.; Fleischmann, M.; Gerhard, D.; Wasserscheid, P.; Hinsch, A.; Gores, H. J., *J. Electrochem. Soc.* **2007**, *154*, B925.

54. Graves, A. D.; Inman, D., *J. Electroanal. Chem.* **1970**, *25*, 357.

55. Costa, R.; Pereira, C. M.; Silva, F., *Phys. Chem. Chem. Phys.* **2010**, *12*, 11125.

56. Silva, F.; Gomes, C.; Figueiredo, M.; Costa, R.; Martins, A.; Pereira, C. M., *J. Electroanal. Chem.* **2008**, *622*, 153.

57. Lockett, V.; Sedev, R.; Ralston, J.; Horne, M.; Rodopoulos, T., *J. Phys. Chem. C* **2008**, *112*, 7486.

58. Holovko, M.; Kapko, V.; Henderson, D.; Boda, D., *Chem. Phys. Lett.* **2001**, *341*, 363.

59. Sangoro, J. R.; Serghei, A.; Naumov, S.; Galvosas, P.; auml; rger, J.; Wespe, C.; Bordusa, F.; Kremer, F., *Phys. Rev. E* **2008**, *77*, 051202.

60. Koddermann, T.; Wertz, C.; Heintz, A.; Ludwig, R., *ChemPhysChem* **2006**, *7*, 1944.

61. Fry, A. J., *J. Electroanal. Chem.* **2003**, *546*, 35.

62. Katoh, R.; Hara, M.; Tsuzuki, S., *J. Phys. Chem. B* **2008**, *112*, 15426.

63. Lehmann, S. B. C.; Roatsch, M.; Schoppke, M.; Kirchner, B., *Phys. Chem. Chem. Phys.* **2010**, *12*, 7473.

64. Zhao, W.; Leroy, F. d. r.; Heggen, B.; Zahn, S.; Kirchner, B.; Balasubramanian, S.; Müller-Plathe, F., *J. Am. Chem. Soc.* **2009**, *131*, 15825.

65. Tokuda, H.; Hayamizu, K.; Ishii, K.; Susan, M. A. B. H.; Watanabe, M., *J. Phys. Chem. B* **2004**, *108*, 16593.

66. Tokuda, H.; Hayamizu, K.; Ishii, K.; Susan, M. A. B. H.; Watanabe, M., *J. Phys. Chem. B* **2005**, *109*, 6103.

67. Tokuda, H.; Ishii, K.; Susan, M. A. B. H.; Tsuzuki, S.; Hayamizu, K.; Watanabe, M., *J. Phys. Chem. B* **2006**, *110*, 2833.

Chapter 5
Thermally Assisted Transfer Printing of Ion Gels for Thin-Film Transistors

5.1 Overview

In this chapter, we transfer-print ion gels using an elastomeric stamp to develop a new route to employ an ion gel layer on a device. To transfer an ion gel, attractive interaction between the gel and substrate should be larger than that at the gel/stamp interface. In this regard, we use thermoresponsive gels at elevated temperatures to achieve good physical contact between the gel and the recipient substrate. By using a gel consisting of poly(styrene-*b*-ethylene oxide-*b*-styrene) SOS and [EMI][TFSA], we successfully transfer-print hexagonal, square, and triangular patterns on three different substrates (polyimide, poly(ethylene terephthalate) PET and SiO_2) with two different thicknesses. We also fabricate organic thin-film transistors using a transfer-printed ion gel as a high capacitance gate insulator (*i.e.* electronic insulator) on SiO_2 and flexible polyimide substrates. The transistors operate at low voltage (< 1 V) with a high ON/OFF current ratio (~10^5). The result in this chapter shows that the transfer printing provides an alternative route to pattern ion gels on thin-film transistors.

5.2 Introduction

In organic and flexible electronics, developing suitable printing routes for functional layers is desirable to realize low cost over large areas and solution processable

fabrication on flexible substrates.[1-7] As a transistor is one of the basic building blocks for electronic devices, finding appropriate, solution processable inks for transistors (electrodes, semiconductors, and gate dielectrics) is a key step to make a flexible electronic device.[8] For printed transistors, there is a challenge to discover novel dielectric materials with better functional properties and solution processability.[9] High capacitance (C) is essential for gate dielectrics to accomplish low-voltage transistor operation, because the same number of charge carriers (Q) can be accumulated in a semiconductor channel with a smaller applied voltage; $Q=C\times(V_G-V_{TH})$, where V_G is the applied gate voltage and V_{TH} is the threshold voltage. Accordingly, polymer electrolytes based on ionic liquids called ion gels have been employed in transistors as gate insulators due to their large capacitance resulting from the electrical double layers at ion gel/electrode interfaces and solution processability.[9-11]

Ion gels have been prepared by either chemically reacting monomers with functional cross-linkers[12-15] or physically creating cross-links by phase separation of block polymers.[16,17] Physical cross-linking is a versatile route because the gel structures and properties can be controlled by changing the polymer block length, identity and sequence. For example, an ABA triblock copolymer with an ionic-liquid soluble B middle block and insoluble A end blocks can form a soft gel by blending a few wt% of the polymer in ionic liquids.[16] Moreover ABA gels with short A end blocks can melt at high temperatures.[18,19] The thermoresponsive gel is particularly advantageous in material processing, because the material can be deposited in the liquid and used in the solid state.

To incorporate ion gels in thin-film transistors, spin coating and aerosol jet printing have been utilized.[9-11,20,21] However, alternative deposition strategies are desirable to give high throughput and to provide a diversity of processing options. Transfer printing that has been employed to pattern films of organic small molecules, polymers, and quantum dots could potentially meet these requirements.[22-35] In this method, an elastomeric stamp (*e.g.* poly(dimethylsiloxane), PDMS) is used to transfer a target layer from a stamp to a receiving substrate (an additive mode) or to remove a functional layer from a substrate by contact with a stamp (a subtractive mode). In the additive mode, transfer of a target layer from the rubber stamp to a receiving substrate is determined by the difference of adhesion force for each layer.[36] To transfer an ink layer, attractive interaction between the ink and the substrate should be larger than that of the ink/stamp interface.[36]

In this chapter, we demonstrate transfer-printed arrays of hexagon-, square-, and triangle-shaped ion gels on polyimde, poly(ethylene terephthalate) (PET) and SiO_2 substrates using patterned PDMS stamps. The ion gel comprises a structuring polymer, poly(styrene-*b*-ethylene oxide-*b*-styrene) SOS or poly(N-isopropyl acrylamide-*b*-styrene-*b*-ethylene oxide-*b*-styrene-*b*-N-isopropyl acrylamide) NSOSN, and a room temperature ionic liquid, 1-ethyl-3-methylimidazolium bis(trifluoromethyl sulfonyl)amide, [EMI][TFSA]; the structures of these materials are shown in Figure 5.1. The SOS ion gel with short PS (M_{PS} = 3.4 kg/mol) end blocks ($IG_{s\text{-}PS}$) is transfer-printable because of its ability to form intimate contact with the substrate, whereas the SOS gel with the long PS (M_{PS} = 11 kg/mol) blocks ($IG_{l\text{-}PS}$) is not. We have fabricated

top-gated organic thin-film transistors (OTFTs) by transfer-printing all active layers (semiconductor, ion gel, and gate electrode) on Au source/drain electrodes. Transfer-printed OTFTs show high transistor-output current (> 1 mA) at low operating voltages (< 1 V).

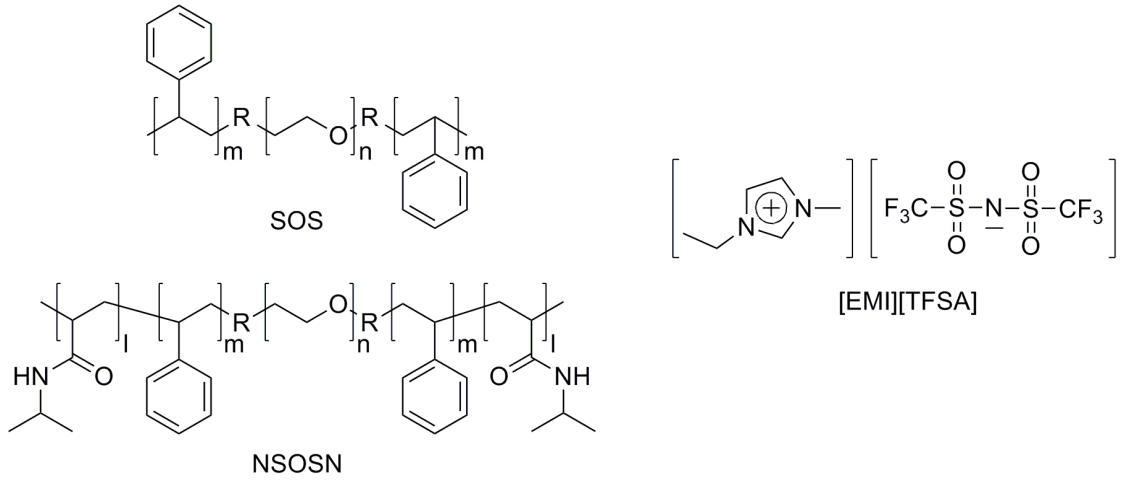

Figure 5.1 Chemical structures of poly(styrene-*b*-ethylene oxide-*b*-styrene) (SOS) (top left), poly(N-isopropyl acrylamide-*b*-styrene-*b*-ethylene oxide-*b*-styrene-*b*-N-isopropyl acrylamide) (NSOSN) (bottom left) and 1-ethyl-3-methylimidazolium bis(trifluoromethylsulfonyl)amide ([EMI][TFSA]) (right). The SOS gels were used to create patterned ion gels and to prepare thin-film transistors. NSOSN ion gels were used to fabricate thin-film transistors.

5.3 Experimental Section

5.3.1 Materials

Poly(styrene-*b*-ethylene oxide-*b*-styrene) (SOS) and poly(N-isopropyl acrylamide-*b*-styrene-*b*-ethylene oxide-*b*-styrene-*b*-N-isopropyl acrylamide) (NSOSN) were synthesized by reversible addition-fragmentation chain transfer (RAFT) polymerization.[18] SOS polymers were synthesized by Yuanyan Gu. NSOSN polymer was

synthesized by Yiyong He. The number average molecular weights of each block were $M_{PS,\ SOS}$ = 3400 or 11000, $M_{PEO,\ SOS}$ = 35000, $M_{PNIPAm,\ NSOSN}$ = 4500, $M_{PS,\ NSOSN}$ = 3300, and $M_{PEO,\ NSOSN}$ = 20000, respectively. Ion gels with SOS(3.4-35-3.4) and NSOSN(4.5-3.3-20-3.3-4.5) polymers were transfer-printable, while the SOS(11-35-11) gel was not. Numbers in parentheses are the number average molecular weights of each polymer block in kg/mol. The SOS(3.4-35-3.4) gel was used to create patterned arrays of ion gels and to fabricate thin-film transistors. NSOSN ion gels were applied to prepare thin-film transistors. 1-Ethyl-3-methylimidazolium bis(trifluoromethylsulfonyl)amide, [EMI][TFSA] (SOLARPUR®), was purchased from Merck. The ionic liquid was dried in a vacuum oven for 24 h at 70 °C and then stored in a nitrogen filled glovebox.

5.3.2 Contact angle and rheology measurements

[EMI][TFSA] contact angles were measured using a microscopic contact angle meter (Kyowa Interface Science Co. Japan) on PDMS, polyimide, SiO_2 and PET substrates. Temperature-dependent dynamic shear moduli measurements were conducted for the SOS ion gels over the temperature ranges of 40 − 150 °C on an ARES rheometer (Rheometric Scientific) using parallel plate geometry. 50 mm diameter plates were used for 10 wt% SOS(3.4-35-3.4) gel and 25 mm plates were used for other samples depending on the gel modulus. For a frequency sweep test, the sample was thermally equilibrated for 20 min at each temperature and the gap was adjusted to compensate for the thermal expansion of the equipment. Dynamic shear moduli were then measured in the linear viscoelastic region.

5.3.3 PDMS stamp fabrication

An elastomeric poly(dimethylsiloxane) PDMS stamp was prepared by curing a PDMS precursor (Sylgard 184, Dow Corning) on a prepatterned master. PDMS precursor and curing agent was mixed with the ratio of 10:1 by weight and then degassed under vacuum. The prepatterned master was created by standard photolithography using SU-8 photoresist (MicroChem Corp.) as described in Chapter 3.

5.3.4 Ion-gel printing

An ion gel layer was directly spin coated on a patterned PDMS stamp. The spin coating solution was prepared by codissolving SOS polymer and [EMI][TFSA] in ethyl acetate. The weight ratio between the two polymers and [EMI][TFSA] was 1:4 or 1:9. The amount of solvent was varied for ion gel films with different thicknesses. Weight ratios between polymer and solvent were 1:9 and 1:8 for 0.8 and 1.5 μm thick ion gels, respectively. The ethyl acetate solution was filtered with 0.45 μm poly(tetrafluoroethylene) filters before spin coating. The ion gel-coated stamp was directly placed on a receiving substrate. No additional pressure was applied except for the PDMS weight. The assembly was then heated at 100 °C for 10 s to facilitate the conformal contact and thereby improve the adhesion between the ion gel/substrate interface. Ion-gel transfer happens by slowly detaching the stamp from the substrate after cooling the assembly for a few seconds at room temperature. Thicknesses of ion gel films were measured by a KLA-Tencor P-16 surface profiler.

5.3.5 Transistor fabrication and characterization

Source and drain contacts (2.5 nm Cr / 37.5 nm Au) were prepared on SiO_2 and flexible polyimide substrates using a standard lithographic lift-off method described in Chapter 3. These patterned substrates were sequentially sonicated in acetone, isopropyl alcohol, and methyl alcohol for 10 min, rinsed with methyl alcohol, and then dried with nitrogen gas prior to active layer printing. Transistor fabrication started from depositing a regioregular poly(3-hexylthiophene) (P3HT) on a flat PDMS stamp by spin coating from chloroform solution (6 mg/mL). The inked stamp was manually cut to a desired size using a razor blade and then placed on a source/drain channel to achieved conformal contact. The device has a channel length and width of 100 μm and 1 mm, respectively. The assembly was then heated at 80 °C for 1 min to facilitate the adhesion of the ink to a receiving substrate. Finally, P3HT was transferred to a source/drain channel by detaching the PDMS mold from the substrate at room temperature. Printing the ion gel followed the same procedure as the P3HT layer on another stamp. The ion gel/substrate assembly was heated at 100 °C for SOS gels and 70 °C for NSOSN gels for 1 min. To create a gate electrode, PEDOT:PSS aqueous solution was drop cast on an oxygen-plasma treated (75 W for 7 sec) PDMS stamp and then transferred on top of ion gels. Typical length and width of printed P3HT, ion gel and PEDOT:PSS were 1 mm and 1.2 mm, respectively. Current–voltage ($I-V$) characteristics were measured in a Desert Cryogenics (Lakeshore) probe station with Keithley 236, 237 and 6517A electrometers. All electronic measurements were conducted in vacuum at ~10^{-6} torr.

5.4 Results and Discussion

5.4.1 Transfer printing ion gels

To transfer print an ion gel from a PDMS stamp to a receiving substrate (an additive mode), first, the gel was directly spin-coated on a patterned PDMS stamp. The spin coating solution was prepared by co-dissolving block polymer and [EMI][TFSA] in ethyl acetate. The inked stamp was manually placed on a receiving substrate. The assembly was then heated at 100 °C, above the gelation temperature (T_{gel}) of the ion gel, for 10 s to facilitate interfacial contact between the ion gel and substrate. Ion-gel transfer happened by slowly detaching the stamp from the substrate after cooling the assembly for a few seconds at room temperature.

Figure 5.2 displays arrays of ion gels with three different shapes (hexagons, squares, and triangles) created on a polyimide substrate by transfer printing. Note that $IG_{s\text{-}PS}$ could be transferred, while $IG_{l\text{-}PS}$ could not. Further discussion about the role of the PS block length is deferred until later. For hexagons the sides are ~60 μm, and inter-pattern spacing between hexagons is ~100 μm. Each square has side length of ~100 μm, and spacing distance is ~100 μm. Triangles have side length of 200 ~μm and pattern spacing of ~50 μm. Clean edges and corners of the patterned ion gels confirm that the transfer printing by PDMS stamps is reliable for a variety of polygons with acute, right, and obtuse angles. Figure 2e shows a height profile of the printed ion gels using a P-16 surface profiler. Ion gels with two different thicknesses (~0.8 μm and ~1.5 μm) were obtained by changing the inking solution concentration as shown in Figure 5.3. We have

also successfully printed ion gels on PET and SiO_2 substrates and the results are displayed in Figure 5.4.

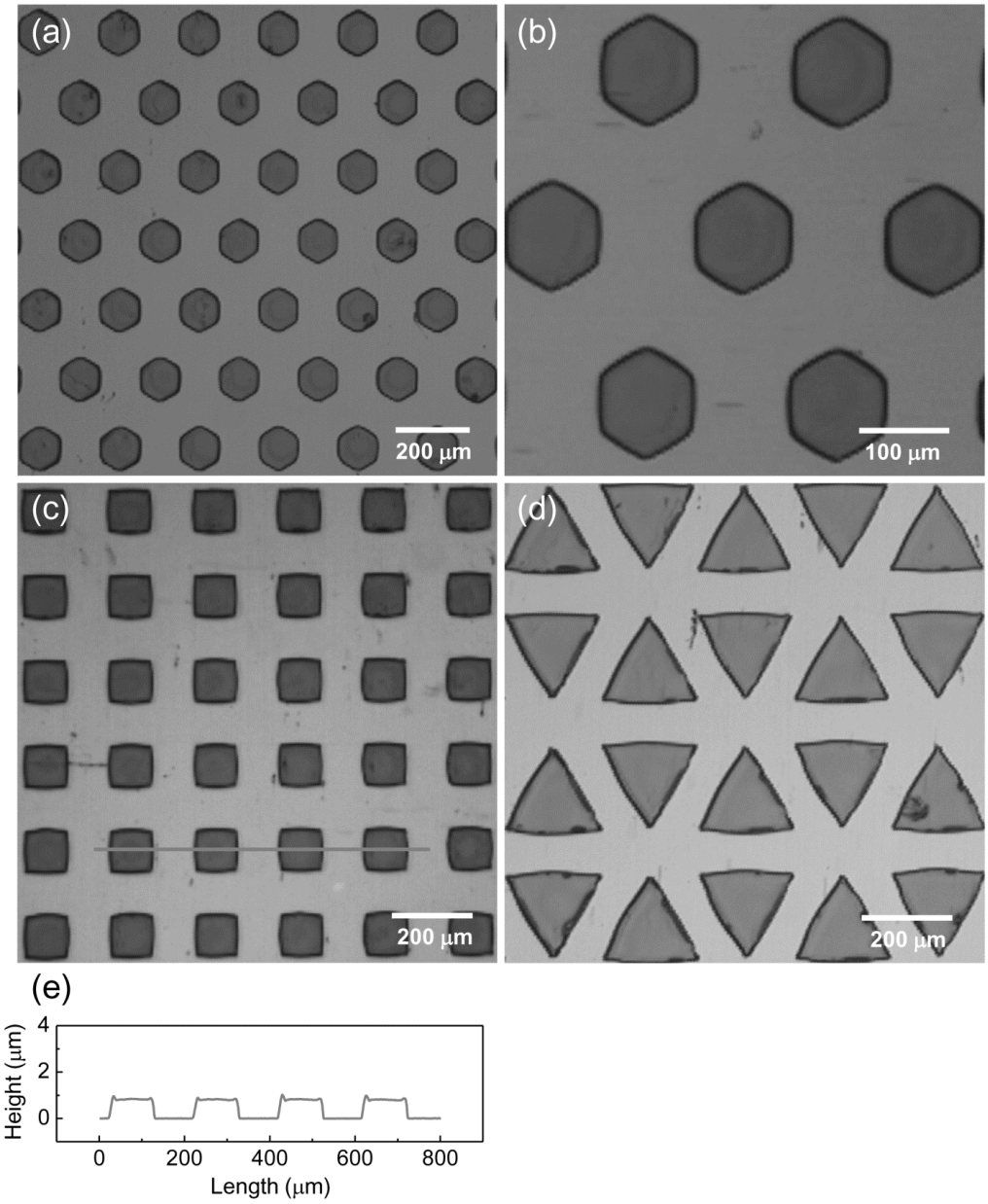

Figure 5.2 Optical microscope images of a patterned ion gel array on polyimide: (a) and (b) hexagons, (c) squares, and (d) triangels. (e) A height profile of patterned squares in (c). Thickness of the squares was 0.8 μm. The ratio between block polymer to ionic liquid was 1:4.

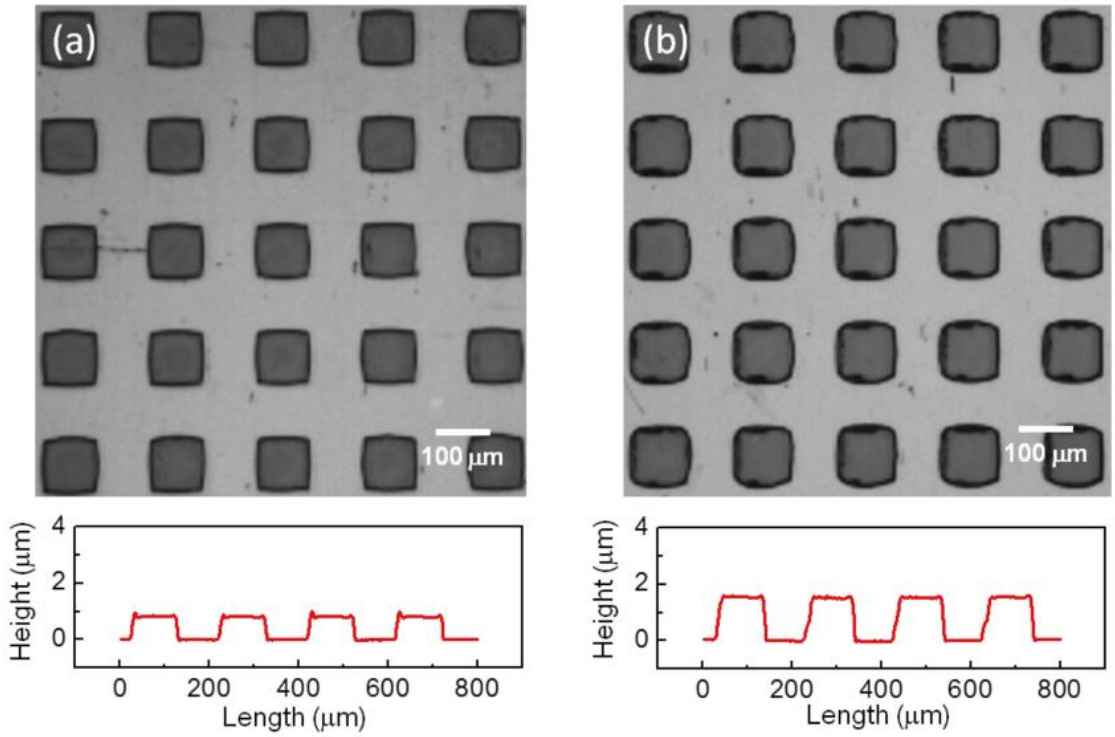

Figure 5.3 Optical microscope images (top) and height profiles (bottom) of patterned ion gels with different thicknesses (0.8 μm: left and 1.5 μm: right) on polyimide.

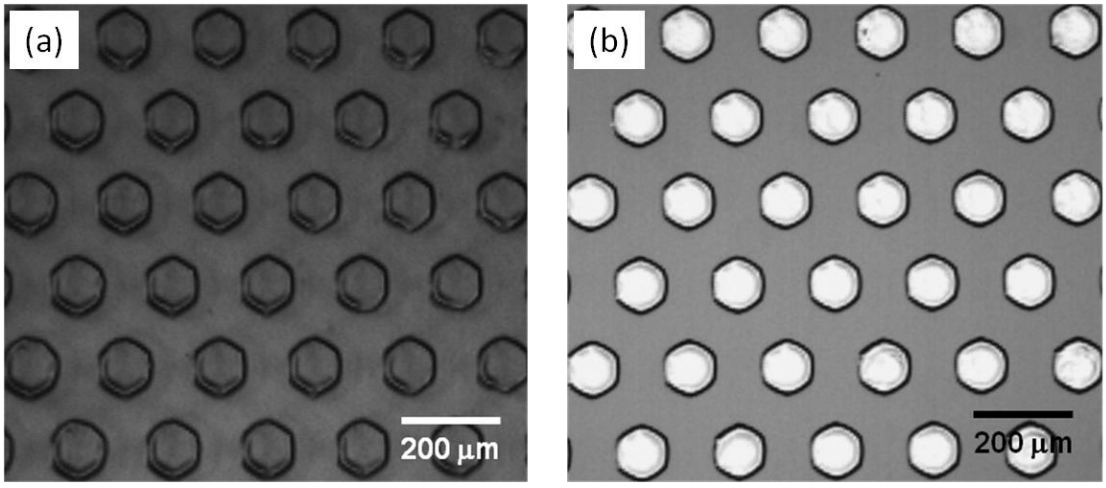

Figure 5.4 Optical microscope images of hexagonal ion gels on (a) PET and (b) SiO_2.

5.4.2 Contact angle and rheology measurements

The physical origin of ion-gel transfer can be explained by the relative adhesion between two interfaces *i.e.*, PDMS/ion gel and the ion gel/receiving substrate. When the ion gel preferentially sticks to the receiving substrate rather than to a PDMS surface, it can be transferred from PDMS to the receiving substrate as a result of adhesive failure at the PDMS surface. As the ion gel is composed mostly of ionic liquid (more than 80 wt%), printability of the ion gel can be estimated by the contact angles of the ionic liquid on donor and acceptor films.

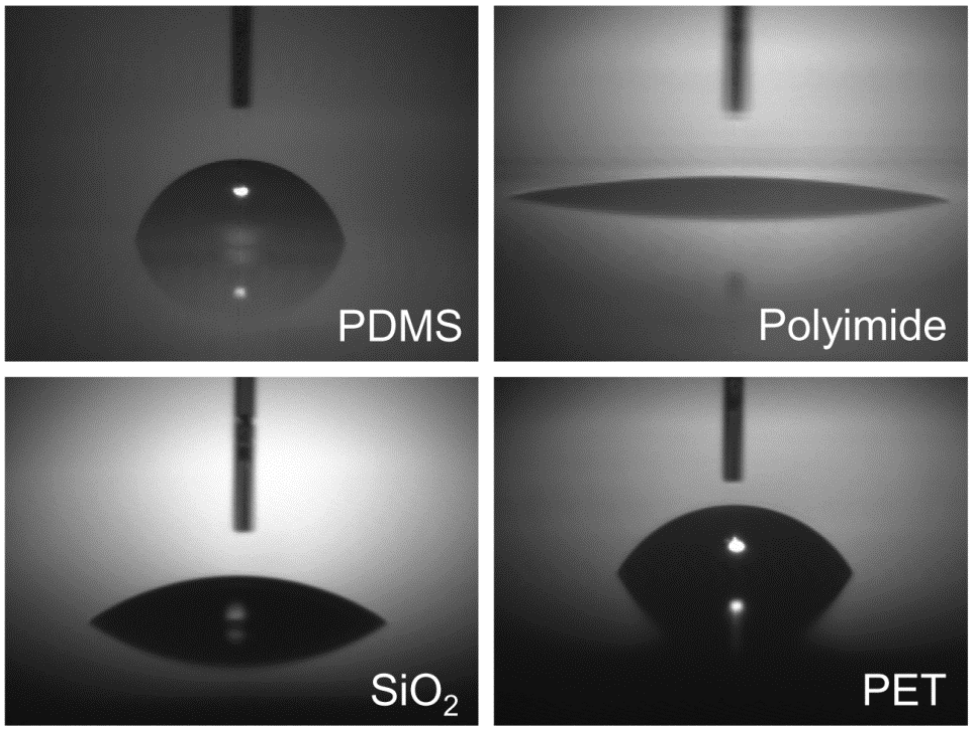

Figure 5.5 Contact angles of [EMI][TFSA] with four different substrates (PDMS, polyimide, SiO_2 and PET). Average contact angles are 80°, 12°, 37°, and 65° for PDMS, polyimide, SiO_2, and PET respectively. [EMI][TFSA] has better wettability to receiving substrates (polyimide, SiO2 and PET) than the PDMS donor substrate. Diameter of a capillary was 30 μm.

Figure 5.5 shows [EMI][TFSA] contact angles on four different materials used in this study: PDMS, polyimide, SiO_2 and PET. Average contact angles of [EMI][TFSA] are 80 ± 2°, 12 ± 2°, 37 ± 1°, and 65 ± 3° on PDMS, polyimide, SiO_2 and PET, respectively. This result indicates [EMI][TFSA] wets the receiving substrates (polyimide, SiO_2 and PET) better than the PDMS interface, which facilitates ion gel transfer from PDMS to the target substrates. In addition to contact angles, the ability of an ion gel to make intimate physical contact with substrates is also important as the gel adhesion contact can be impeded by the polymer network.

For a successful transfer, the ion gel must be in intimate contact with the substrate to maximize gel-substrate adhesion. Importantly, $IG_{s\text{-}PS}$ is printable after annealing the sample at temperatures above T_{gel}. Figure 5.6 illustrates how the ion gel/polyimide interface determines the printability for two ion gels: $IG_{s\text{-}PS}$ (b and c) and $IG_{l\text{-}PS}$ (d and e). As shown in Figure 5.6a, when the ion gel-coated stamp is put on a substrate, the ion gel primarily touches protruded regions of the rough substrate. For example, the surface roughness of a polyimide substrate is ~3 nm. At temperatures above T_{gel}, the PS cores in the $IG_{s\text{-}PS}$ melt and the gel becomes more fluid-like. The melted solution then wets the substrate and achieves intimate physical contact. Cooling below T_{gel} the gel reforms tensile force then causes adhesive failure at the PDMS interface, because the ion gel prefers to stick on the recipient surfaces. However, $IG_{l\text{-}PS}$ with SOS (11-35-11) polymer cannot achieve conformal contact with substrates even at elevated temperatures, due to the high enthalpic barrier for pulling PS chains out from the network cores, which results in failure of ion gel transfer.

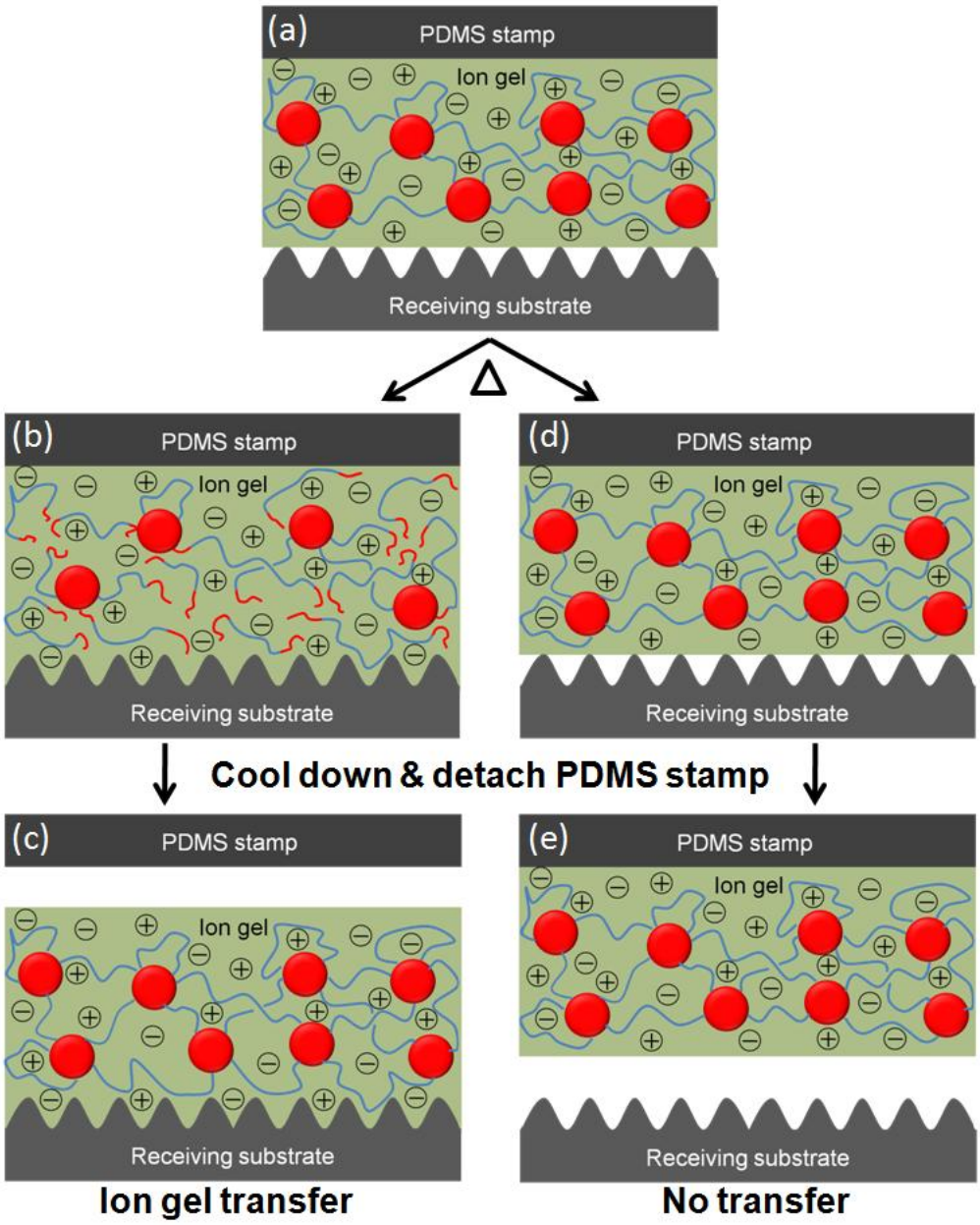

Figure 5.6 Schematic of ion-gel transfer from a PDMS stamp to a receiving substrate. (a) Initial contact is made between ion gel-coated PDMS and a substrate. (b) An ion gel with short PS end blocks achieves intimate contact with a receiving substrate upon heating above T_{gel}. (c) Ion gel is transferred upon detaching PDMS. For an ion gel with long PS end blocks (d and e), ion gel cannot achieve conformal contact due to a permanent polymer network, which results in failure of ion gel transfer.

Viscoelastic properties of ion gels can provide an explanation for a role of the PS block length in the printing process. Figure 5.7a shows the sol-gel transition of $IG_{s\text{-}PS}$ with 10 wt% of SOS (3.4-35-3.4) in [EMI][TFSA] upon varying the temperature between 40 °C and 150 °C with heating and cooling rates of ±1 °C/min. At low temperature, the values of G' and G'' are high, and $G' > G''$, indicating solid-like behavior. With increasing temperature both G' and G'' decrease, and G'' is greater than G', indicating a liquid-like molten state. The crossover of G' and G'', or T_{gel}, is ~80 °C for the $IG_{s\text{-}PS}$ used in this study.

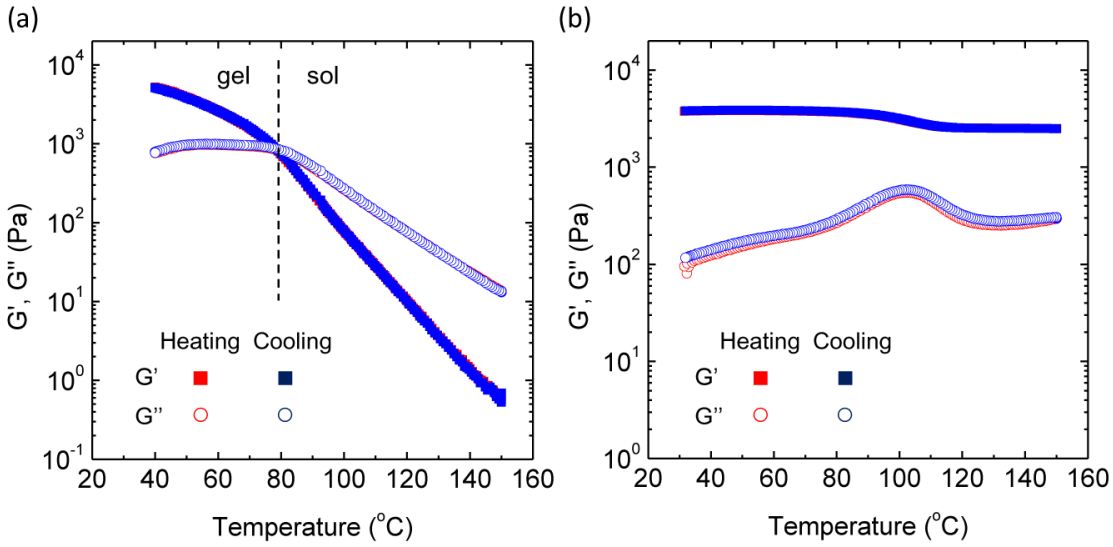

Figure 5.7 Temperature dependent dynamic shear moduli (G' and G'') for (a) $IG_{s\text{-}PS}$ (10 wt% SOS (3.4-35-3.4) in [EMI][TFSA]) and (b) $IG_{l\text{-}PS}$ (10 wt% SOS (11-35-11) in [EMI][TFSA]) at a frequency $\omega = 0.3$ rad/s and strain $\gamma = 5\%$ (for a) or 1% (for b) with heating and cooling rates of ±1 °C/min.

The terminal flow behavior of $IG_{s\text{-}PS}$ is also observed from a time-temperature superposition (tTS) master curve created by a dynamic frequency sweep measurement, as evidenced by $G' < G''$ and power law dependence of G' and G'' on angular frequency ω

in the low frequency regime: $G' \sim \omega^2$ and $G'' \sim \omega$ (Figure 5.8). Therefore at $T > T_{gel}$, PS chains in $IG_{s\text{-}SP}$ can be pulled-out from the cores and the gel intimately wets recipient materials, which is a critical step for the gel transfer.

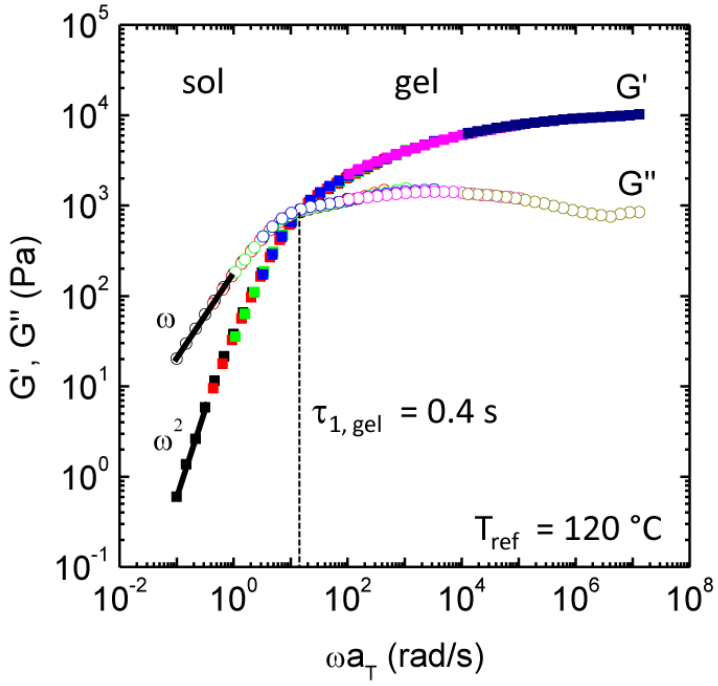

Figure 5.8 tTS master curves of dynamic storage and loss moduli (G' and G'') referenced to 120 °C at strain $\gamma = 1\%$ for the ion gel with 10 wt% SOS(3.4-35-3.4) in 90 wt% [EMI][TFSA].

Note that $IG_{s\text{-}PS}$ with 20 wt% of SOS (3.4-35-3.4) in [EMI][TFSA] is also transferrable although the system remains an elastic solid ($G' > G''$) with two plateaus over the entire temperature range (Figure 5.9a). At low temperatures G' shows a rubbery plateau of a physically cross-linked network because PS chains do not have enough energy to be pulled-out from the cores. At high temperature, PS chains can diffuse out from the cross-links and form a congested micelle solution with PS cores and PEO coronas.[18,19] Our previous study on another ion gel with SOS (3-35-3) reveals that the PS

chain pull-out rate from the network cores does not depend strongly on the polymer concentration for this type of thermoresponsive ion gel, as evidenced by the concentration independent crossover frequency or temperature.[18,19] This result implies that PS chains in $IG_{s\text{-}PS}$ with 20 wt% polymer can be pulled-out at $T > T_{gel}$ and the gel wets the substrate.

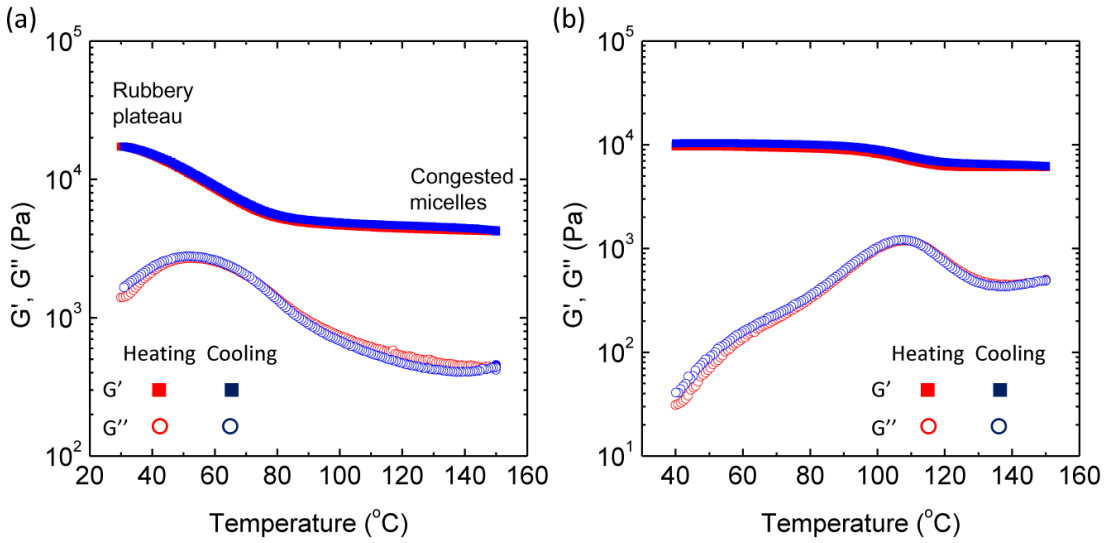

Figure 5.9 Temperature dependent dynamic shear moduli (G' and G'') for (a) 20 wt% SOS (3.4-35-35) and (b) 20 wt% SOS (11-35-11) in 80 wt% [EMI][TFSA] at a frequency $\omega = 0.3$ rad/s and strain $\gamma = 1\%$ with heating and cooling rates of ±1 °C/min.

However, $IG_{l\text{-}PS}$ shows characteristic features of a cross-linked network in the entire temperature range, $G' > G''$ (Figures 5.7b and 5.9b). This implies that PS chains in $IG_{l\text{-}PS}$ cannot be pulled out from the cores, which results in poor contact between $IG_{l\text{-}PS}$ and a rough substrate. Note that the relaxation observed at ~100 °C in Figures 5.7b and 5.9b corresponds to the glass transition of the PS chains. This observation is consistent with the patterning result for $IG_{l\text{-}PS}$ shown in Figure 5.10.

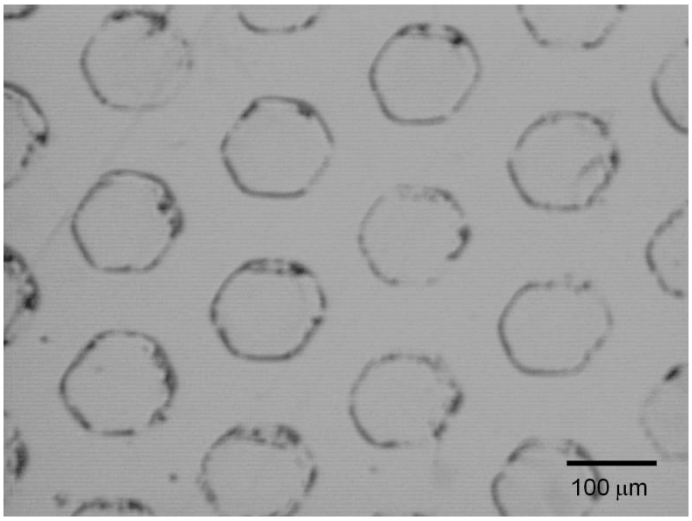

Figure 5.10 Patterning result for ion gels using SOS (11-35-11) on polyimide. Transfer printing was unsuccessful due to the gel's poor contact with substrate. The image shows residues of ion gel on edges.

5.4.3 Transistor measurements

By transfer-printing $IG_{s\text{-}PS}$ as a high capacitance gate insulator, we have fabricated top-gated organic thin-film transistors (Gel-OTFTs). The other two polymer layers (semiconductor and gate electrode) were also prepared using the same method. Figure 5.11 shows a schematic procedure for fabricating a top-gated transistor using transfer printing. A Gel-OTFT was created by sequentially transfer-printing the semiconductor regioregular poly(3-hexylthiophene) (P3HT), the $IG_{s\text{-}PS}$, and the poly(3,4-ethylene dioxythiophene):poly(styrene sulfonate) (PEDOT:PSS) gate electrode on a source/drain channel in a bottom-contact configuration. To deposit polymeric inks on a PDMS stamp, solution casting methods (spin coating or drop casting) were used. P3HT and the gel were spin coated on a flat PDMS stamp, while the PEDOT:PSS gate electrode was deposited by drop casting. The inked stamp was manually cut to the desired size using a razor blade

and then placed on a source/drain channel. The assembly was then heated at elevated temperature (80 °C for P3HT and PEDOT:PSS and 100 °C for the ion gel) to facilitate adhesion between the ink/substrate interfaces. Functional-layer transfer happens upon detaching the stamp from the substrate at room temperature.

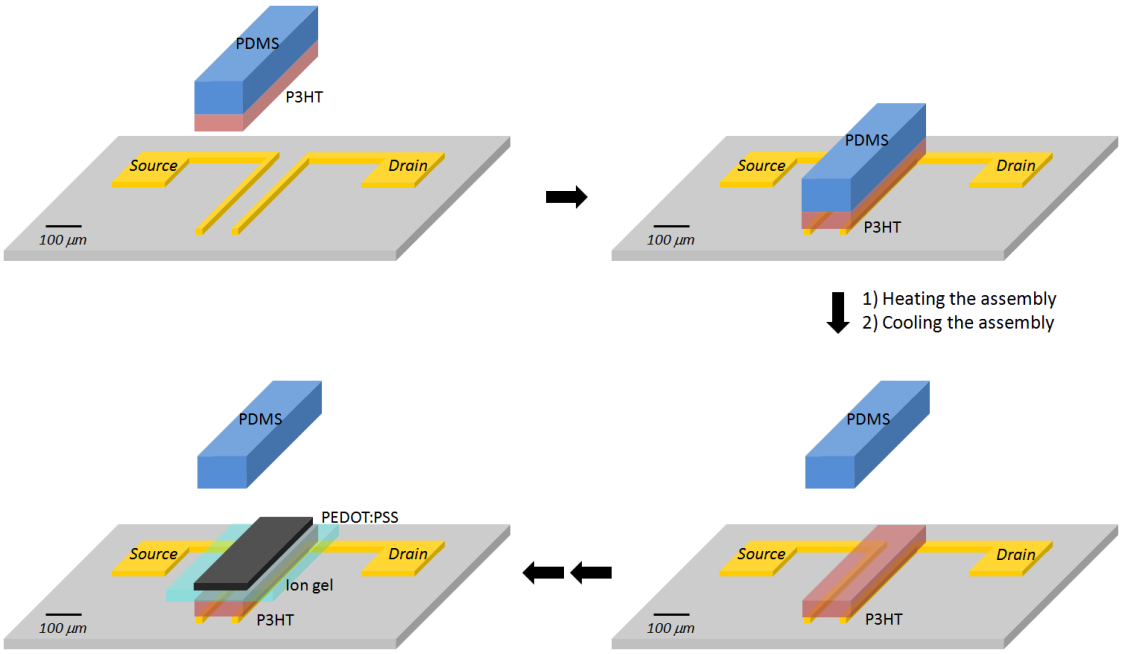

Figure 5.11 Schematic procedures for an all-printed transistor using transfer printing. P3HT was deposited on a PDMS stamp by spin casting and then transferred on a source/drain channel. Ion gel and PEDOT:PSS layers were sequentially created on P3HT to fabricate a top-gated transistor by the same process. Ion gel was inked on the stamp by spin coating, while drop casting was used to prepare a PEDOT:PSS layer on PDMS.

A cross-sectional schematic and an optical image of the transistor are shown in Figure 5.12a. The channel length (L) and width (W) of the devices are 100 μm and 1 mm, respectively. Figure 5.12b displays an optical image of an array of transfer-printed

OTFTs on a flexible polyimide substrate. It is noteworthy that all active layers (the semiconductor, the gate insulator, and the gate electrode) of the transistor were prepared by the simple lamination and detachment processes. These processes may be compatible with roll-to-roll (R2R) fabrication.

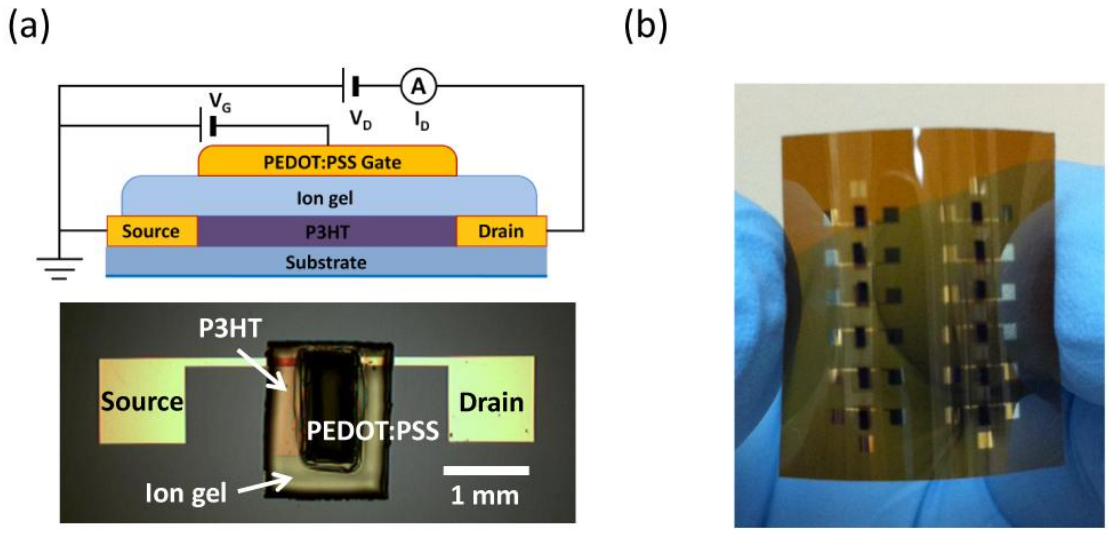

Figure 5.12 a) Cross sectional schematic of an ion gel-gated organic thin-film transistor (Gel-OTFT) (top) and an optical image of a Gel-OTFT on SiO_2 (bottom). b) Optical image of an all-printed transistor array fabricated on a flexible polyimide substrate. The device has channel length of 100 μm and width of 1 mm.

Figure 5.13a shows the quasi-static output characteristics (I_D–V_D, where I_D is the drain current and V_D is the drain voltage) of a transfer-printed Gel-OTFT at five different gate voltages (V_Gs). The output characteristics exhibited an increase in channel current with increasing V_G. A saturation current above 2 mA was obtained at V_G = −1 V and V_D = −1 V. Low voltage transistor operation can be attributed to the large capacitance of the PEDOT:PSS/ion gel interface. Because the capacitor at the ion gel/P3HT interface is in series with PEDOT:PSS/ion gel capacitor, a large number of holes (*i.e.* high drain current)

can be accumulated in the P3HT film to balance the capacitor charges at the gate-electrode side.[38] Accumulated hole density in the P3HT film will be discussed shortly.

Figure 5.13b shows the quasi-static transfer characteristic (I_D−V_G) of the OTFT. Drain current was measured while sweeping V_G from 1 V to −1 V and then back to 1 V at a rate of 5 mV/s at constant V_D = −0.1 V. A small V_D was applied to ensure the device operated in the linear regime. The device displayed a reasonable ON/OFF current ratio >10^5 within a very small gate voltage range.

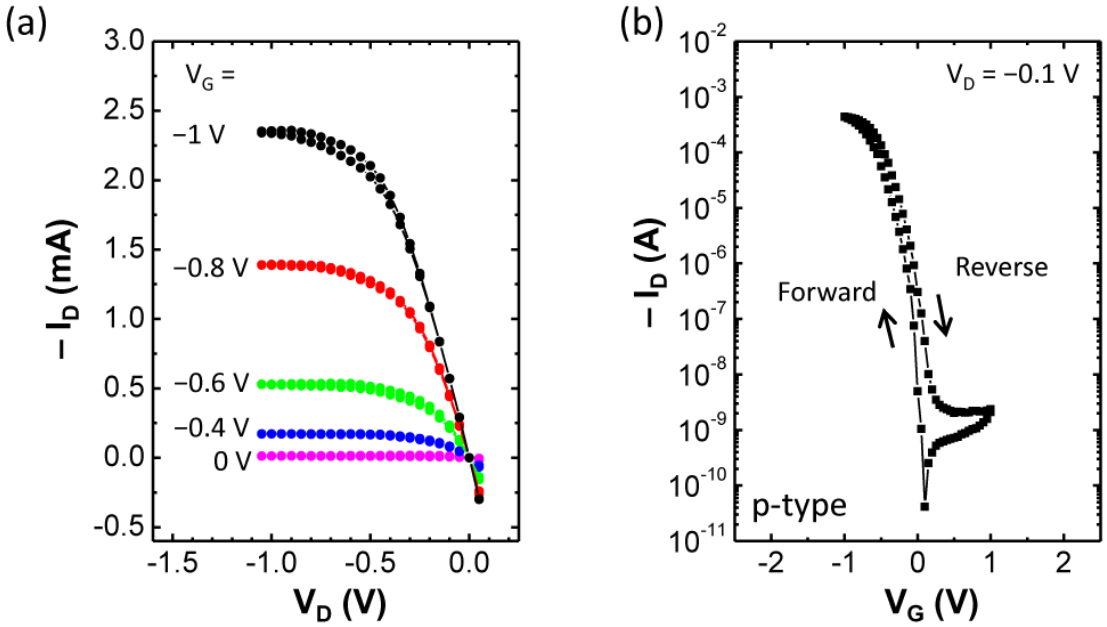

Figure 5.13 a) Quasi-static I_D-V_D characteristics of a Gel-OTFT. b) Quasi-static I_D-V_G characteristics of a Gel-OTFT. The gate voltage was swept at a rate of 5 mV/s.

The hole mobility (μ) of the transistors is calculated in the linear regime using the following equation (5.1):

$$\mu = \frac{L}{W}\frac{I_D}{epV_D} \tag{5.1}$$

where e is the elementary charge and p is the induced hole density in P3HT. The value p was obtained by dynamic gate-displacement current (I_{disp}) measurements (Figure 5.14). In the measurement, the source and drain contacts were linked to ground while the gate potential was swept at different rates. By plotting $\int I_{disp} dV_G/(r_V eA)$ *versus* $1/r_V$, where r_V is the gate potential sweep rate and A is the area of the ion gel, hole density (p) accumulated in the semiconductor channel can be extracted from the y-intercept.[39,40] From the measurements, a high hole density of 1.2×10^{15} cm^{-2} was obtained. This is due to electrochemical doping in the P3HT film, which results in a three dimensional carrier conduction. In this case, a 3D hole density, which we estimate to be 2.4×10^{20} cm^{-3} from the thickness of the P3HT film, may be more appropriate.[41] The average room temperature mobility for P3HT gated with the transfer-printed ion gel is 1.5 cm^2/Vs, which is comparable to that of P3HT using an ion gel with other deposition methods.[41,42] This mobility is orders of magnitude larger than that of P3HT gated with conventional dielectrics.[43, 44] This is presumably due to the extremely large number of holes induced by the ion gel that fills the carrier traps in the P3HT film. However, some I_D hysteresis is observed between forward and reverse sweeps. This may be due to ion motion in the porous PEDOT:PSS and P3HT films, which delays discharging of holes from the semiconductor.[42]

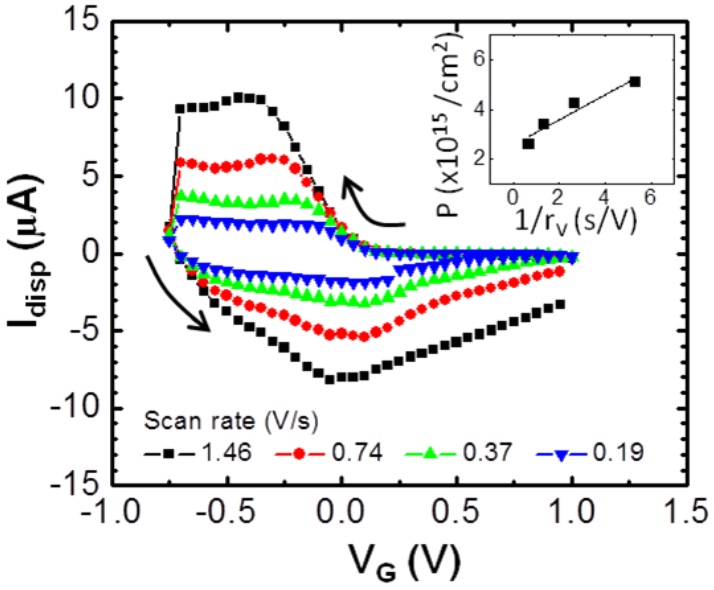

Figure 5.14 Dynamic gate-displacement current (I_{disp}) measurements with 4 different scan rates for a Gel-OTFT. Inset shows $\int I_{disp} dV_G/(r_V eA)$ *versus* $1/r_V$ plot. Hole density (p) can be obtained from the y-intercept of the plot.

We have also fabricated Gel-OTFTs using another thermoresponsive ion gel based on poly(N-isopropyl acrylamide-*b*-styrene-*b*-ethylene oxide-*b*-styrene-*b*-N-isopropyl acrylamide) (NSOSN) polymer and [EMI][TFSA]. NSOSN ion gel is transfer-printed at 70 °C due to the low T_{gel} of ~50 °C.[18] This suggests that the process temperature can be controlled by simply tailoring the block-polymer architecture. Figure 5.15a displays the I_D-V_G curves for 35 transistors prepared on a SiO_2 substrate. The 35 transistors behave nearly identically with an average hole mobility of 1.5 ± 0.5 cm^2/Vs and ON/OFF current ratio of 4.3 (± 3.2) × 10^5. The turn on voltage where the drain current in the forward sweep passes the off current of the reverse sweep for all transistor remains around zero volt for all transistors. These results indicate that transfer printing provides a reliable alternative for processing ion gels with high reproducibility.

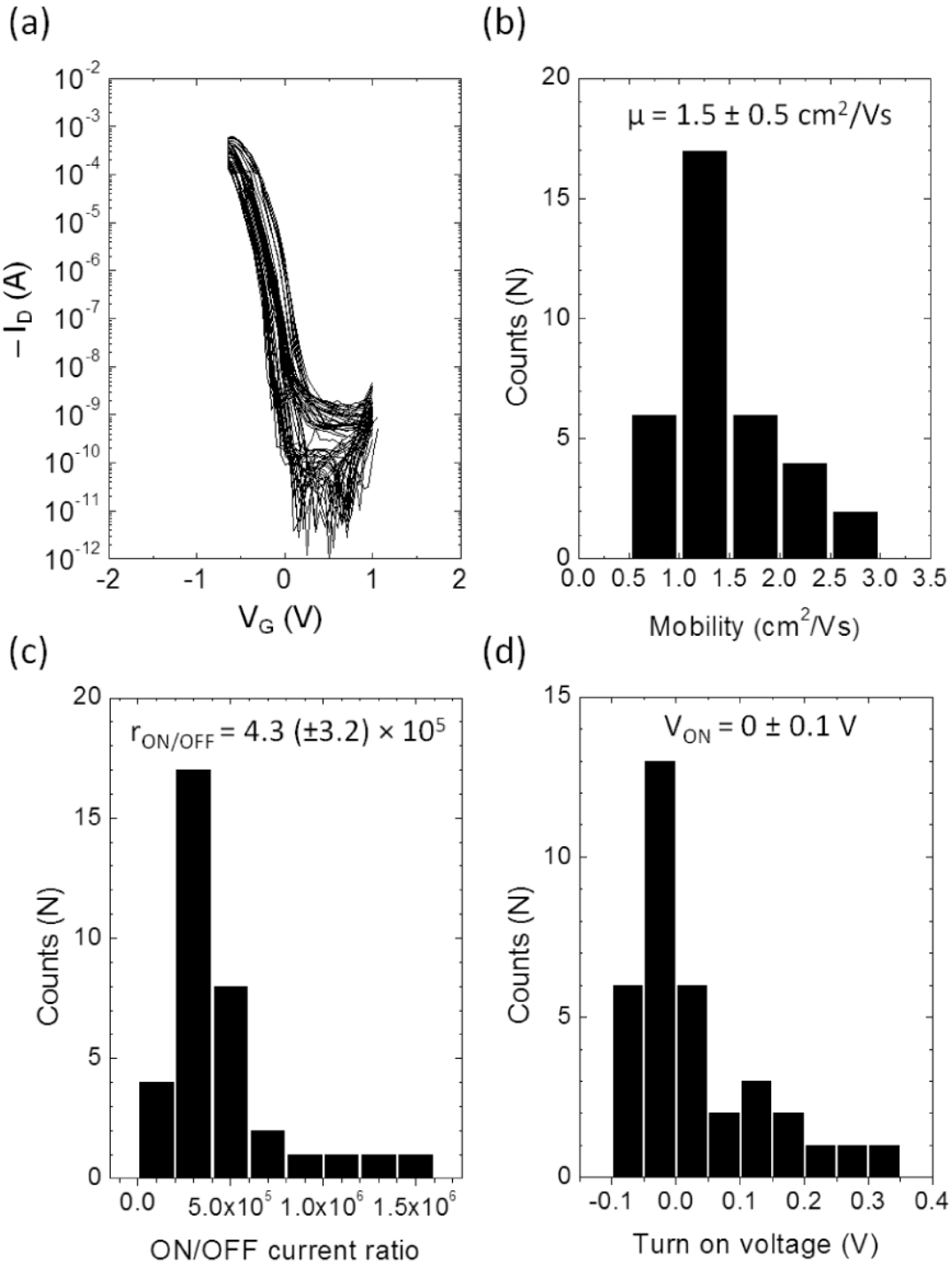

Figure 5.15 Summary of the device characteristics for 35 transistors fabricated by transfer printing. a) Transfer curves b) mobility c) ON/OFF current ratio and d) turn ON voltage. For these devices NSOSN gels were used as gate insulators.

5.5 Summary

In this chapter, we have successfully transfer-printed hexagonal, square, and triangular $IG_{s\text{-}PS}$ on three different substrates with two different thicknesses. Interestingly, $IG_{s\text{-}PS}$ is transfer-printable because of its ability to form intimate wetting contact with the substrate, while $IG_{l\text{-}PS}$ is not due to the high enthalpic barrier keeping the PS chains in their cores. Contact angle measurements of [EMI][TFSA] on a donor PDMS and recipient polyimide, PET and SiO_2 surfaces suggests that the ion gel wets the receiving substrates better than the PDMS. We have fabricated organic thin-film transistors using a transfer-printed ion gel as a high capacitance gate insulator on SiO_2 and flexible polyimide substrates. All printed OTFTs operate in low voltage (< 1 V) and displayed a high ON/OFF current ratio (~10^5). Device statistics of carrier mobility, turn on voltage, and ON/OFF current ratio exhibited the excellent reproducibility of the printing technique. Overall, our results demonstrate that the transfer printing provides an attractive option to pattern an electrolyte layer for use in devices.

5.6 References

1. Garnier, F.; Hajlaoui, R.; Yassar, A.; Srivastava, P., *Science* **1994,** *265*, 1684.
2. Forrest, S. R., *Nature* **2004,** *428*, 911.
3. Gelinck, G. H.; Huitema, H. E. A.; van Veenendaal, E.; Cantatore, E.; Schrijnemakers, L.; van der Putten, J. B. P. H.; Geuns, T. C. T.; Beenhakkers, M.; Giesbers, J. B.; Huisman, B.-H.; Meijer, E. J.; Benito, E. M.; Touwslager, F. J.; Marsman, A. W.; van Rens, B. J. E.; de Leeuw, D. M., *Nat. Mater.* **2004,** *3*, 106.

4. Someya, T.; Kato, Y.; Sekitani, T.; Iba, S.; Noguchi, Y.; Murase, Y.; Kawaguchi, H.; Sakurai, T., *Proc. Natl. Acad. Sci. USA* **2005,** *102,* 12321.

5. Noh, Y.-Y.; Zhao, N.; Caironi, M.; Sirringhaus, H., *Nat. Nanotech.* **2007,** *2,* 784.

6. Sekitani, T.; Takamiya, M.; Noguchi, Y.; Nakano, S.; Kato, Y.; Sakurai, T.; Someya, T., *Nat. Mater.* **2007,** *6*, 413.

7. Facchetti, A., *Nat. Mater*. **2008,** *7*, 839.

8. Sirringhaus, H.; Kawase, T.; Friend, R. H.; Shimoda, T.; Inbasekaran, M.; Wu, W.; Woo, E. P., *Science* **2000,** *290*, 2123.

9. Cho, J. H.; Lee, J.; Xia, Y.; Kim, B.; He, Y.; Renn, M. J.; Lodge, T. P.; Daniel Frisbie, C., *Nat. Mater.* **2008,** *7*, 900.

10. Xia, Y.; Zhang, W.; Ha, M.; Cho, J. H.; Renn, M. J.; Kim, C. H.; Frisbie, C. D., *Adv. Funct. Mater.* **2010,** *20*, 587.

11. Ha, M.; Xia, Y.; Green, A. A.; Zhang, W.; Renn, M. J.; Kim, C. H.; Hersam, M. C.; Frisbie, C. D., *ACS Nano* **2010,** *4*, 4388.

12. Noda, A.; Watanabe, M., *Electrochim. Acta* **2000,** *45*, 1265.

13. Susan, M. A. B. H.; Kaneko, T.; Noda, A.; Watanabe, M., *J. Am. Chem. Soc.* **2005,** *127*, 4976.

14. Klingshirn, M. A.; Spear, S. K.; Subramanian, R.; Holbrey, J. D.; Huddleston, J. G.; Rogers, R. D., *Chem. Mater.* **2004,** *16*, 3091.

15. Matsumoto, K.; Endo, T., *Macromolecules* **2008,** *41*, 6981.

16. He, Y.; Boswell, P. G.; Buhlmann, P.; Lodge, T. P., *J. Phys. Chem. B* **2007,** *111*, 4645.

17. Lodge, T. P., *Science* **2008,** *321*, 50.

18. He, Y.; Lodge, T. P., *Macromolecules* **2008,** *41*, 167.

19. Zhang, S.; Lee, K. H.; Sun, J.; Frisbie, C. D.; Lodge, T. P., *Macromolecules* **2011,** *44*, 8981.

20. Lee, K. H.; Zhang, S.; Lodge, T. P.; Frisbie, C. D., *J. Phys. Chem. B* **2011,** *115*, 3315.

21. Lee, K. H.; Kang, M. S.; Zhang, S.; Gu, Y.; Lodge, T. P.; Frisbie, C. D., *Adv. Mater.* **2012,** *24*, 4457.

22. Menard, E.; Meitl, M. A.; Sun, Y.; Park, J.-U.; Shir, D. J.-L.; Nam, Y.-S.; Jeon, S.; Rogers, J. A., *Chem. Rev.* **2007,** *107*, 1117.

23. Xia, Y.; Whitesides, G. M., *Angew. Chem. Int. Ed. Engl.* **1998,** *37*, 550.

24. Xia, Y.; Whitesides, G. M., *Annu. Rev. Mater. Sci.* **1998,** *28*, 153.

25. Suh, D.; Choi, S. J.; Lee, H. H., *Adv. Mater.* **2005,** *17*, 1554.

26. Meitl, M. A.; Zhu, Z.-T.; Kumar, V.; Lee, K. J.; Feng, X.; Huang, Y. Y.; Adesida, I.; Nuzzo, R. G.; Rogers, J. A., *Nat. Mater.* **2006,** *5*, 33.

27. Granlund, T.; Nyberg, T.; Stolz Roman, L.; Svensson, M.; Inganäs, O., *Adv. Mater.* **2000,** *12*, 269.

28. Lee, T.-W.; Zaumseil, J.; Bao, Z.; Hsu, J. W. P.; Rogers, J. A., *Proc. Natl. Acad. Sci. USA* **2004,** *101*, 429.

29. Li, D.; Guo, L. J., *Appl. Phys. Lett.* **2006,** *88*, 063513.

30. Cosseddu, P.; Bonfiglio, A., *Appl. Phys. Lett.* **2006,** *88*, 023506.

31. Emah, J. B.; Curry, R. J.; Silva, S. R. P., *Appl. Phys. Lett.* **2008,** *93*, 103301.

32. Chen, L.; Degenaar, P.; Bradley, D. D. C., *Adv. Mater.* **2008,** *20*, 1679.

33. Serban, D. A.; Greco, P.; Melinte, S.; Vlad, A.; Dutu, C. A.; Zacchini, S.; Iapalucci, M. C.; Biscarini, F.; Cavallini, M., *Small* **2009,** *5*, 1117.

34. Kim, T.-H.; Cho, K.-S.; Lee, E. K.; Lee, S. J.; Chae, J.; Kim, J. W.; Kim, D. H.; Kwon, J.-Y.; Amaratunga, G.; Lee, S. Y.; Choi, B. L.; Kuk, Y.; Kim, J. M.; Kim, K., *Nat. Photon.* **2011,** *5*, 176.

35. Kang, S. J.; Kim, B.; Kim, K. S.; Zhao, Y.; Chen, Z.; Lee, G. H.; Hone, J.; Kim, P.; Nuckolls, C., *Adv. Mater.* **2011,** *23*, 3531.

36. Park, S. Y.; Kwon, T.; Lee, H. H., *Adv. Mater.* **2006,** *18*, 1861.

37. Zhang, S.; Lee, K. H.; Frisbie, C. D.; Lodge, T. P., *Macromolecules* **2011,** *44*, 940.

38. Larsson, O.; Laiho, A.; Schmickler, W.; Berggren, M.; Crispin, X., *Adv. Mater.* **2011,** *23*, 4764.

39. Liang, Y.; Frisbie, C. D.; Chang, H.-C.; Ruden, P. P., *J. Appl. Phys.* **2009,** *105*, 024514.

40. Xie, W.; Frisbie, C. D., *J. Phys. Chem. C* **2011,** *115*, 14360.

41. Lee, J.; Kaake, L. G.; Cho, J. H.; Zhu, X. Y.; Lodge, T. P.; Frisbie, C. D., *J. Phys. Chem. C* **2009,** *113*, 8972.

42. Cho, J. H.; Lee, J.; He, Y.; Kim, B. S.; Lodge, T. P.; Frisbie, C. D., *Adv. Mater.* **2008,** *20*, 686.

43. Bao, Z.; Dodabalapur, A.; Lovinger, A. J., *Appl. Phys. Lett.* **1996,** *69*, 4108.

44. Sirringhaus, H.; Brown, P. J.; Friend, R. H.; Nielsen, M. M.; Bechgaard, K.; Langeveld-Voss, B. M. W.; Spiering, A. J. H.; Janssen, R. A. J.; Meijer, E. W.; Herwig, P.; de Leeuw, D. M., *Nature* **1999,** *401*, 685.

Chapter 6
Free-Standing P(VDF-HFP) Ion Gels for Thin-Film Transistors[2]

6.1 Overview

In this chapter, we study mechanically free-standing ion gels that can be cut by hand and laminated on a layer of semiconductor using tweezers. This study aims to develop a new route to incorporate an ion gel layer on a device to provide diversity and universality in ion gel processing. The ion gel consists of a structuring poly(vinylidene fluoride-*co*-hexafluoropropylene) P(VDF-HFP) polymer swollen in an ionic liquid. The 'cut and stick' processing strategy developed in this study allows very convenient fabrication of electrolyte-gated transistors based on various semiconductors. The transistors using P(VDF-HFP) gel as a gate insulator operate within a low voltage range (< 2 V) and show a high ON/OFF current ratio (~10^5). We also observe that the ion gel can accumulate both holes and electrons in organic and inorganic semiconductors, respectively.

6.2 Introduction

Ionic liquids consisting of low molar mass cations and anions have attracted great attention as high capacitance gate insulators in field effect transport experiments in which a gate electrode is employed to modulate the carrier concentration of a semiconductor.[1-4]

---

[*] Reproduced in part with permission from Lee, K.H.; Kang, M.S.; Zhang, S.; Gu, Y.; Lodge, T. P.; Frisbie, C. D. *Advanced Materials* **2012**, *24*, 4457-4462. Copyright 2012 WILEY-VCH Verlag GmbH & Co. KGaA, Weinheim

The primary figure of merit for a gate insulator is specific capacitance, as the charge induced in the transistor channel is directly proportional to capacitance ($Q = C \times (V_G - V_{TH})$, where Q is the electric charge, C is the capacitance, V_G is the applied gate voltage, and V_{TH} is the threshold voltage). Ionic liquids feature exceptionally large specific capacitances originating from nanometer-thick electrical double layers at electrolyte/electrode interfaces, and wide electrochemical windows.[5-9] Using ionically conducting but electronically insulating ionic liquids as gate insulators, the number of charge carriers in a transistor channel can be tuned beyond 10^{14} cm^{-2}.[10] Accessing such large carrier densities by ionic liquid gating is extremely valuable for examining transport behavior and critical phenomena (*e.g.*, the insulator-to-metal transition) in semiconductors.[11]

To enhance the practicality of employing ionic liquids in gating experiments, it is desirable to blend them with structuring polymers to form a chemically or physically crosslinked network. The resulting solid polymer electrolyte is referred to as an ion gel.[12] The most promising ion gels retain a large fraction of the ionic conductivity and capacitance of the neat ionic liquid but can be incorporated into devices as thin solid films. Chemically crosslinked ion gels have been prepared by *in situ* radical polymerization of vinyl monomers[12,13] or by gelation of molecular crosslinkers with telechelic polymers.[14,15] Physically crosslinked ion gels can be obtained by using block polymers that are partially compatible with ionic liquids.[16] For example, ABA triblock copolymers, where the A end blocks are insoluble and the B middle block is soluble in an ionic liquid, have been utilized to obtain soft gels by combining a few wt% of the

polymer with the ionic liquid.[17] Ion gels have been demonstrated as high capacitance gate insulators in thin-film transistors and, importantly, they can be processed by spin coating or direct-write printing from solvents.[18,19] During solution processing, however, solvents can contaminate the active channel of a transistor, which may limit the application of ion gels in specific test environments.

In this chapter, we demonstrate solvent-free, free-standing ion gels based on poly(vinylidene fluoride-*co*-hexafluoropropylene), P(VDF-HFP),[20-30] and the ionic liquid 1-ethyl-3-methylimidazolium bis(trifluoromethylsulfonyl)amide, [EMI][TFSA], as high capacitance gate dielectrics for transistor-gating experiments. Due to the high tensile strength, a free-standing P(VDF-HFP) ion gel can be cut by hand and laminated on a layer of semiconductor. This 'cut and stick' processing strategy allows very convenient fabrication of transistors based on a variety of semiconductor materials.[31] Gate electrodes can be deposited directly on the gel by printing, or an even simpler side-gate configuration can also be employed. We observed that the ion gel can induce both holes and electrons in organic and inorganic semiconductors, respectively. Overall, the results indicate that the free-standing ion gel provides a convenient route to incorporate a high capacitance electrolyte layer in a transistor.

6.3 Experimental Section

6.3.1 Materials

Poly(vinylidene fluoride-*co*-hexafluoropropylene), P(VDF-HFP) with M_n = 130000 g/mol and M_w = 400000 g/mol, was purchased from Sigma-Aldrich. 1-Ethyl-3-methylimidazolium bis(trifluoromethylsulfonyl)amide, [EMI][TFSA] (high purity), was

purchased from EMD Chemicals Inc. The ionic liquid was dried in a vacuum oven for 24 h at a temperature of 70 °C. The dried ionic liquid was stored in a glovebox.

6.3.2 Ion gel preparation

The free-standing ion gel layer was first spin coated on a glass slide, cut with a razor blade, and then transferred onto the device using tweezers. The spin coating solution was prepared by codissolving P(VDF-HFP) and [EMI][TFSA] in acetone. The weight ratio between the polymer, ionic liquid, and the solvent was kept to 1:4:7 in the experiments. Spin-coated ion gels were placed in a vacuum oven at 70 °C for 24 h to remove the residual solvent. Thicknesses of spin-coated ion gel films were measured by a KLA-Tencor P-16 surface profiler.

6.3.3 Capacitance measurements and tensile test

Capacitance measurements were carried out using Solartron 1255B frequency analyzer with SI 1287 electrochemical interface controlled by ZPlot and ZView software at room temperature. Metal-ion gel-metal (MIM) capacitors were created by following the procedures described in Chapter 4. The experiments were conducted over the frequency range of $1 \sim 10^5$ Hz with an AC amplitude of 10 mV. Tensile tests were conducted on an ARES rheometer (Rheometric Scientific) using rectangular specimens with a deformation rate of 0.1 mm/s. Solvent-cast ion gels with an average length of 16 mm, width of 6 mm, and thickness of 0.6 mm were used for the tensile tests.

6.3.4 Transistor fabrication and characterization

Source and drain contacts (2.5 nm Cr / 37.5 nm Au) were patterned on SiO_2 substrates using standard lift-off techniques described in Chapter 3. These patterned

substrates were sequentially sonicated in acetone, isopropyl alcohol, and methyl alcohol for 10 min, rinsed with methyl alcohol, and then dried with nitrogen gas. Regioregular poly-3-hexylthiophene (P3HT) was spin coated at a speed of 2000 rpm for 60 s from chloroform solution (6 mg/mL) on Au contacts. The free-standing ion gel was transfered onto the P3HT using tweezers. A gate PEDOT:PSS contact was prepared by aerosol jet printing on the gel for top-gated transistors. For side-gated transistors, the ion gel was laminated over both a semiconductor channel and a side-gate electrode placed 700 μm away from the center of the channel. ZnO films were prepared by spin coating a zinc hydroxide precursor followed by sintering at 300 °C for 10 min.[32] 40 nm thick Al source, drain, and side gate contacts were thermally deposited using a stainless steel stencil mask after the ZnO layer was prepared. Al electrodes were chosen to facilitate electron injection into *n*-type ZnO. However, similar to other low work function metals, Al can undergo oxidation reactions upon exposure to atmospheric oxygen or water. To avoid this, the entire device fabrication process was carried out in a nitrogen-filled glove box after the ZnO layer was created. Current–voltage ($I-V$) characteristics were measured in a Desert Cryogenics (Lakeshore) probe station with Keithley 236, 237 and 6517A electrometers. All electronic measurements were conducted in vacuum at ~10^{-6} torr.

6.4 Results and Discussion

6.4.1 P(VDF-HFP) ion gels and their properties

Figure 6.1 shows the chemical structures of P(VDF-HFP) and [EMI][TFSA]. We have gelled the ionic liquid by selective dissolution of the copolymer, where PVDF crystals are insoluble in the liquid.[33] The gelation happens through bridging these crystals

by polymer chains dissolved in the solution. This ion gel is thermally stable above 300 °C as shown by the thermogravimetric analysis (TGA) result in Figure 6.2.

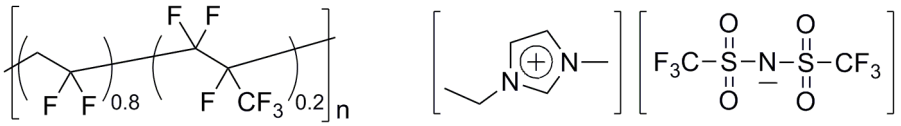

P(VDF-HFP) [EMI][TFSA]

Figure 6.1 Chemical structures of the copolymer and the ionic liquid: poly(vinylidene fluoride-*co*-hexafluoropropylene) (P(VDF-HFP)) (left) and 1-ethyl-3-methylimidazolium bis(trifluoromethylsulfonyl)amide ([EMI][TFSA]) (right).

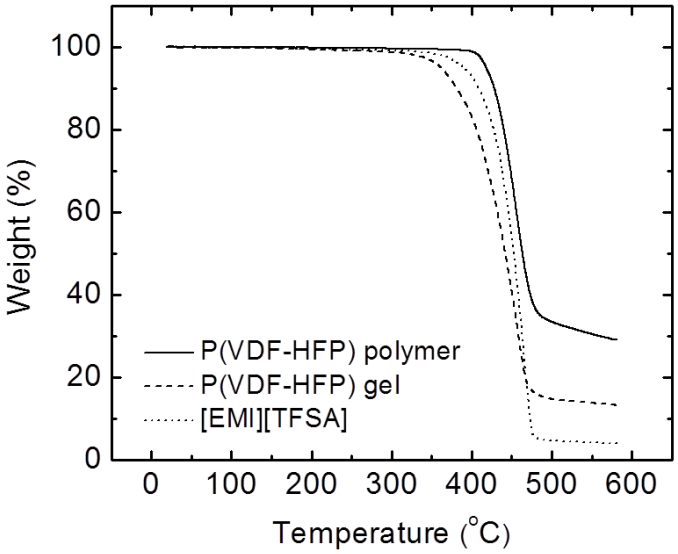

Figure 6.2 TGA thermogram of P(VDF-HFP) polymer, P(VDF-HFP) ion gel and [EMI][TFSA] under nitrogen atmosphere. Heating rate was 10 °C/min.

Both spin coating (Figure 6.3a) and solvent casting methods (Figures 6.3b and c) are applied to prepare the ion gels. Optical images in Figure 6.3 clearly show the self-supporting nature of the ion gel. Films of the gels can be easily twisted or bent without damage because of their high mechanical strength and elasticity.

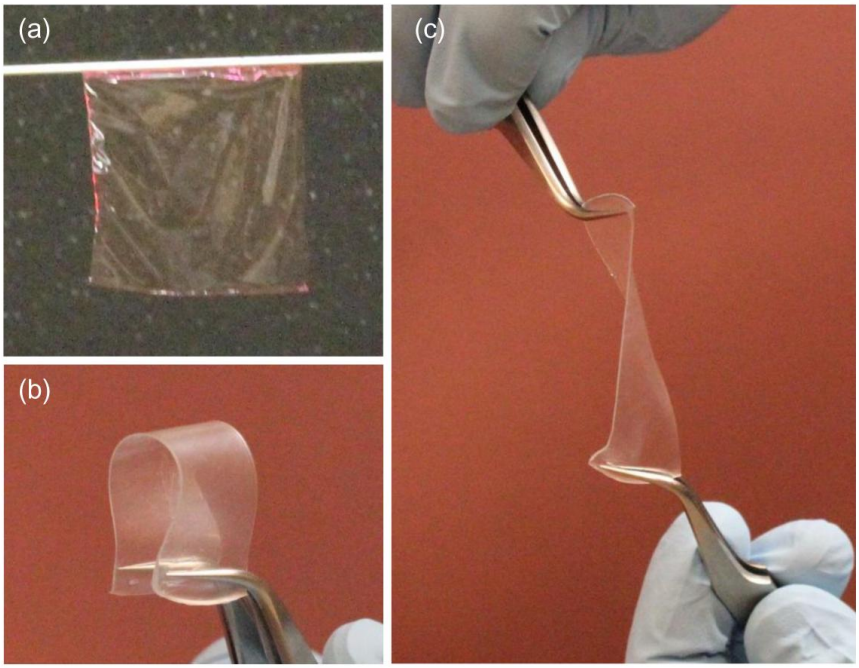

Figure 6.3 Optical images of the free-standing ion gel based on P(VDF-HFP) and [EMI][TFSA]. The weight ratio between the polymer and the ionic liquid was 1:4. Ion gel films were prepared by (a) spin coating (~10 μm thick) or by (b and c) solvent casting (~0.6 mm thick). Spin-coated ion gels were applied in transistor measurements, while thick ion gel films prepared by solvent casting were used in tensile tests.

Figure 6.4 displays a stress versus strain curve for a solvent-casted ion gel with 20 wt% P(VDF-HFP) in [EMI][TFSA]. A Young's modulus of ~1.3 ± 0.1 MPa calculated from the ratio of tensile stress to tensile strain in the elastic region. For the tensile test, rectangular shaped samples were used under an extension rate of 0.1 mm/s. The

measured modulus is ~2 orders of magnitude smaller than that of pure P(VDF-HFP), due to addition of "zero modulus" ionic liquid, and the reduction in ion-gel crystallinity shown by differential scanning calorimetry (DSC) (Figure 6.5).[33] The amplitudes of the crystallization and meting peaks for the ion gel are reduced to ~18 % of those for pure polymer. The peaks shift to lower temperature and become broader relative to P(VDF-HFP) polymer, indicating plasticization by the ionic liquid. However, the modulus value is still ~2 orders of magnitude higher than the typical modulus of ion gels based on ABA block copolymers at the same polymer concentration.[17,34,35] Accordingly, the free-standing ion gel can be cut into any size with a razor blade and can be transferred to substrates using tweezers. This process provides a convenient and solvent-free route to incorporate the ion gel in transistors.

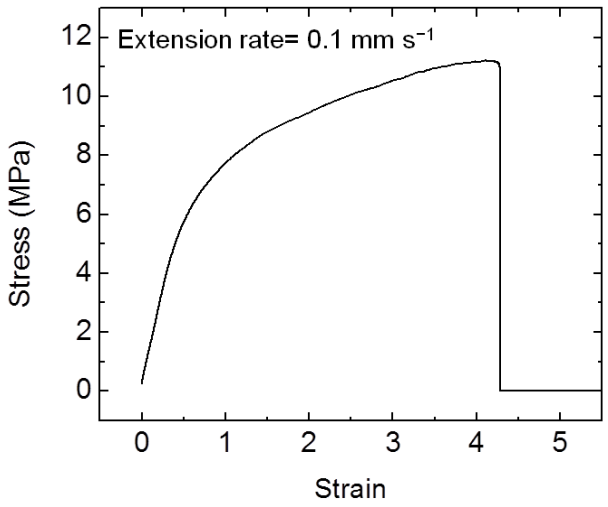

Figure 6.4 Stress *versus* strain curve for P(VDF-HFP) ion gel. Tensile tests were conducted on an ARES rheometer using solvent casted ion gels (thickness = 0.6 mm) with an extension rate of 0.1 mm/s. A Young's modulus of ~1.3 ± 0.1 MPa was measured from the initial slopes of stress-strain curves.

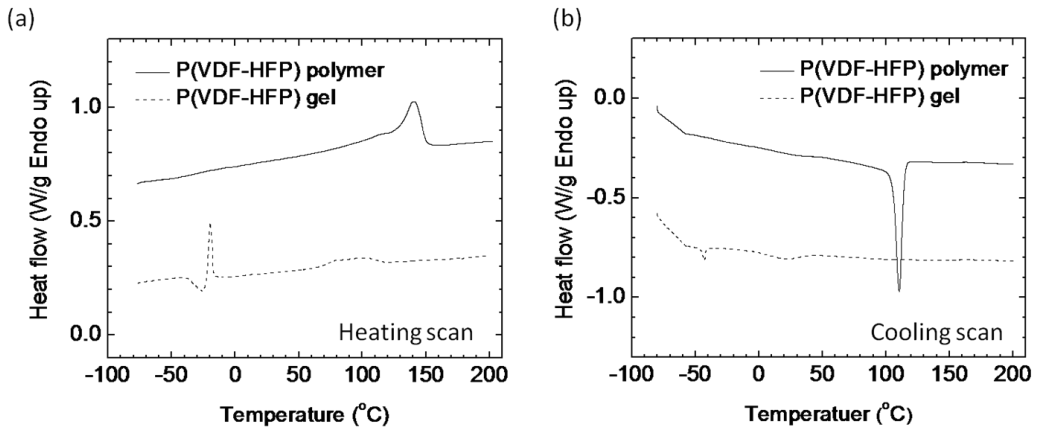

Figure 6.5 DSC thermogram of P(VDF-HFP) ion gel, and P(VDF-HFP) polymer. Curves are sifted vertically for clarity. The samples were tightly sealed in Al pans, and the measurements were carried out while heating up the sample to 200 °C, followed by cooling down to –80 °C, and reheating up to 200 °C, at a heating and cooling rate of 10 °C/min. Curves were obtained during the 2nd heating scan (a) to remove any prior thermal history and the cooling scan (b).

The specific capacitance of a 10 μm thick P(VDF-HFP) ion gel sandwiched between two gold electrodes was measured as a function of frequency ($C = -1/2\pi fZ''$, where Z'' is the imaginary impedance and f is the frequency), and the results are displayed in Figure 6.6. The measured capacitances are as large as 10 μF/cm^2 at low frequency and still remain above 1 μF/cm^2 at 100 kHz. Note that a traditional dielectric such as SiO_2 with a thickness of 300 nm shows a specific capacitance value of ~10 nF/cm^2. The large capacitance values of the ion gel result from the formation of electrical double layers at the electrode/ion gel interfaces. Moreover, the capacitance values are comparable to those of softer ion gels based on block copolymers reported previously (open symbols).[19] This suggests that the formation of double layers in ion gels is not influenced significantly by the type of structuring polymer. Capacitance values increase

with decreasing frequency, also known as capacitance dispersion. This has been attributed to the interaction between electric charges on the electrode and counterions in the electrolyte, and is typical for electrolytes in contact with solid electrodes.[36-38] It is also common to analyze impedance data with an equivalent circuit using a constant phase element (CPE); this allows a frequency independent capacitance of ~4 μF/cm^2 to be extracted.[34] This capacitance value is comparable to our previous reports and the literature values.[7,19,34,39,40]

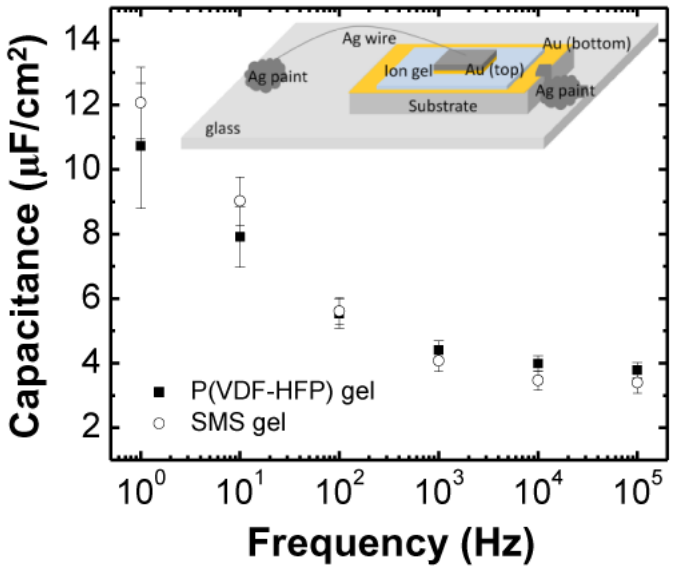

Figure 6.6 Frequency dependence of specific capacitance for a 10 μm thick free-standing ion gel based on P(VDF-HFP) random copolymer (■) and an ion gel based on poly(styrene-*b*-methyl methacrylate-*b*-styrene), (SMS), triblock copolymer (○). The molecular weights of each block are M_{PS} = 13000 and M_{PMMA} = 65000, respectively. [EMI][TFSA] was used as the ionic liquid. Inset shows schematic of an Au/ion gel/Au capacitor (not to scale).

6.4.2 Organic P3HT transistors

Top-gated transistors were fabricated by laminating the free-standing ion gel on a film of the organic semiconductor regioregular poly-3-hexylthiophene (P3HT). Au contacts were used as source and drain electrodes in a bottom-contact configuration. The conducting polymer, poly(3,4-ethylene dioxythiophene) doped with poly(styrene sulfonate), (PEDOT:PSS), was deposited on the ion gel by aerosol jet printing to serve as the gate electrode.[18] A cross-sectional schematic of the transistor is shown in Figure 6.7a. The channel length (L) and width (W) of the devices were 100 μm and 1 mm, respectively. Figure 6.7b displays an optical microscope image of a transistor. Clean edges and corners of the transferred ion gel confirm that the free-standing ion gel is easily transferable.

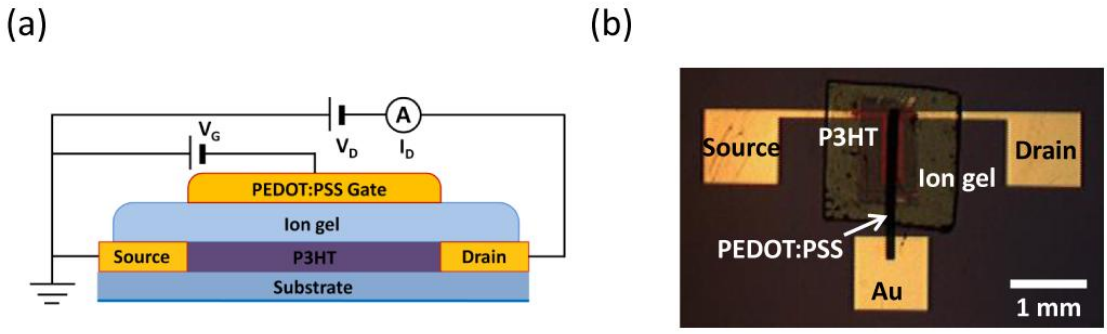

Figure 6.7 a) Cross sectional schematic of ion gel-gated organic thin-film transistor (Gel-OTFT) b) Optical image of a Gel-OTFT. The device has channel length of 100 μm and channel width of 1 mm. Au source, drain electrodes and Au pad were patterned by electron beam evaporation. P3HT was spin coated from chloroform solution. Ion gel was spin coated on a glass slide from acetone solution and then transferred onto P3HT using tweezers. PEDOT:PSS gate electrode was deposited by aerosol jet printing.

For stable device operation the ion gel needs to stick on the semiconductor channel during measurements. In this regard we tested adhesion of the gel to semiconductors (P3HT and ZnO) at 4 K by immersing the gel/semiconductor assembly upside down in liquid helium. Even through a simple lamination process, the ion gel adhered well on the surfaces for several hours at 4 K.

Figure 6.8a displays the quasi-static output characteristics (I_D−V_D, where I_D is the drain current and V_D is the drain voltage) of a free-standing ion gel based organic thin-film transistor (Gel-OTFT) at seven different gate voltages (V_Gs). The output characteristics show an increase in channel conductance with increasing V_G. Also, saturation in the drain current is observed in the high drain voltage regime. A saturation current as high as 1.5 mA is obtained at modest V_G = −1.3 V and V_D = −1 V as a result of the large capacitance of the ion gel gate dielectric.

Figure 6.8b shows the quasi-static transfer characteristic (I_D−V_G) of the OTFT. The drain current was measured while sweeping V_G from 1 V to −1.3 V and then back to 1 V at a rate of 25 mV/s at a constant V_D of −0.1 V. A small V_D was applied to ensure the device operated in the linear regime. The measured I_D in Figure 6.8b shows the expected linear dependence on V_G (open symbols). The device showed a reasonable ON/OFF current ratio of ~10^5.

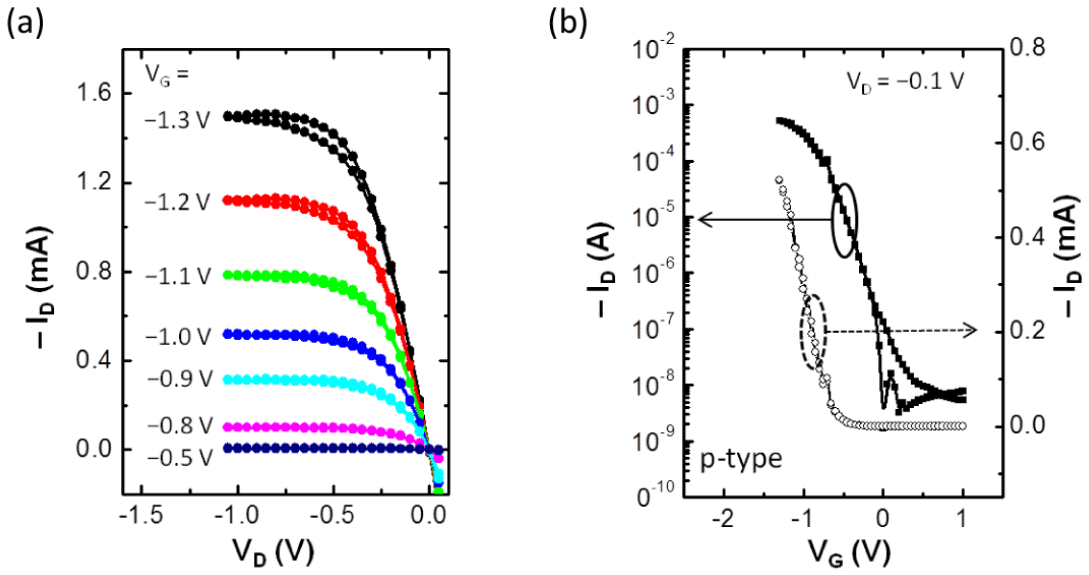

Figure 6.8 a) Quasi-static I_D-V_D characteristics of a Gel-OTFT and b) quasi-static I_D-V_G characteristics of a Gel-OTFT. The gate voltage was swept at a rate of 25 mV/s.

The hole mobility (μ) of the transistors was calculated in the linear regime using the following equation:

$$\mu = \frac{L}{W}\frac{I_D}{epV_D} \tag{6.1}$$

where e is the elementary charge, and p is the injected hole density in the semiconductor. The hole density was obtained from gate-displacement current (I_{disp}) measurements and the result is shown in Figure 6.9.[41,42] In these measurements, the source and drain contacts were connected to ground while the gate potential was swept at different rates. By plotting $\int I_{disp} dV_G/(r_V eA)$ *versus* $1/r_V$, where r_V is the sweep rate and A is the area of the ion gel, p can be obtained from the y-intercept.[41,42] Using this method, a high hole density of $\sim 1\times10^{15}$ cm^{-2} was obtained. The large value was probably due to ion penetration into the polymer semiconductor, which resulted in the formation of a three

dimensional conduction channel. (It may be more appropriate in this case to consider the 3D charge density, which we estimate to be ~2×10^{20} cm^{-3} based on the 50 nm thickness of the P3HT film).[43] The average room temperature mobility for P3HT gated with the free-standing ion gel is 1.7 ± 0.3 cm^2/Vs, which is comparable to that of P3HT using an ion gel based on block copolymers as the gate dielectric.[43,44] This mobility is significantly larger than that of a P3HT transistor gated with conventional dielectrics.[45,46] This is attributed to an exceptionally high hole density induced by the ion gel, which fills the carrier traps in the film.

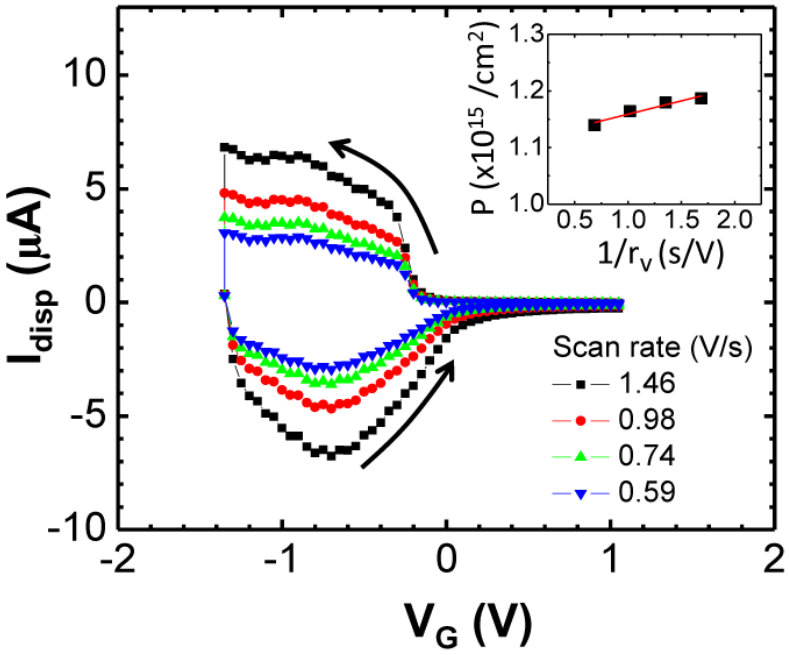

Figure 6.9 Dynamic gate-displacement current (I_{disp}) measurements with 4 different sweep rates for a top-gated P3HT Gel-OTFT. Inset shows $\int I_{disp} dV_G/(r_V eA)$ *versus* $1/r_V$ plot. Hole density (p) can be obtained from the y-intercept of the plot.

The drain current in the saturation regime was also measured at a larger drain bias of −1 V. The measured $I_D^{1/2}$ in Figure 6.10 shows the expected linear dependence on V_G. The hole mobility calculated from the slope of the $I_D^{1/2}$ *versus* V_G curve in the saturation regime is 2.3 ± 0.2 cm^2/Vs.

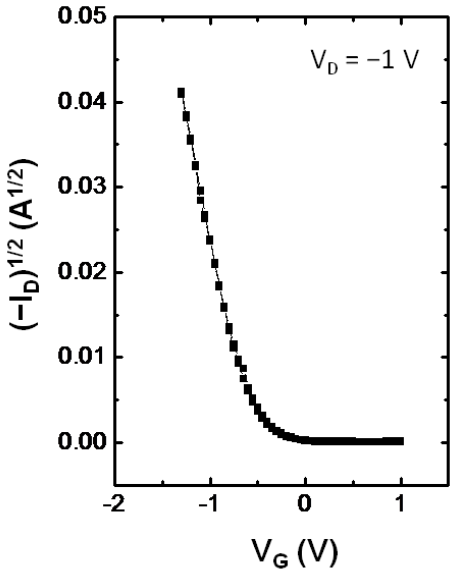

Figure 6.10 $I_D^{1/2}$–V_G graph for a top-gated P3HT Gel-OTFT in the saturation regime. Applied V_D was −1 V. The curve shows linear increase in $I_D^{1/2}$ with applied V_G. V_G was swept at a rate of 25 mV s^{-1}.

We have also fabricated a P3HT transistor using aerosol-printed P(VDF-HFP) ion gels and the results is shown in Figure 6.11a. A transistor with the printed-gel shows similar characteristics relative to a transistor with a laminated P(VDF-HFP) ion gel in Figure 6.11b. The device operates at low voltage (< 2 V) and showed a high ON/OFF current ratio of ~10^5. The devices with P(VDF-HFP) ion gels exhibit almost the same performance compared to a transistor with aerosol-printed ion gels using SMS triblock

copolymer in [EMI][TFSA] in Figure 6.11c. This is to be expected, based on the similar capacitance of the ion gel presented in Figure 6.6. The data in Figure 6.11c is regenerated from ref. 18 for comparison. In all cases, the ion gels consist mostly (more than 80 wt%) of an ionic liquid, [EMI][TFSA]. These results suggest that the charge accumulation in a semiconductor channel is not influenced significantly by the type of structuring polymers or deposition methods.

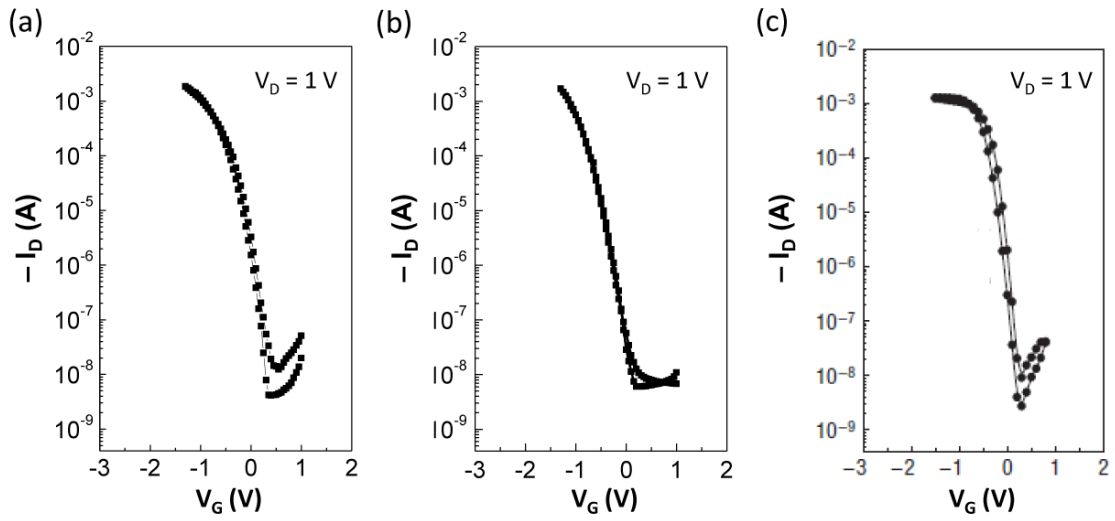

Figure 6.11 a) Quasi-static I_D-V_G characteristics of a top-gated Gel-OTFT using aerosol-printed P(VDF-HFP) gel on printed P3HT, b) laminated P(VDF-HFP) gel on the spin-coated P3HT, and c) aerosol-printed ion gel based on poly (styrene-*b*-methyl methacrylate-*b*-styrene) (SMS) triblock copolymers on printed P3HT. The transfer curve in (c) is regenerated from ref. 18 for comparison. PEDOT:PSS gate electrodes were printed on top of the ion gels. Applied V_D was −1 V. V_G was swept at rates of 25 mV/s for (a) and (b) and 50 mV/s for (c). The devices have L of 100 μm and W of 1 mm for (a) and (b), and L of 20 μm and W of 1.4 μm for (c).

We have also investigated side-gated transistors using organic P3HT as a semiconductor. To prepare a transistor, the free-standing ion gel was simply laid over a

semiconductor channel and a side-gate electrode, which is possible because of the gel's high mechanical strength. In the side-gated transistor configuration, both a gate electrode and a source-drain channel were patterned concurrently in one plane, as shown schematically in Figure 6.12. Such an unconventional device configuration has the advantage that the device-fabrication process is simple because all electrodes were patterned simultaneously, and precise alignment of the gate electrode on the semiconductor channel was not required. The channel length and the width of the side-gated devices were 100 μm and 1 mm, respectively. The gate electrode was located 700 μm away from the center of the channel. The free-standing ion gel was simply laid over the P3HT channel and the side-gate electrode.

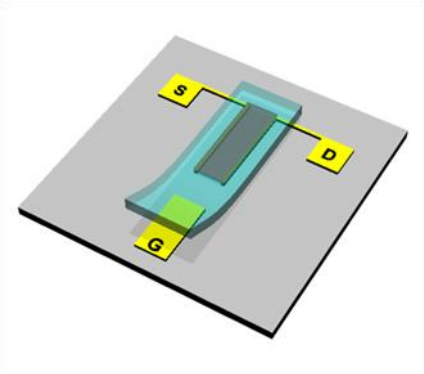

Figure 6.12 Schematic of a side-gated transistor (not to scale). The free-standing ion gel is simply laid over a semiconductor channel and a side-gate electrode to fabricate the device. This simple lamination method allows for the ion gels to be applied on any type of substrates.

Figure 6.13a displays a cross-sectional schematic (top) and an optical microscope image (bottom) of a side-gated transistor using P3HT as the semiconductor. The transfer characteristic of the P3HT transistors is shown in Figure 6.13b. A slow V_G sweep rate of

5 mV/s was used for side-gated transistors to allow sufficient time for ion migration. The transistors operate at low voltage (< 2 V) and show high ON/OFF current ratios (~10^5). In spite of the slow V_G sweep rate, current hysteresis was observed between forward and reverse sweeps in side-gated transistors. Essentially, this is due to the large effective gate-to-channel separation distance. A gate aligned over the channel should result in a faster device. The side-gated devices thus sacrifice speed for convenience. The results from P3HT transistors and our previous reports demonstrate that the ion gel can accumulate holes in organic semiconductors.[1,18,44]

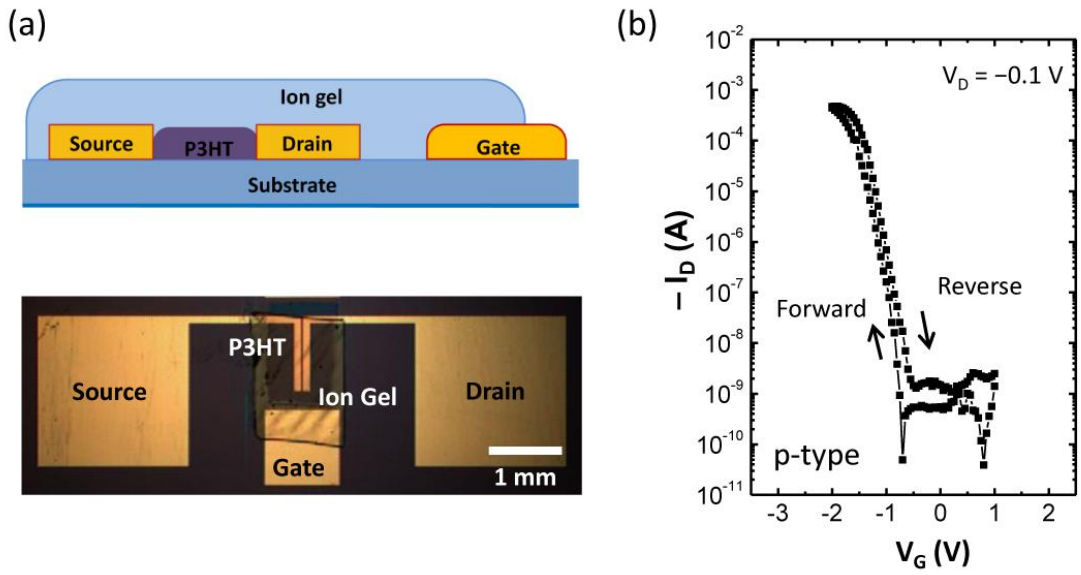

Figure 6.13 a) Schematic diagram (top) and an optical microscope image (bottom) of side-gated P3HT Gel-OTFTs. Gate electrodes are 700 μm away from the center of the channel. b) Quasi-static I_D-V_G characteristic of a side-gated P3HT transistor. The gate voltage was swept at a rate of 5 mV/s.

6.4.3 Inorganic ZnO transistors

In addition to p-type (hole transport) devices, an important objective is to demonstrate n-type (electron transport) transistors for complementary circuits with low power consumption. In this regard, an inorganic n-type ZnO was studied. A ZnO semiconductor was created by spin coating a zinc hydroxide precursor followed by sintering at 300 °C for 10 min.[32] A smooth ZnO film with surface roughness of 0.3 nm, is obtained as shown by atomic force microscopy (AFM) image in Figure 6.14.

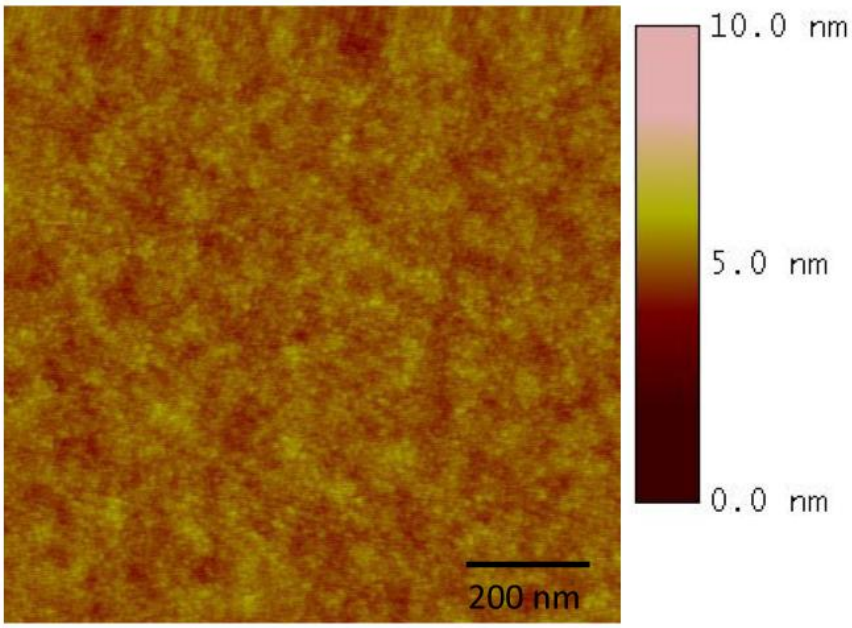

Figure 6.14 AFM height image of a ZnO film. Surface roughness of the film is 0.3 nm. Image taken by Yanfei Wu.

Output characteristics for side-gated ZnO transistors in Figure 6.15a demonstrate that the free-standing ion gel can modulate the electron current properly. The transfer curve in Figure 6.15b exhibits I_D hysteresis similar to P3HT transistors with the same configuration. A maximum drain current above 100 μA, ON/OFF current ratio of ~10^4,

and high electron mobility of 2.3±0.3 cm^2/Vs were obtained, comparable values to those of ion-gel gated ZnO transistors reported previously.[47] An ion-gel capacitance of 10.7 μF/cm^2 at 1 Hz was used for the mobility calculation. Overall, side-gated transistors broaden opportunities to exploit ion gels as the dielectric material in a wide variety of test environments.

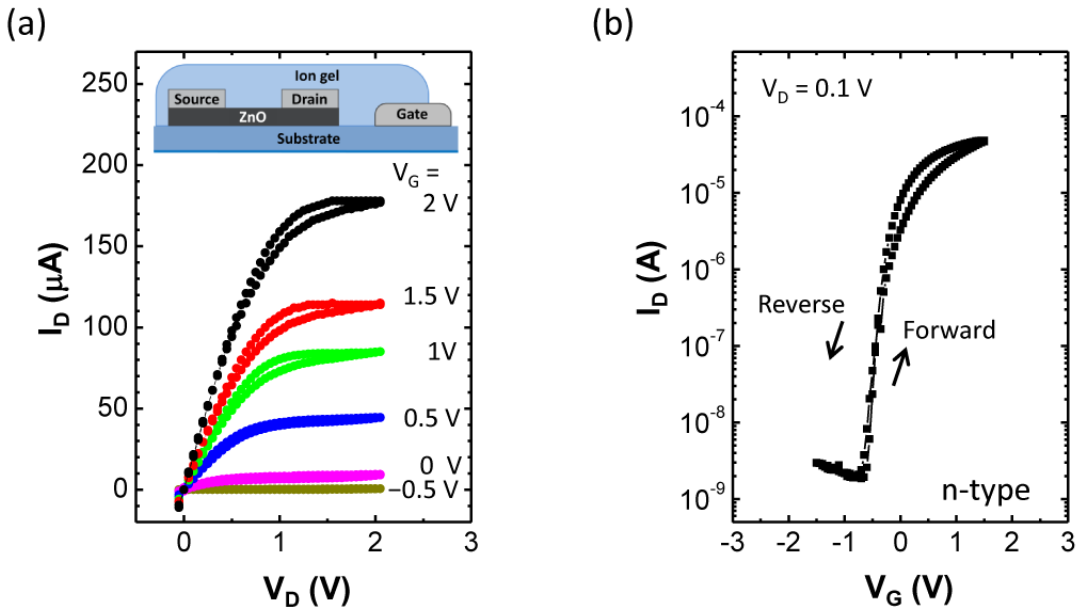

Figure 6.15 a) Quasi-static I_D-V_D and d) I_D-V_G characteristics of a side-gated ZnO transistor. Al source, drain and gate electrodes were thermally deposited after a ZnO layer was created. Inset shows schematic of a side-gated ZnO transistor. The devices had channel lengths of 100 μm and channel widths of 1 mm. The gate voltage was swept at a rate of 5 mV/s.

6.5 Summary

In this chapter, we have fabricated both organic and inorganic thin-film transistors using free-standing ion gels as the high capacitance gate dielectric layer. The ion gel

layer was transferred and laminated onto a device using tweezers, which was possible because of the gel's high mechanical strength. The capacitance of the free-standing ion gel was as large as 10 $\mu F/cm^2$ at low frequency, a value that is comparable to that of ion gels based on block copolymers and other solid polymer electrolytes consisting of PEO and lithium salts. Top-gated P3HT Gel-OTFTs operated within a low voltage range of < 1.5 V and showed a high ON/OFF current ratio of ~10^5. A convenient side-gating transistor configuration was also demonstrated using these gels. Overall, our results demonstrate that the free-standing ion gels provide a simple and solvent-free route to apply an electrolyte dielectric for transistor-gating experiments.

6.6 References

1. Lee, J.; Panzer, M. J.; He, Y.; Lodge, T. P.; Frisbie, C. D., *J. Am. Chem. Soc.* **2007,** *129,* 4532.
2. Shimotani, H.; Asanuma, H.; Tsukazaki, A.; Ohtomo, A.; Kawasaki, M.; Iwasa, Y., *Appl. Phys. Lett.* **2007,** *91*, 082106.
3. Ye, J. T.; Inoue, S.; Kobayashi, K.; Kasahara, Y.; Yuan, H. T.; Shimotani, H.; Iwasa, Y., *Nat. Mater.* **2009,** *9,* 125.
4. Kim, B. J.; Jang, H.; Lee, S.-K.; Hong, B. H.; Ahn, J.-H.; Cho, J. H., *Nano Lett.* **2010,** *10,* 3464.
5. Ohno, H., *Electrochemical aspects of ionic liquids* Wiley: Hoboken, New Jersey, 2005.
6. Galinski, M.; Lewandowski, A.; Stepniak, I., *Electrochim. Acta* **2006,** *51,* 5567.

7. Nanjundiah, C.; McDevitt, S. F.; Koch, V. R., *J. Electrochem. Soc.* **1997,** *144*, 3392.

8. Alam, M. T.; Islam, M. M.; Okajima, T.; Ohsaka, T., *J. Phys. Chem. C* **2007,** *111*, 18326.

9. Bonhote, P.; Dias, A.-P.; Papageorgiou, N.; Kalyanasundaram, K.; Gratzel, M., *Inorg. Chem.* **1996,** *35*, 1168.

10. Yuan, H.; Shimotani, H.; Tsukazaki, A.; Ohtomo, A.; Kawasaki, M.; Iwasa, Y., *Adv. Funct. Mater.* **2009,** *19*, 1046.

11. Ahn, C. H.; Triscone, J. M.; Mannhart, J., *Nature* **2003,** *424*, 1015.

12. Susan, M. A. B. H.; Kaneko, T.; Noda, A.; Watanabe, M., *J. Am. Chem. Soc.* **2005,** *127*, 4976.

13. Noda, A.; Watanabe, M., *Electrochim. Acta* **2000,** *45*, 1265.

14. Klingshirn, M. A.; Spear, S. K.; Subramanian, R.; Holbrey, J. D.; Huddleston, J. G.; Rogers, R. D., *Chem. Mater.* **2004,** *16*, 3091.

15. Matsumoto, K.; Endo, T., *Macromolecules* **2008,** *41*, 6981.

16. Lodge, T. P., *Science* **2008,** *321*, 50.

17. He, Y.; Boswell, P. G.; Buhlmann, P.; Lodge, T. P., *J. Phys. Chem. B* **2007,** *111*, 4645.

18. Cho, J. H.; Lee, J.; Xia, Y.; Kim, B.; He, Y.; Renn, M. J.; Lodge, T. P.; Daniel Frisbie, C., *Nat. Mater.* **2008,** *7*, 900.

19. Lee, K. H.; Zhang, S.; Lodge, T. P.; Frisbie, C. D., *J. Phys. Chem. B* **2011,** *115*, 3315.

20. Sekitani, T.; Noguchi, Y.; Hata, K.; Fukushima, T.; Aida, T.; Someya, T., *Science* **2008,** *321*, 1468.

21. Fuller, J.; Breda, A. C.; Carlin, R. T., *J. Electrochem. Soc.* **1997,** *144*, L67.

22. Ogihara, W.; Sun, J.; Forsyth, M.; MacFarlane, D. R.; Yoshizawa, M.; Ohno, H., *Electrochim. Acta* **2004,** *49*, 1797.

23. Singh, B.; Sekhon, S. S., *J. Phys. Chem. B* **2005,** *109*, 16539.

24. Wang, P.; Zakeeruddin, S. M.; Exnar, I.; Grätzel, M., *Chem. Commun.* **2002,** 2972.

25. Bansal, D.; Cassel, F.; Croce, F.; Hendrickson, M.; Plichta, E.; Salomon, M., *J. Phys. Chem. B* **2005,** *109*, 4492.

26. Yeon, S.-H.; Kim, K.-S.; Choi, S.; Cha, J.-H.; Lee, H., *J. Phys. Chem. B* **2005,** *109*, 17928.

27. Sekhon, S. S.; Lalia, B. S.; Park, J.-S.; Kim, C.-S.; Yamada, K., *J. Mater. Chem.* **2006,** *16*.

28. Ye, H.; Huang, J.; Xu, J. J.; Khalfan, A.; Greenbaum, S. G., *J. Electrochem. Soc.* **2007,** *154*, A1048.

29. Kim, D.-W.; Sivakkumar, S. R.; MacFarlane, D. R.; Forsyth, M.; Sun, Y.-K., *J. Power Sources* **2008,** *180*, 591.

30. Randriamahazaka, H.; Asaka, K., *J. Phys. Chem. C* **2010,** *114*, 17982.

31. Shimamura, K.; Chiba, D.; Ono, S.; Fukami, S.; Ishiwata, N.; Kawaguchi, M.; Kobayashi, K.; Ono, T., *Appl. Phys. Lett.* **2012,** *100*, 122402.

32. Meyers, S. T.; Anderson, J. T.; Hung, C. M.; Thompson, J.; Wager, J. F.; Keszler, D. A., *J. Am. Chem. Soc.* **2008,** *130*, 17603.

33. Jansen, J. C.; Friess, K.; Clarizia, G.; Schauer, J.; Izák, P., *Macromolecules* **2011,** *44*, 39.

34. Zhang, S.; Lee, K. H.; Frisbie, C. D.; Lodge, T. P., *Macromolecules* **2011,** *44*, 940.

35. Zhang, S.; Lee, K. H.; Sun, J.; Frisbie, C. D.; Lodge, T. P., *Macromolecules* **2011,** *44*, 8981.

36. Pajkossy, T., *J. Electroanal. Chem.* **1994,** *364*, 111.

37. Kerner, Z.; Pajkossy, T., *Electrochim. Acta* **2000,** *46*, 207.

38. Pajkossy, T., *Solid State Ionics* **2005,** *176*, 1997.

39. Drüschler, M.; Huber, B.; Passerini, S.; Roling, B., *J. Phys. Chem. C* **2010,** *114*, 3614.

40. Alam, M. T.; Islam, M. M.; Okajima, T.; Ohsaka, T., *J. Phys. Chem. C* **2008,** *112*, 16600.

41. Liang, Y.; Frisbie, C. D.; Chang, H.-C.; Ruden, P. P., *J. Appl. Phys.* **2009,** *105*, 024514.

42. Xie, W.; Frisbie, C. D., *J. Phys. Chem. C* **2011,** *115*, 14360.

43. Lee, J.; Kaake, L. G.; Cho, J. H.; Zhu, X. Y.; Lodge, T. P.; Frisbie, C. D., *J. Phys. Chem. C* **2009,** *113*, 8972.

44. Cho, J. H.; Lee, J.; He, Y.; Kim, B. S.; Lodge, T. P.; Frisbie, C. D., *Adv. Mater.* **2008,** *20*, 686.

45. Bao, Z.; Dodabalapur, A.; Lovinger, A. J., *Appl. Phys. Lett.* **1996,** *69*, 4108.

46. Sirringhaus, H.; Brown, P. J.; Friend, R. H.; Nielsen, M. M.; Bechgaard, K.; Langeveld-Voss, B. M. W.; Spiering, A. J. H.; Janssen, R. A. J.; Meijer, E. W.; Herwig, P.; de Leeuw, D. M., *Nature* **1999,** *401*, 685.

47. Bong, H.; Lee, W. H.; Lee, D. Y.; Kim, B. J.; Cho, J. H.; Cho, K., *Appl. Phys. Lett.* **2010,** *96*, 192115.

Chapter 7

Summary and Outlook

7.1 Summary

The objective of this thesis project is to study electrical and mechanical properties of ionic-liquid based polymer gel electrolytes (ion gels) to better understand the operation mechanisms of ion-gel gated transistors, and to develop new routes to employ an ion gel layer on transistors. An ion gel consists of a structuring polymer network infused in an ionic liquid. In this composite, polymers impart a solid, rubbery network with tunable mechanical properties, while ionic liquids provide high ionic conductivity and capacitance.

For the first goal, the electrical properties of ion gels were studied systematically to understand how the ion gel works as a capacitor for transistors and to further improve the device performance. As a result, resistance, specific capacitance, and conductivity of ion gels were successfully characterized as a function of film geometry (thickness and area) and temperature. As expected, the resistance was directly proportional to the thickness and the reciprocal area, whereas the specific capacitance and conductivity were independent of the film geometry. The polarization response time, or *RC* time constant, that is inversely proportional to the maximum device operating frequency, decreased when reducing the thickness of ion gel films. For the thinnest spin-coated ion gels (~2 μm thick) an *RC* time constant of ~3 μs was achieved. Conductivity and capacitance of the ion gels both increased with increasing temperature. The conductivity increase with

temperature was much stronger than the capacitance increase with temperature. This result implies that *RC* time constant will decrease, and as a result the device operating speed will increase with increasing temperature.

This thesis research also aimed to develop new routes to incorporate an ion gel layer on a device to provide diversity and universality in ion gel processing. The first effort was devoted to preparing smooth and uniform ion gels by spin casting. Through this method ion gels with typical thickness of 1~20 μm were successfully prepared. Spin-coated films were used to study the electrical properties of the ion gels, as described in Chapter 4. The technique was also employed to deposit ion gels on a patterned PDMS stamp for transfer printing (Chapter 5) and to create micrometer-thick free-standing ion gels (Chapter 6).

By using a thermoresponsive gel consisting of poly(styrene-*b*-ethylene oxide-*b*-styrene) SOS block polymer and 1-ethyl-3-methylimidazolium bis(trifluoromethylsulfonyl)amide [EMI][TFSA], hexagonal, square, and triangular ion gels with two different thicknesses (0.8 and 1.5 μm) were successfully transfer-printed on three different substrates (polyimide, PET and SiO_2), as demonstrated in Chapter 5. In this process, an elastomeric PDMS stamp was used to transfer the gel layer from a donor stamp to a receiving substrate. Using this ion gel as a gate insulator, organic thin-film transistors were fabricated on SiO_2 and flexible polyimide. The other two layers (P3HT semiconductor and PEDOT:PSS gate electrode) of a transistor were created using the same transfer-printing method. The transistors operated at low voltage (< 1 V) with a high ON/OFF current ratio (~10^5).

Alternatively, mechanically free-standing ion gels that can be cut by hand and laminated on a semiconductor using tweezers were demonstrated. The ion gel consists of a structuring poly(vinylidene fluoride-*co*-hexafluoropropylene) P(VDF-HFP) polymer swollen in [EMI][TFSA]. With this ion gel a convenient side-gate configuration (side-gate transistor) was realized by simply laying the free-standing gel over a semiconductor and a side-gate electrode. Both organic (P3HT) and inorganic (ZnO) transistors were successfully fabricated, demonstrating the free-standing ion gel can induce both holes and electrons in P3HT and ZnO semiconductors, respectively. All three processes developed in this thesis provide reliable routes to incorporate ion gels on electrical and electrochemical devices including thin-film transistors.

7.2 Outlook

From an applications perspective, it is desirable for ion gels to have several features such as high capacitance, wide electrochemical-stability window, air stability, solution processability or printability, fast response to external signal, and accumulation of both electrons and holes. Recent research efforts including this thesis expand the knowledge about the ion gels including mechanical and electrical properties, device operating speed, deposition methods and practical application in thin-film transistors. However, there are still several research directions to pursue for these gel electrolytes and ion-gel gated transistors.

7.2.1 Mechanical stability of ion gel gated transistors

There has been increasing interest in stretchable and flexible electronics to realize electric circuits on curved surfaces or movable parts.[1-9] Ion-gel gated organic transistors can provide a solution for these applications because they can potentially be bendable, rollable and stretchable. In this regard, it is worthwhile to perform mechanical stability tests on ion gel gated transistors. These experiments might include inward and outward bending, stretching and twisting modes, as shown in Figure 7.1. In the bending tests, plastic substrates such as polyimide and PET can be employed to fabricate transistors. In the measurement, transistor characteristics with different bending radii and the number of stress cycles would be interesting to investigate. In stretching and twisting experiments, however, rubbery substrates such as PMDS (thickness ~1 mm) might be more appropriate to prevent substrate failure upon external stresses.[10] For these tests, stretching/twisting speed and extent/number of deformations can be changed to study the corresponding effects on transistor characteristics.

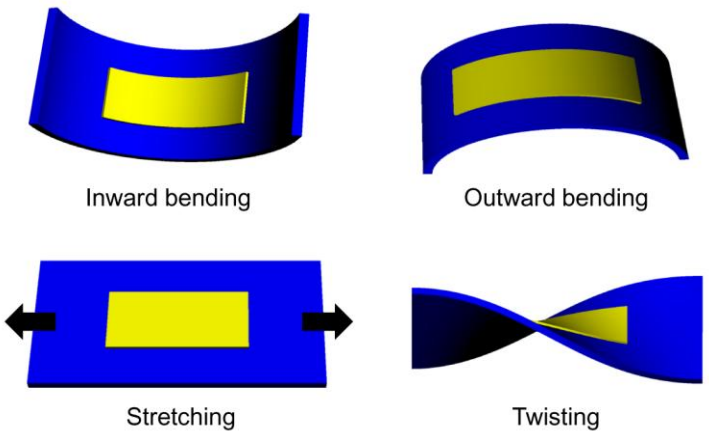

Figure 7.1 Schematic modes of mechanical stability tests: inward and outward bending, stretching and twisting modes.

7.2.2 Ion gel gated n-type transistors and complementary circuits

Most previous results on ion-gel gated transistors focus mainly on p-type (hole conducting) semiconductors.[11-14] However, to make complementary circuits that operate at low voltage and consume low power, n-channel (electron conducting) transistors need to be demonstrated using ion gels. Based on the results presented in Chapter 6, a solution processable ZnO semiconductor can be a candidate to realize hybrid organic/inorganic complementary circuits. Figure 7.2 shows output (I_D–V_D) and transfer curve (I_D–V_G) for a top-gated ZnO transistor prepared by aerosol jet printing on Au source/drain electrodes. The device has a channel length and width of 100 μm and 1 mm, respectively. The device exhibits low voltage operation (< 1.5 V) and high ON to OFF current ratio (10^5).

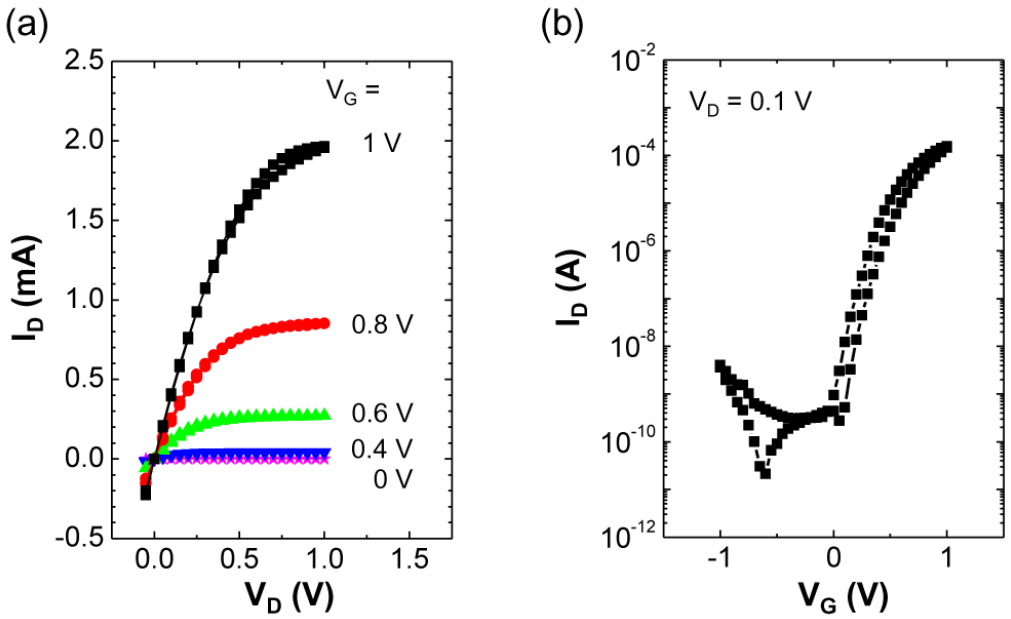

Figure 7.2 a) I_D-V_D and b) I_D-V_G characteristics of an aerosol printed ZnO transistor. The device had a channel length and width of 100 μm and 1 mm, respectively. The gate voltage was swept at a rate of 0.1 V/s.

Figure 7.3 shows a schematic circuit diagram of a complementary inverter based on p-channel (P3HT) and n-channel (ZnO) transistors and the resulting input−output voltage (V_{in}–V_{out}) characteristic at V_{supply} = 2 V. Both transistors were prepared by aerosol jet printing with channel lengths and widths of 70 and 500 μm, respectively. The hybrid inverter shows a good inverting characteristic, where the output voltage was switched between the supply voltage (2 V) and the ground (0 V) when the input gate voltage was swept from 0 V to 2 V and back to 0 V. Based on this P3HT/ZnO complementary inverter, various logic circuits including NAND, NOR, NOT, and ring oscillators can be realized.

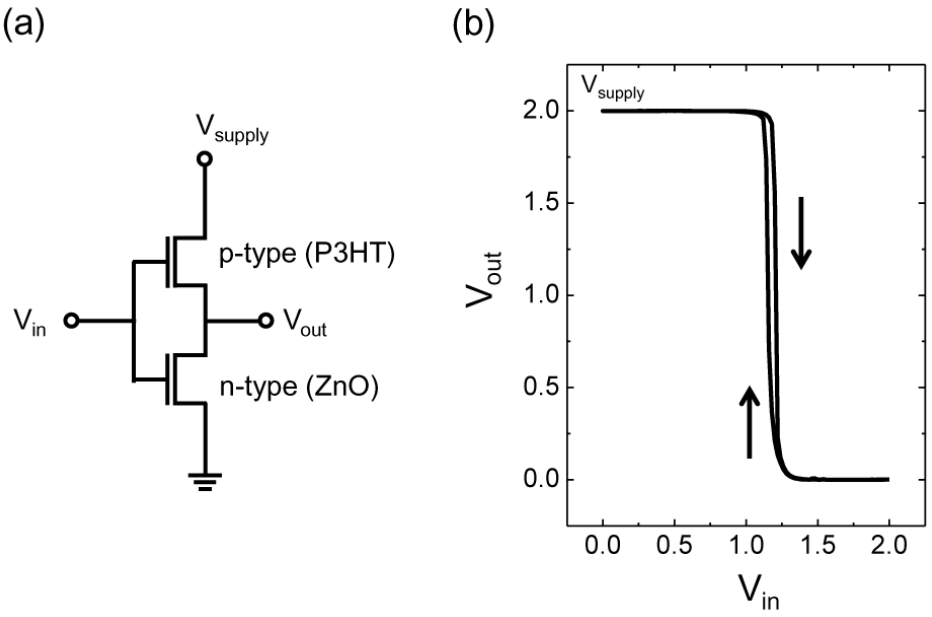

Figure 7.3 a) Schematic circuit diagram of a complementary inverter based on p-channel (P3HT) and n-channel (ZnO) transistors and b) the resulting input−output voltage characteristic at V_{supply} = 2 V.

However, the mechanical stability of inorganic ZnO transistors turned out to be relatively poor compared to organic P3HT transistors in outward bending tests with a bending radius of 0.5 cm. The channel currents (I_Ds) for ZnO transistors decreased to ~70 % of their initial current after 10,000 bending cycles, whereas I_Ds for P3HT transistors remained unchanged. This result indicates that inorganic ZnO semiconductor might not be a proper n-type semiconductor for flexible electronics because it is inherently brittle. This issue could be addressed by incorporating organic n-type semiconductors. Among various kinds of the organic n-channel materials, N,N"-bis(n-alkyl)-(1,7 and 1,6)-dicyanoperylene-3,4:9,10-bis (dicarboximide)s (PDIF-CN2),[15] poly{[*N*,*N'*-bis(2-octyldodecyl)- naphthalene - 1,4,5,8 - bis(dicarboximide) - 2,6 - diyl]-*alt* - 5,5' -(2,2'-bithiophene)} P(NDI2OD-T2),[16,17] 7,7,8,8-tetracyanoquinodimethane (TCNQ)[18] and fullerene (C_{60})[18] semiconductors can be considered first because they have been reported to be gated with electrolytes. To efficiently inject electrons into the lowest unoccupied molecular orbit (LUMO) of these semiconductors (typically at ~2−3 eV), low work function metals such as calcium, magnesium and aluminum might need to be used.

7.2.3 Patterning chemically crosslinkable ion gels

As described in Chapter 5, thermoresponsive SOS and poly(N-isopropyl acrylamide-*b*-styrene-*b*-ethylene oxide-*b*-styrene-*b*-N-isopropyl acrylamide) NSOSN gels were successfully transfer-printed and incorporated in thin-film transistors. In the printing process the gels needed to be heated at temperatures above the gelation temperature (T_{gel}) of the ion gels to achieve physical contact between the gels and substrates. For SOS and NSOSN gels used in Chapter 5, T_{gel}s were 80 and 50 °C, respectively.[19] From the process

point of view, thermoresponsiveness of the ion gels is helpful as described previously. However, this property might be detrimental to mechanical stability of the transfer-printed ion gels because at $T > T_{gel}$ the gels can potentially be melted and flow. This issue can be addressed by using the chemically corsslinkable block-polymer based ion gels recently developed in the Lodge and Frisbie groups. In this ion gel, a chemically crosslinkable azide functionality is introduced into polystyrene (PS) end blocks. Before chemical crosslinking, the gel shows the typical characteristics of thermoresponsive gels (solid-like gels at low temperature and liquid-like response at high temperature). After a chemical gel is obtained by thermal curing at 200 °C, however, the ion gel will retain the network structure because PS chains are locked inside of the micelle cores. Therefore this chemical gel could provide advantages of both physical (*e.g.* easy process) and chemical (*e.g.* persistent structure) gels when transfer printing is employed to deposit ion gels on transistors.

The chemically crosslinkable ion gel can also provide another processing option: photopatterning of an ion gel.[20] It has been reported that an azide group can be chemically corsslinked by UV light (λ = 254 nm).[21] This ion gel may be compatible with roll-to-roll (R2R) processes. In the R2R patterning process, a uniform layer of a physical gel is deposited on a substrate by doctor blading or spin coating. UV light is then irradiated on the ion gel-coated substrate through a patterned mask to chemically crosslink the ion gel. Only chemically crosslinked ion gel will remain after removing uncrosslinked regions with solvent (*e.g.* methylene chloride or ethyl acetate). One challenge in the UV crosslinking is component ionic liquids can be degraded by UV

irradiation. It has been reported that imidazolium- and pyridinium-based ionic liquids can absorb UV light (*e.g.* [EMI][TFSA] shows a strong absorption peak at λ = 211 nm).[22] In this regard, optimization of UV irradiating condition such as light intensity and exposure time is needed to achieve photopatterned ion gels without damaging component ionic liquids.

7.3 References

1. Hamedi, M.; Forchheimer, R.; Inganas, O., *Nat. Mater.* **2007**, *6*, 357.
2. Sekitani, T.; Someya, T., *Adv. Mater.* **2010**, *22*, 2228.
3. Sekitani, T.; Noguchi, Y.; Hata, K.; Fukushima, T.; Aida, T.; Someya, T., *Science* **2008**, *321*, 1468.
4. Someya, T.; Sekitani, T.; Iba, S.; Kato, Y.; Kawaguchi, H.; Sakurai, T., *Proc. Natl. Acad. Sci. USA* **2004**, *101*, 9966.
5. Forrest, S. R., *Nature* **2004**, *428*, 911.
6. Cao, Q.; Kim, H. S.; Pimparkar, N.; Kulkarni, J. P.; Wang, C.; Shim, M.; Roy, K.; Alam, M. A.; Rogers, J. A., *Nature* **2008**, *454*, 495.
7. Kim, D.-H.; Viventi, J.; Amsden, J. J.; Xiao, J.; Vigeland, L.; Kim, Y.-S.; Blanco, J. A.; Panilaitis, B.; Frechette, E. S.; Contreras, D.; Kaplan, D. L.; Omenetto, F. G.; Huang, Y.; Hwang, K.-C.; Zakin, M. R.; Litt, B.; Rogers, J. A., *Nat. Mater.* **2010**, *9*, 511.
8. Kim, D.-H.; Lu, N.; Ghaffari, R.; Kim, Y.-S.; Lee, S. P.; Xu, L.; Wu, J.; Kim, R.-H.; Song, J.; Liu, Z.; Viventi, J.; de Graff, B.; Elolampi, B.; Mansour, M.; Slepian,

M. J.; Hwang, S.; Moss, J. D.; Won, S.-M.; Huang, Y.; Litt, B.; Rogers, J. A., *Nat. Mater.* **2011**, *10*, 316.

9. Briseno, A. L.; Mannsfeld, S. C. B.; Ling, M. M.; Liu, S.; Tseng, R. J.; Reese, C.; Roberts, M. E.; Yang, Y.; Wudl, F.; Bao, Z., *Nature* **2006**, *444*, 913.

10. Kim, D.-H.; Song, J.; Choi, W. M.; Kim, H.-S.; Kim, R.-H.; Liu, Z.; Huang, Y. Y.; Hwang, K.-C.; Zhang, Y.-w.; Rogers, J. A., *Proc. Natl. Acad. Sci. USA* **2008**, *105*, 18675.

11. Lee, J.; Panzer, M. J.; He, Y.; Lodge, T. P.; Frisbie, C. D., *J. Am. Chem. Soc.* **2007**, *129*, 4532.

12. Cho, J. H.; Lee, J.; He, Y.; Kim, B. S.; Lodge, T. P.; Frisbie, C. D., *Adv. Mater.* **2008**, *20*, 686.

13. Cho, J. H.; Lee, J.; Xia, Y.; Kim, B.; He, Y.; Renn, M. J.; Lodge, T. P.; Frisbie, C. D., *Nat. Mater.* **2008**, *7*, 900.

14. Lee, J.; Kaake, L. G.; Cho, J. H.; Zhu, X. Y.; Lodge, T. P.; Frisbie, C. D., *J. Phys. Chem. C* **2009**, *113*, 8972.

15. Ono, S.; Minder, N.; Chen, Z.; Facchetti, A.; Morpurgo, A. F., *Appl. Phys. Lett.* **2010**, *97*, 143307.

16. Malti, A.; Gabrielsson, E. O.; Berggren, M.; Crispin, X., *Appl Phys. Lett.* **2011**, *99*, 063305.

17. Herlogsson, L.; Crispin, X.; Tierney, S.; Berggren, M., *Adv. Mater.* **2011**, *23*, 4684.

18. Uemura, T.; Yamagishi, M.; Ono, S.; Takeya, J., *Appl. Phys. Lett.* **2009**, *95*, 103301.

19. He, Y.; Lodge, T. P., *Macromolecules* **2008**, *41*, 167.

20. Lee, S. W.; Lee, H. J.; Choi, J. H.; Koh, W. G.; Myoung, J. M.; Hur, J. H.; Park, J. J.; Cho, J. H.; Jeong, U., *Nano Lett.* **2009**, *10*, 347.

21. Lee, S.; Lee, B.; Kim, B. J.; Park, J.; Yoo, M.; Bae, W. K.; Char, K.; Hawker, C. J.; Bang, J.; Cho, J., *J. Am. Chem. Soc.* **2009**, *131*, 2579.

22. Wang, C.; Luo, H.; Li, H.; Dai, S., *Phys. Chem. Chem. Phys.* **2010**, *12*, 7246.

Bibliography

- Abbott, A. P., *ChemPhysChem* **2004**, *5*, 1242.
- Abbott, A. P., *ChemPhysChem.* **2005**, *6*, 2502.
- Abedin, S. Z. E.; Endres, F., *Acc. Chem. Res.* **2007**, *40*, 1106.
- Adebahr, J.; Best, A. S.; Byrne, N.; Jacobsson, P.; MacFarlane, D. R.; Forsyth, M., *Phys. Chem. Chem. Phys.* **2003**, *5*, 720.
- Ahn, C. H.; Triscone, J. M.; Mannhart, J., *Nature* **2003**, *424*, 1015.
- Alam, M. T.; Islam, M. M.; Okajima, T.; Ohsaka, T., *J. Phys. Chem. C* **2007**, *111*, 18326.
- Alam, M. T.; Islam, M. M.; Okajima, T.; Ohsaka, T., *J. Phys. Chem. C* **2008**, *112*, 16600.
- Armand, M.; Endres, F.; MacFarlane, D. R.; Ohno, H.; Scrosati, B., *Nat. Mater.* **2009**, *8*, 621.
- Baldelli, S., *J. Phys. Chem. B* **2005**, *109*, 13049.
- Baldelli, S., *Acc. Chem. Res.* **2008**, *41*, 421.
- Balducci, A.; Bardi, U.; Caporali, S.; Mastragostino, M.; Soavi, F., *Electrochem. Commun.* **2004**, *6*, 566.
- Bansal, D.; Cassel, F.; Croce, F.; Hendrickson, M.; Plichta, E.; Salomon, M., *J. Phys. Chem. B* **2005**, *109*, 4492.
- Bao, Z.; Dodabalapur, A.; Lovinger, A. J., *Appl. Phys. Lett.* **1996**, *69*, 4108.
- Bao, Z.; Dodabalapur, A.; Lovinger, A. J., *Appl. Phys. Lett.* **1996**, *69*, 4108.

- Bard, A. J.; Faulkner, L. R., *Electrochemical Methods: Fundamentals and Applications*. Wiley: New York, 2001.
- Berns, B.; Deligöz, H.; Tieke, B.; Kremer, F., *Macromol. Mater. Eng.* **2008**, *293*, 409.
- Boda, D.; Henderson, D.; Chan , K.-Y., *J. Chem. Phys.* **1999**, *110*, 5346.
- Bong, H.; Lee, W. H.; Lee, D. Y.; Kim, B. J.; Cho, J. H.; Cho, K., *Appl. Phys. Lett.* **2010**, *96*, 192115.
- Bonhote, P.; Dias, A.-P.; Papageorgiou, N.; Kalyanasundaram, K.; Gratzel, M., *Inorg. Chem.* **1996**, *35*, 1168.
- Brandrup, J.; Immergut, E. H.; Grulke, E. A., *Polymer Handbook* Wiley-Interscience: New York, 1999; Vol. 4th ed.
- Brattain, W. H.; Garrett, C. G. B., *Bell. Telephone Syst. Tech. Publ. Monogr.* **1955**, *2372*, 1.
- Brattain, W. H.; Gibney, R. B. *US patent 2,524,034*, **1948**.
- Briseno, A. L.; Mannsfeld, S. C. B.; Ling, M. M.; Liu, S.; Tseng, R. J.; Reese, C.; Roberts, M. E.; Yang, Y.; Wudl, F.; Bao, Z., *Nature* **2006**, *444*, 913.
- Brug, G. J.; van den Eeden, A. L. G.; Sluyters-Rehbach, M.; Sluyters, J. H., *J. Electroanal. Chem.* **1984**, *176*, 275.
- Buzzeo, M. C.; Hardacre, C.; Compton, R. G., *ChemPhysChem.* **2006**, *7*, 176.
- Cao, Q.; Kim, H. S.; Pimparkar, N.; Kulkarni, J. P.; Wang, C.; Shim, M.; Roy, K.; Alam, M. A.; Rogers, J. A., *Nature* **2008**, *454*, 495.
- Chao, S.; Wrighton, M. S., *J. Am. Chem. Soc.* **1987**, *109*, 2197.

- Chao, S.; Wrighton, M. S., *J. Am. Chem. Soc.* **1987**, *109*, 6627.
- Chen, L.; Degenaar, P.; Bradley, D. D. C., *Adv. Mater.* **2008**, *20*, 1679.
- Cheng, H.-C.; Chen, C.-F.; Lee, C.-C., *Thin Solid Films* **2006**, *498*, 142.
- Cheng, J.-A.; Chuang, C.-S.; Chang, M.-N.; Tsai, Y.-C.; Shieh, H.-P. D., *Org. Electron.* **2008**, *9*, 1069.
- Cheung, I. W.; Chin, K. B.; Greene, E. R.; Smart, M. C.; Abbrent, S.; Greenbaum, S. G.; Prakash, G. K. S.; Surampudi, S., *Electrochim. Acta* **2003**, *48*, 2149.
- Cho, J. H.; Lee, J.; He, Y.; Kim, B. S.; Lodge, T. P.; Frisbie, C. D., *Adv. Mater.* **2008**, *20*, 686.
- Cho, J. H.; Lee, J.; Xia, Y.; Kim, B.; He, Y.; Renn, M. J.; Lodge, T. P.; Frisbie, C. D., *Nat. Mater.* **2008**, *7*, 900.
- Cosseddu, P.; Bonfiglio, A., *Appl. Phys. Lett.* **2006**, *88*, 023506.
- Costa, R.; Pereira, C. M.; Silva, F., *Phys. Chem. Chem. Phys.* **2010**, *12*, 11125.
- Cussler, E. L., *Diffusion: Mass Transfer in Fluid Systems*. Cambridge University Press: New York, 1997.
- Daniel, V. V., *Dielectric Relaxation* Academic Press: London and New York 1965.
- de Souza, R. F.; Padilha, J. C.; Gonçalves, R. S.; Dupont, J., *Electrochem. Commun.* **2003**, *5*, 728.
- Dhoot, A. S.; Israel, C.; Moya, X.; Mathur, N. D.; Friend, R. H., *Phys. Rev. Lett.* **2009**, *102*, 136402.

- DiBenedetto, S. A.; Frattarelli, D.; Ratner, M. A.; Facchetti, A.; Marks, T. J., *J. Am. Chem. Soc.* **2008**, *130*, 7528.
- DiBenedetto, S. A.; Frattarelli, D. L.; Facchetti, A.; Ratner, M. A.; Marks, T. J., *J. Am. Chem. Soc.* **2009**, *131*, 11080.
- Drüschler, M.; Huber, B.; Passerini, S.; Roling, B., *J. Phys. Chem. C* **2010**, *114*, 3614.
- Dzyuba, S. V.; Bartsch, R. A., *ChemPhysChem.* **2002**, *3*, 161.
- Emah, J. B.; Curry, R. J.; Silva, S. R. P., *Appl. Phys. Lett.* **2008**, *93*, 103301.
- Every, H.; Bishop, A. G.; Forsyth, M.; MacFarlane, D. R., *Electrochim. Acta* **2000**, *45*, 1279.
- Every, H. A.; Bishop, A. G.; MacFarlane, D. R.; Oradd, G.; Forsyth, M., *Phys. Chem. Chem. Phys.* **2004**, *6*, 1758.
- Facchetti, A., *Nat. Mater*. **2008**, *7*, 839.
- Fedorov, M. V.; Kornyshev, A. A., *Electrochim. Acta* **2008**, *53*, 6835.
- Forrest, S. R., *Nature* **2004**, *428*, 911.
- Freemantle, M., *Chem. Eng. News* **1998**, *76*, 32.
- Fry, A. J., *J. Electroanal. Chem.* **2003**, *546*, 35.
- Fukushima, T.; Kosaka, A.; Ishimura, Y.; Yamamoto, T.; Takigawa, T.; Ishii, N.; Aida, T., *Science* **2003**, *300*, 2072.
- Fuller, J.; Breda, A. C.; Carlin, R. T., *J. Electrochem. Soc.* **1997**, *144*, L67.
- Galinski, M.; Lewandowski, A.; Stepniak, I., *Electrochim. Acta* **2006**, *51*, 5567.
- Garnier, F.; Hajlaoui, R.; Yassar, A.; Srivastava, P., *Science* **1994**, *265*, 1684.

- Gary, F. M., *Solid polymer electrolytes: fundamentals and technological applications*. Wiley-VCH: New York, 1991.
- Gelinck, G. H.; Huitema, H. E. A.; van Veenendaal, E.; Cantatore, E.; Schrijnemakers, L.; van der Putten, J. B. P. H.; Geuns, T. C. T.; Beenhakkers, M.; Giesbers, J. B.; Huisman, B.-H.; Meijer, E. J.; Benito, E. M.; Touwslager, F. J.; Marsman, A. W.; van Rens, B. J. E.; de Leeuw, D. M., *Nat. Mater.* **2004**, *3*, 106.
- Granlund, T.; Nyberg, T.; Stolz Roman, L.; Svensson, M.; Inganäs, O., *Adv. Mater.* **2000**, *12*, 269.
- Graves, A. D.; Inman, D., *J. Electroanal. Chem.* **1970**, *25*, 357.
- Guilherme, L. A.; Borges, R. S.; Moraes, E. M. S.; Silva, G. G.; Pimenta, M. A.; Marletta, A.; Silva, R. A., *Electrochim. Acta* **2007**, *53*, 1503.
- Ha, M.; Frisbie, C. D., *Manuscript in preparation*.
- Ha, M.; Xia, Y.; Green, A. A.; Zhang, W.; Renn, M. J.; Kim, C. H.; Hersam, M. C.; Frisbie, C. D., *ACS Nano* **2010**, *4*, 4388.
- Halik, M.; Klauk, H.; Zschieschang, U.; Schmid, G.; Dehm, C.; Schutz, M.; Maisch, S.; Effenberger, F.; Brunnbauer, M.; Stellacci, F., *Nature* **2004**, *431*, 963.
- Hamedi, M.; Forchheimer, R.; Inganas, O., *Nat. Mater.* **2007**, *6*, 357.
- Hapiot, P.; Lagrost, C., *Chem. Rev.* **2008**, *108*, 2238.
- He, Y.; Boswell, P. G.; Buhlmann, P.; Lodge, T. P., *J. Phys. Chem. B* **2007**, *111*, 4645.
- He, Y.; Lodge, T. P., *Chem. Commun.* **2007**, 2732.
- He, Y.; Lodge, T. P., *Macromolecules* **2008**, *41*, 167.

- Herlogsson, L.; Crispin, X.; Robinson, N. D.; Sandberg, M.; Hagel, O. J.; Gustafsson, G.; Berggren, M., *Adv. Mater.* **2007**, *19*, 97.
- Herlogsson, L.; Crispin, X.; Tierney, S.; Berggren, M., *Adv. Mater.* **2011**, *23*, 4684.
- Herlogsson, L.; Noh, Y.-Y.; Zhao, N.; Crispin, X.; Sirringhaus, H.; Berggren, M., *Adv. Mater.* **2008**, *20*, 4708.
- Hiemenz, P. C.; Lodge, T. P., *Polymer Chemistry*. CRC Press: New York, 2007.
- Holovko, M.; Kapko, V.; Henderson, D.; Boda, D., *Chem. Phys. Lett.* **2001**, *341*, 363.
- Howlett, P. C.; Izgorodina, E. I.; Forsyth, M.; MacFarlane, D. R., *Z. Phys. Chem.* **2006**, *220*, 1483.
- Hu, H.; Zhu, C.; Lu, Y. F.; Wu, Y. H.; Liew, T.; Li, M. F.; Cho, B. J.; Choi, W. K.; Yakovlev, N., *J. Appl. Phys.* **2003**, *94*, 551.
- Huddleston, J. G.; Visser, A. E.; Reichert, W. M.; Willauer, H. D.; Broker, G. A.; Rogers, R. D., *Green Chem.* **2001**, *3*, 156.
- Hyk, W.; Caban, K.; Donten, M.; Stojek, Z., *J. Phys. Chem. B* **2001**, *105*, 6943.
- Ignat'ev, N. V.; Welz-Biermann, U.; Kucheryna, A.; Bissky, G.; Willner, H., *J. Fluorine Chem.* **2005**, *126*, 1150.
- Islam, M. M.; Alam, M. T.; Ohsaka, T., *J. Phys. Chem. C* **2008**, *112*, 16568.
- Islam, M. M.; Alam, M. T.; Okajima, T.; Ohsaka, T., *J. Phys. Chem. C* **2009**, *113*, 3386.

- Izgorodina, E. I.; Forsyth, M.; MacFarlane, D. R., *Phys. Chem. Chem. Phys.* **2009**, *11*, 2452.
- Jackson, N. F., *Phys. Educ.* **1968**, *3*, 253.
- Jana, S.; Parthiban, A.; Chai, C. L. L., *Chem. Commun.* **2010**, *46*, 1488.
- Jansen, J. C.; Friess, K.; Clarizia, G.; Schauer, J.; Izak, P., *Macromolecules* **2011**, *44*, 39.
- Jansen, J. C.; Friess, K.; Clarizia, G.; Schauer, J.; Izák, P., *Macromolecules* **2011**, *44*, 39.
- Kang, S. J.; Kim, B.; Kim, K. S.; Zhao, Y.; Chen, Z.; Lee, G. H.; Hone, J.; Kim, P.; Nuckolls, C., *Adv. Mater.* **2011**, *23*, 3531.
- Kaskhedikar, N.; Burjanadze, M.; Karatas, Y.; Wiemhofer, H. D., *Solid State Ionics* **2006**, *177*, 3129.
- Katoh, R.; Hara, M.; Tsuzuki, S., *J. Phys. Chem. B* **2008**, *112*, 15426.
- Kawano, R.; Kubo, W.; Masaki, N.; Kitamura, T.; Wada, Y.; Watanabe, M.; Yanagida, S., *J. Phys. Chem. B* **2007**, *111*, 4763.
- Kawano, R.; Watanabe, M., *Chem. Commun.* **2003**, 330.
- Kazarian, S. G.; Briscoe, B. J.; Welton, T., *Chem. Commun.* **2000**, 2047.
- Kelley, T. W.; Baude, P. F.; Gerlach, C.; Ender, D. E.; Muyres, D.; Haase, M. A.; Vogel, D. E.; Theiss, S. D., *Chemistry of Materials* **2004**, *16*, 4413.
- Kerner, Z.; Pajkossy, T., *Electrochim. Acta* **2000**, *46*, 207.
- Kim, B. J.; Jang, H.; Lee, S.-K.; Hong, B. H.; Ahn, J.-H.; Cho, J. H., *Nano Lett.* **2010**, *10*, 3464.

- Kim, D.-H.; Lu, N.; Ghaffari, R.; Kim, Y.-S.; Lee, S. P.; Xu, L.; Wu, J.; Kim, R.-H.; Song, J.; Liu, Z.; Viventi, J.; de Graff, B.; Elolampi, B.; Mansour, M.; Slepian, M. J.; Hwang, S.; Moss, J. D.; Won, S.-M.; Huang, Y.; Litt, B.; Rogers, J. A., *Nat. Mater.* **2011**, *10*, 316.
- Kim, D.-H.; Song, J.; Choi, W. M.; Kim, H.-S.; Kim, R.-H.; Liu, Z.; Huang, Y. Y.; Hwang, K.-C.; Zhang, Y.-w.; Rogers, J. A., *Proc. Natl. Acad. Sci. USA* **2008**, *105*, 18675.
- Kim, D.-H.; Viventi, J.; Amsden, J. J.; Xiao, J.; Vigeland, L.; Kim, Y.-S.; Blanco, J. A.; Panilaitis, B.; Frechette, E. S.; Contreras, D.; Kaplan, D. L.; Omenetto, F. G.; Huang, Y.; Hwang, K.-C.; Zakin, M. R.; Litt, B.; Rogers, J. A., *Nat. Mater.* **2010**, *9*, 511.
- Kim, D.-W.; Sivakkumar, S. R.; MacFarlane, D. R.; Forsyth, M.; Sun, Y.-K., *J. Power Sources* **2008**, *180*, 591.
- Kim, T.-H.; Cho, K.-S.; Lee, E. K.; Lee, S. J.; Chae, J.; Kim, J. W.; Kim, D. H.; Kwon, J.-Y.; Amaratunga, G.; Lee, S. Y.; Choi, B. L.; Kuk, Y.; Kim, J. M.; Kim, K., *Nat. Photon.* **2011**, *5*, 176.
- Kitazawa, Y.; Ueki, T.; Niitsuma, K.; Imaizumi, S.; Lodge, T. P.; Watanabe, M., *Soft Matter* **2012**, *8*, 8067.
- Klauk, H., *Chem. Soc. Rev.* **2010**, *39*, 2643.
- Klingshirn, M. A.; Spear, S. K.; Subramanian, R.; Holbrey, J. D.; Huddleston, J. G.; Rogers, R. D., *Chem. Mater.* **2004**, *16*, 3091.

- Koch, V. R.; Dominey, L. A.; Nanjundiah, C.; Ondrechen, M. J., *J. Electrochem. Soc.* **1996**, *143*, 798.
- Koddermann, T.; Wertz, C.; Heintz, A.; Ludwig, R., *ChemPhysChem* **2006**, *7*, 1944.
- Krossing, I.; Slattery, J. M.; Daguenet, C.; Dyson, P. J.; Oleinikova, A.; Weingärtner, H., *J. Am. Chem. Soc.* **2006**, *128*, 13427.
- Larsson, O.; Laiho, A.; Schmickler, W.; Berggren, M.; Crispin, X., *Adv. Mater.* **2011**, *23*, 4764.
- Larsson, O.; Said, E.; Berggren, M.; Crispin, X., *Adv. Funct. Mater.* **2009**, *19*, 3334.
- Lee, J.; Kaake, L. G.; Cho, J. H.; Zhu, X. Y.; Lodge, T. P.; Frisbie, C. D., *J. Phys. Chem. C* **2009**, *113*, 8972.
- Lee, J.; Kim, J. H.; Im, S., *Appl. Phys. Lett.* **2003**, *83*, 2689.
- Lee, J.; Panzer, M. J.; He, Y.; Lodge, T. P.; Frisbie, C. D., *J. Am. Chem. Soc.* **2007**, *129*, 4532.
- Lee, K. H.; Kang, M. S.; Zhang, S.; Gu, Y.; Lodge, T. P.; Frisbie, C. D., *Adv. Mater.* **2012**, *24*, 4457.
- Lee, K. H.; Zhang, S.; Lodge, T. P.; Frisbie, C. D., *J. Phys. Chem. B* **2011**, *115*, 3315.
- Lee, S.; Lee, B.; Kim, B. J.; Park, J.; Yoo, M.; Bae, W. K.; Char, K.; Hawker, C. J.; Bang, J.; Cho, J., *J. Am. Chem. Soc.* **2009**, *131*, 2579.

- Lee, S. W.; Lee, H. J.; Choi, J. H.; Koh, W. G.; Myoung, J. M.; Hur, J. H.; Park, J. J.; Cho, J. H.; Jeong, U., *Nano Lett.* **2009**, *10*, 347.
- Lee, T.-W.; Zaumseil, J.; Bao, Z.; Hsu, J. W. P.; Rogers, J. A., *Proc. Natl. Acad. Sci. USA* **2004**, *101*, 429.
- Lehmann, S. B. C.; Roatsch, M.; Schoppke, M.; Kirchner, B., *Phys. Chem. Chem. Phys.* **2010**, *12*, 7473.
- Lei, Y.; Lodge, T. P., *Soft Matter* **2012**, *8*, 2110.
- Li, D.; Guo, L. J., *Appl. Phys. Lett.* **2006**, *88*, 063513.
- Liang, Y.; Frisbie, C. D.; Chang, H.-C.; Ruden, P. P., *J. Appl. Phys.* **2009**, *105*, 024514.
- Liu, X.; Osaka, T., *J. Electrochem. Soc.* **1996**, *143*, 3982.
- Lockett, V.; Sedev, R.; Ralston, J.; Horne, M.; Rodopoulos, T., *J. Phys. Chem. C* **2008**, *112*, 7486.
- Lodge, T. P., *Science* **2008**, *321*, 50.
- MacCallum, J. R.; VIncent, C. A., *Polymer electrolyte Review 1 and 2*. Elsevier: New York, 1987, 1989.
- MacFarlane, D. R.; Meakin, P.; Sun, J.; Amini, N.; Forsyth, M., *J. Phys. Chem. B* **1999**, *103*, 4164.
- MacFarlane, D. R.; Seddon, K. R., *Aust. J. Chem.* **2007**, *60*, 3.
- Majewski, L. A.; Schroeder, R.; Grell, M., *J. Phys. D: Appl. Phys.* **2004**, *37*, 21.
- Majewski, L. A.; Schroeder, R.; Grell, M., *Adv. Mater.* **2005**, *17*, 192.

- Malti, A.; Gabrielsson, E. O.; Berggren, M.; Crispin, X., *Appl Phys. Lett.* **2011**, *99*, 063305.
- Matsumoto, K.; Endo, T., *Macromolecules* **2008**, *41*, 6981.
- Matyjaszewski, K.; Xia, J., *Chem. Rev.* **2001**, *101*, 2921.
- McEwen, A. B.; Ngo, H. L.; LeCompte, K.; Goldman, J. L., *J. Electrochem. Soc.* **1999**, *146*, 1687.
- McFarlane, D. R.; Sun, J.; Golding, J.; Meakin, P.; Forsyth, M., *Electrochim. Acta* **2000**, *45*, 1271.
- Meitl, M. A.; Zhu, Z.-T.; Kumar, V.; Lee, K. J.; Feng, X.; Huang, Y. Y.; Adesida, I.; Nuzzo, R. G.; Rogers, J. A., *Nat. Mater.* **2006**, *5*, 33.
- Memming, R., *Semiconductor electrochemistry*. Wiley-VCH: Weinheim ; New York, 2001.
- Menard, E.; Meitl, M. A.; Sun, Y.; Park, J.-U.; Shir, D. J.-L.; Nam, Y.-S.; Jeon, S.; Rogers, J. A., *Chem. Rev.* **2007**, *107*, 1117.
- Meyers, S. T.; Anderson, J. T.; Hung, C. M.; Thompson, J.; Wager, J. F.; Keszler, D. A., *J. Am. Chem. Soc.* **2008**, *130*, 17603.
- Min, Y.; Akbulut, M.; Sangoro, J. R.; Kremer, F.; Prud'homme, R. K.; Israelachvili, J., *J. Phys. Chem. C* **2009**, *113*, 16445.
- Motheo, A. J.; Sadkowski, A.; Neves, R. S., *J. Electroanal. Chem.* **1997**, *430*, 253.
- Muller, D. A.; Sorsch, T.; Moccio, S.; Baumann, F. H.; Evans-Lutterodt, K.; Timp, G., *Nature* **1999**, *399*, 758.

- Naber, R. C. G.; Tanase, C.; Blom, P. W. M.; Gelinck, G. H.; Marsman, A. W.; Touwslager, F. J.; Setayesh, S.; de Leeuw, D. M., *Nat. Mater.* **2005**, *4*, 243.
- Nakamoto, H.; Noda, A.; Hayamizu, K.; Hayashi, S.; Hamaguchi, H.; Watanabe, M., *J. Phys. Chem. C* **2007**, *111*, 1541.
- Nanjundiah, C.; McDevitt, S. F.; Koch, V. R., *J. Electrochem. Soc.* **1997**, *144*, 3392.
- Neouze, M.-A.; Bideau, J. L.; Leroux, F.; Vioux, A., *Chem. Commun.* **2005**, 1082.
- Noda, A.; Hayamizu, K.; Watanabe, M., *J. Phys. Chem. B* **2001**, *105*, 4603.
- Noda, A.; Susan, M. A. B. H.; Kudo, K.; Mitsushima, S.; Hayamizu, K.; Watanabe, M., *J. Phys. Chem. B* **2003**, *107*, 4024.
- Noda, A.; Watanabe, M., *Electrochim. Acta* **2000**, *45*, 1265.
- Noh, Y.-Y.; Zhao, N.; Caironi, M.; Sirringhaus, H., *Nat. Nanotech.* **2007**, *2*, 784.
- Noro, A.; Hayashi, M.; Matsushita, Y., *Soft Matter* **2012**, *8*, 6416.
- Noro, A.; Matsushita, Y.; Lodge, T. P., *Macromolecules* **2008**, *41*, 5839.
- Noro, A.; Matsushita, Y.; Lodge, T. P., *Macromolecules* **2009**, *42*, 5802.
- Ofer, D.; Crooks, R. M.; Wrighton, M. S., *J. Am. Chem. Soc.* **1990**, *112*, 7869.
- Ofer, D.; Park, L. Y.; Schrock, R. R.; Wrighton, M. S., *Chem. Mater.* **1991**, *3*, 573.
- Ogihara, W.; Sun, J.; Forsyth, M.; MacFarlane, D. R.; Yoshizawa, M.; Ohno, H., *Electrochim. Acta* **2004**, *49*, 1797.

- Ohno, H., *Electrochemical aspects of ionic liquids*. Wiley: Hoboken, New Jersey, 2005.
- Ono, S.; Minder, N.; Chen, Z.; Facchetti, A.; Morpurgo, A. F., *Appl. Phys. Lett.* **2010**, *97*, 143307.
- Ono, S.; Seki, S.; Hirahara, R.; Tominari, Y.; Takeya, J., *Appl. Phys. Lett.* **2008**, *92*, 103313.
- Owens, R. M.; Malliaras, G. G., *MRS Bull.* **2010**, *35*, 449.
- Pajkossy, T., *J. Electroanal. Chem.* **1994**, *364*, 111.
- Pajkossy, T., *Solid State Ionics* **2005**, *176*, 1997.
- Panzer, M. J.; Frisbie, C. D., *Advanced Functional Materials* **2006**, *16*, 1051.
- Panzer, M. J.; Frisbie, C. D., *J. Am. Chem. Soc.* **2007**, *129*, 6599.
- Panzer, M. J.; Frisbie, C. D., *Adv. Mater.* **2008**, *20*, 3177.
- Panzer, M. J.; Newman, C. R.; Frisbie, C. D., *Appl. Phys. Lett.* **2005**, *86*, 103503.
- Papageorgiou, N.; Athanassov, Y.; Armand, M.; Bonhote, P.; Pettersson, H.; Azam, A.; Grätzel, M., *J. Electrochem. Soc.* **1996**, *143*, 3099.
- Parashkov, R.; Becker, E.; Ginev, G.; Riedl, T.; Johannes, H.-H.; Kowalsky, W., *J. Appl. Phys.* **2004**, *95*, 1594.
- Park, S. Y.; Kwon, T.; Lee, H. H., *Adv. Mater.* **2006**, *18*, 1861.
- Patten, T. E.; Xia, J.; Abernathy, T.; Matyjaszewski, K., *Science* **1996**, *272*, 866.
- Randriamahazaka, H.; Asaka, K., *J. Phys. Chem. C* **2010**, *114*, 17982.
- Ratner, M. A.; Shriver, D. F., *Chem. Rev.* **1988**, *88*, 109.
- Redinger, D.; Subramanian, V., *IEEE Trans. Electron Devices* **2007**, *54*, 1301.

- Reichardt, C., *Org. Process Res. Dev.* **2007**, *11*, 105.
- Sangoro, J. R.; Serghei, A.; Naumov, S.; Galvosas, P.; auml; rger, J.; Wespe, C.; Bordusa, F.; Kremer, F., *Phys. Rev. E* **2008**, *77*, 051202.
- Sarjeant, W. J.; Zirnheld, J.; MacDougall, F. W., *IEEE Trans. Plasma Sci.* **1998**, *26*, 1368.
- Schroder, U.; Wadhawan, J. D.; Compton, R. G.; Marken, F.; Suarez, P. A. Z.; Consorti, C. S.; Souza, R. F. d.; Dupont, J., *New J. Chem.* **2000**, *24*, 1009.
- Sekhon, S. S.; Lalia, B. S.; Park, J.-S.; Kim, C.-S.; Yamada, K., *J. Mater. Chem.* **2006**, *16*.
- Sekitani, T.; Noguchi, Y.; Hata, K.; Fukushima, T.; Aida, T.; Someya, T., *Science* **2008**, *321*, 1468.
- Sekitani, T.; Someya, T., *Adv. Mater.* **2010**, *22*, 2228.
- Sekitani, T.; Takamiya, M.; Noguchi, Y.; Nakano, S.; Kato, Y.; Sakurai, T.; Someya, T., *Nat. Mater.* **2007**, *6*, 413.
- Serban, D. A.; Greco, P.; Melinte, S.; Vlad, A.; Dutu, C. A.; Zacchini, S.; Iapalucci, M. C.; Biscarini, F.; Cavallini, M., *Small* **2009**, *5*, 1117.
- Shi, F.; Deng, Y., *Spectrochim. Acta A* **2005**, *62*, 239.
- Shi, F.; Zhang, Q.; Li, D.; Deng, Y., *Chem. Eur. J.* **2005**, *11*, 5279.
- Shimamura, K.; Chiba, D.; Ono, S.; Fukami, S.; Ishiwata, N.; Kawaguchi, M.; Kobayashi, K.; Ono, T., *Appl. Phys. Lett.* **2012**, *100*, 122402.
- Shimotani, H.; Asanuma, H.; Tsukazaki, A.; Ohtomo, A.; Kawasaki, M.; Iwasa, Y., *Appl. Phys. Lett.* **2007**, *91*, 082106.

- Shipp, D. A.; Wang, J.; Matyjaszewski, K., *Macromolecules* **1998**, *31*, 8005.
- Silva, F.; Gomes, C.; Figueiredo, M.; Costa, R.; Martins, A.; Pereira, C. M., *J. Electroanal. Chem.* **2008**, *622*, 153.
- Singh, B.; Sekhon, S. S., *J. Phys. Chem. B* **2005**, *109*, 16539.
- Singh, K. P.; Gupta, P. N., *Eur. Polym. J.* **1998**, *34*, 1023.
- Sirringhaus, H.; Brown, P. J.; Friend, R. H.; Nielsen, M. M.; Bechgaard, K.; Langeveld-Voss, B. M. W.; Spiering, A. J. H.; Janssen, R. A. J.; Meijer, E. W.; Herwig, P.; de Leeuw, D. M., *Nature* **1999**, *401*, 685.
- Sirringhaus, H.; Kawase, T.; Friend, R. H.; Shimoda, T.; Inbasekaran, M.; Wu, W.; Woo, E. P., *Science* **2000**, *290*, 2123.
- Someya, T.; Kato, Y.; Sekitani, T.; Iba, S.; Noguchi, Y.; Murase, Y.; Kawaguchi, H.; Sakurai, T., *Proc. Natl. Acad. Sci. USA* **2005**, *102*, 12321.
- Someya, T.; Sekitani, T.; Iba, S.; Kato, Y.; Kawaguchi, H.; Sakurai, T., *Proc. Natl. Acad. Sci. USA* **2004**, *101*, 9966.
- Stathatos, E.; Lianos, P.; Zakeeruddin, S. M.; Liska, P.; Gratzel, M., *Chem. Mater.* **2003**, *15*, 1825.
- Stoppa, A.; Zech, O.; Kunz, W.; Buchner, R., *J. Chem. Eng. Data* **2009**, *55*, 1768.
- Suarez, P. A. Z.; Consorti, C. S.; Souza, R. F. d.; Dupont, J.; Gonçalves, R. S., *J. Braz. Chem. Soc.* **2002**, *13*, 106.
- Suarez, P. A. Z.; Selbach, V. i. M.; Dullius, J. E. L.; Einloft, S.; Piatnicki, C. M. S.; Azambuja, D. S.; de Souza, R. F.; Dupont, J., *Electrochim. Acta* **1997**, *42*, 2533.

- Suh, D.; Choi, S. J.; Lee, H. H., *Adv. Mater.* **2005**, *17*, 1554.
- Sun, J.; Forsyth, M.; MacFarlane, D. R., *J. Phys. Chem. B* **1998**, *102*, 8858.
- Susan, M. A. B. H.; Kaneko, T.; Noda, A.; Watanabe, M., *J. Am. Chem. Soc.* **2005**, *127*, 4976.
- Takeya, J.; Yamada, K.; Hara, K.; Shigeto, K.; Tsukagoshi, K.; Ikehata, S.; Aoyagi, Y., *Appl. Phys. Lett.* **2006**, *88*, 112102.
- Tardy, J. E., M.; Deman, A. L.; Gagnaire, A.; Teodorescu, V.; Blanchin, M. G.; Canut, B.; Barau, A.; Zaharescu, M. , *Microelectron. Reliab.* **2007**, *47*, 372.
- Tate, J.; Rogers, J. A.; Jones, C. D. W.; Vyas, B.; Murphy, D. W.; Li, W.; Bao, Z.; Slusher, R. E.; Dodabalapur, A.; Katz, H. E., *Langmuir* **2000**, *16*, 6054.
- Thiemann, S.; Sachnov, S.; Porscha, S.; Wasserscheid, P.; Zaumseil, J., *J. Phys. Chem. C* **2012**, *116*, 13536.
- Tokuda, H.; Hayamizu, K.; Ishii, K.; Susan, M. A. B. H.; Watanabe, M., *J. Phys. Chem. B* **2004**, *108*, 16593.
- Tokuda, H.; Hayamizu, K.; Ishii, K.; Susan, M. A. B. H.; Watanabe, M., *J. Phys. Chem. B* **2005**, *109*, 6103.
- Tokuda, H.; Ishii, K.; Susan, M. A. B. H.; Tsuzuki, S.; Hayamizu, K.; Watanabe, M., *J. Phys. Chem. B* **2006**, *110*, 2833.
- Tsuzuki, S.; Tokuda, H.; Hayamizu, K.; Watanabe, M., *J. Phys. Chem. B* **2005**, *109*, 16474.
- Turner, E. A.; Pye, C. C.; Singer, R. D., *J. Phys. Chem. A* **2003**, *107*, 2277.

- Ue, M.; Takeda, M.; Takahashi, T.; Takehara, M., *Electrochem. Solid-State Lett.* **2002**, *5*, A119.
- Ueki, T.; Watanabe, M., *Chem. Lett.* **2006**, *35*, 964.
- Uemura, T.; Yamagishi, M.; Ono, S.; Takeya, J., *Appl. Phys. Lett.* **2009**, *95*, 103301.
- Ueno, K.; Hata, K.; Katakabe, T.; Kondoh, M.; Watanabe, M., *J. Phys. Chem. B* **2008**, *112*, 9013.
- Ueno, K.; Tokuda, H.; Watanabe, M., *Phys. Chem. Chem. Phys.* **2010**, *12*, 1649.
- Ukshe, E. A.; Bukun, N. G.; Leikis, D. I.; Frumkin, A. N., *Electrochim. Acta* **1964**, *9*, 431.
- Uno, T.; Kawaguchi, S.; Kubo, M.; Itoh, T., *J. Power Sources* **2008**, *178*, 716.
- Usui, H.; Matsui, H.; Tanabe, N.; Yanagida, S., *J.Photoch. Photobio. A* **2004**, *164*, 97.
- Vincent, C. A., *Prog. Solid State Chem.* **1987**, *17*, 145.
- Wakai, C.; Oleinikova, A.; Ott, M.; Weingärtner, H., *J. Phys. Chem. B* **2005**, *109*, 17028.
- Walden, P., *Bull. Acad. Imp. Sci. St Petersbourg* **1914**, *8*, 405.
- Wang, C.; Luo, H.; Li, H.; Dai, S., *Phys. Chem. Chem. Phys.* **2010**, *12*, 7246.
- Wang, G.; Moses, D.; Heeger, A. J.; Zhang, H.-M.; Narasimhan, M.; Demaray, R. E., *J. Appl. Phys.* **2004**, *95*, 316.
- Wang, P.; Zakeeruddin, S. M.; Comte, P.; Exnar, I.; Gratzel, M., *J. Am. Chem. Soc.* **2003**, *125*, 1166.

- Wang, P.; Zakeeruddin, S. M.; Exnar, I.; Grätzel, M., *Chem. Commun.* **2002**, 2972.
- Wang, P.; Zakeeruddin, S. M.; Moser, J.; Grätzel, M., *J. Phys. Chem. B* **2003**, *107*, 13280.
- Wei, C.-Y.; F., A.; Lin, Y.-J.; Li, Y.-C.; Huang, T.-J.; Chou, D.-W.; Wang, Y.-H., *IEEE Electron Device Lett.* **2009**, *30*, 1039.
- Welton, T., *Chem. Rev.* **1999**, *99*, 2071.
- Weston, J. E.; Steele, B. C. H., *Solid State Ionics* **1982**, *7*, 75.
- White, H. S.; Kittlesen, G. P.; Wrighton, M. S., *J. Am. Chem. Soc.* **1984**, *106*, 5375.
- Wilk, G. D.; Wallace, R. M.; Anthony, J. M., *J. Appl. Phys.* **2001**, *89*, 5243.
- Xia, J.; Matyjaszewski, K., *Macromolecules* **1997**, *30*, 7697.
- Xia, Y.; Whitesides, G. M., *Angew. Chem. Int. Ed. Engl.* **1998**, *37*, 550.
- Xia, Y.; Zhang, W.; Ha, M.; Cho, J. H.; Renn, M. J.; Kim, C. H.; Frisbie, C. D., *Adv. Funct. Mater.* **2010**, *20*, 587.
- Xie, W.; Frisbie, C. D., *J. Phys. Chem. C* **2011**, *115*, 14360.
- Yan, H.; Chen, Z.; Zheng, Y.; Newman, C.; Quinn, J. R.; Dotz, F.; Kastler, M.; Facchetti, A., *Nature* **2009**, *457*, 679.
- Ye, H.; Huang, J.; Xu, J. J.; Khalfan, A.; Greenbaum, S. G., *J. Electrochem. Soc.* **2007**, *154*, A1048.
- Ye, J. T.; Inoue, S.; Kobayashi, K.; Kasahara, Y.; Yuan, H. T.; Shimotani, H.; Iwasa, Y., *Nat. Mater.* **2009**, *9*, 125.

- Yeon, S.-H.; Kim, K.-S.; Choi, S.; Cha, J.-H.; Lee, H., *J. Phys. Chem. B* **2005**, *109*, 17928.
- Yoon, M.-H.; Yan, H.; Facchetti, A.; Marks, T. J., *J. Am. Chem. Soc.* **2005**, *127*, 10388.
- Yu, X. J.; Xu, J. B.; Cheung, W. Y.; Ke, N., *J. Appl. Phys.* **2007**, *102*, 103711.
- Yuan, H.; Shimotani, H.; Tsukazaki, A.; Ohtomo, A.; Kawasaki, M.; Iwasa, Y., *Adv. Funct. Mater.* **2009**, *19*, 1046.
- Zaumseil, J.; Sirringhaus, H., *Chem. Rev.* **2007**, *107*, 1296.
- Zech, O.; Stoppa, A.; Buchner, R.; Kunz, W., *J. Chem. Eng. Data* **2010**, *55*, 1774.
- Zhang, S.; Lee, K. H.; Frisbie, C. D.; Lodge, T. P., *Macromolecules* **2011**, *44*, 940.
- Zhang, S.; Lee, K. H.; Sun, J.; Frisbie, C. D.; Lodge, T. P., *Macromolecules* **2011**, *44*, 8981.
- Zhao, F.; Wu, X.; Wang, M.; Liu, Y.; Gao, L.; Dong, S., *Anal. Chem.* **2004**, *76*, 4960.
- Zhao, W.; Leroy, F. d. r.; Heggen, B.; Zahn, S.; Kirchner, B.; Balasubramanian, S.; Müller-Plathe, F., *J. Am. Chem. Soc.* **2009**, *131*, 15825.
- Zistler, M.; Wachter, P.; Schreiner, C.; Fleischmann, M.; Gerhard, D.; Wasserscheid, P.; Hinsch, A.; Gores, H. J., *J. Electrochem. Soc.* **2007**, *154*, B925.